Dynamic Cone Penetrometer Criteria for Evaluation of Subgrade and Aggregate Base Courses

By

Mohammed A. Gabr

Philip C. Lambe

Jeffrey W. Coonse

Kelly P. Hopkins

Department of Civil Engineering

North Carolina State University

In Cooperation with

The North Carolina Department of Transportation

and

The institute for Transportation Research and Education

Center for Transportation Engineering Studies

North Carolina State University

Raleigh, North Carolina

August, 1999

Technical Report Documentation Page

1. Report No. FHWA/NC/2002-013	2. Government Accession No.	3. Recipient's Catalog No.
4. Title and Subtitle Dynamic Cone Penetrometer Criteria for Evaluation of Subgrade and Aggregate Base Courses		5. Report Date August, 1999
		6. Performing Organization Code
7. Author(s) M. A. Gabr, P. C. Lambe, J. W. Coonse, and K. P. Hopkins		8. Performing Organization Report No.
9. Performing Organization Name and Address Department of Civil Engineering North Carolina State University Campus Bos 7908 Raleigh, NC 27695-7908		10. Work Unit No. (TRAIS)
		11. Contract or Grant No.
12. Sponsoring Agency Name and Address North Carolina Department of Transportation Research and Analysis Group 1 South Wilmington Street Raleigh, NC 27601		13. Type of Report and Period Covered Final Report July, 1998 - June 1999
		14. Sponsoring Agency Code 1999-04
15. Supplementary Notes		

16. Abstract

This report summarizes the findings of one-year research study sponsored by the North Carolina Department of Transportation on the use of the DCP to develop a pavement distress evaluation model. Work included laboratory and field testing programs as well as modeling effort. In this report, a method was proposed by which the DCP PR data were utilized to evaluate pavement distress state. Such evaluation is needed on regular basis in order to categorize the implementation of rehabilitation measures. The principle idea was to use the DCP data to discern the integrity of the subase and ABC layers. Accordingly, if the structural integrity of subgrade and ABC layers is found to be adequate, maintenance measures can include simply resurfacing or treating the surface layer. However, in situations where the structural integrity of the ABC, the subgrade, or both, is found inadequate, extensive stabilization and soil improvement measures maybe needed and resurfacing alone will not be sufficient.

The laboratory work on the subgrade materials was performed on three residual soil types taken from test sites in Davidson County, North Carolina. Testing included compaction of soil specimens in a 150 mm (6 in) mold, performing the CBR test on the prepared specimens, and then penetrating the specimens with the DCP probe. In parallel, the laboratory testing on the ABC materials included the preparation of thirty-two CBR specimens using material from two different sources. The field testing included work at seven sites with three CBR tests, seven DCP penetrations, three nuclear gauge measurements, three FWD tests and one bulk sample extraction conducted at each site. A second phase of field testing at three sites was also performed. Modeling work included development of correlation between the PR and CBR of subgrade soils, PR and CBR of the ABC material, and PR and compaction unit weight and moisture content of the subgrade soils. In addition, the coupled PR-subgrade and PR- ABC data were used to develop a pavement distress level that provided an indication of the test sites pavement's serviceability level.

17. Key Words Aggregate Base Course, Cones, Compaction, Dynamic Cone Laboratory, Penetrometers, Penetration, Residual Soils, Subgrade	18. Distribution Statement		
19. Security Classif. (of this report) Unclassified	20. Security Classif. (of this page) Unclassified	21. No. of Pages 115	22. Price

Form DOT F 1700.7 (8-72) **Reproduction of completed page authorized**

ACKNOWLEDGEMENTS

This research project entitled "Dynamic Cone Penetrometer Criteria for Evaluation of Subgrade and Aggregate Base Courses" was sponsored by North Carolina Department of Transportation (NCDOT). The authors would like to thank Mr. Pat Strong and Dr. Moy Biswas of NCDOT research and development for their support of this project. Mr. Dick Reaves and his staff at the Materials Testing Unit provided excellent assistance in performing the laboratory tests. Special thanks goes to C. K Su, Mehdi Haeri and Hisham El Boulaki for their input to the experimental program. Thanks are also extended to Mr. Tom Hearne and Mr. Shane Kepley, NC Pavement Management System, for sharing their knowledge of the DCP test and performing the field work. Mr. Njoroge Wainaina provided valuable input to the direction of the research program. Dr. Roy Borden, NCSU, suggested innovative ways to reduce the test data. Mr. Dan Grissom and Mr. David Spainhour provided helpful comments on the direction of the research. Mr. James Travis was the FHWA representative on the project. The opinions, findings and conclusions expressed are those of the authors and do not necessarily represent those of the NCDOT.

ABSTRACT

This report summarizes the findings of one-year research study sponsored by the North Carolina Department of Transportation on the use of the DCP to develop a pavement distress evaluation model. Work included laboratory and field testing programs as well as modeling effort. In this report, a method was proposed by which the DCP PR data were utilized to evaluate pavement distress state. Such evaluation is needed on regular basis in order to categorize the implementation of rehabilitation measures. The principle idea was to use the DCP data to discern the integrity of the subase and ABC layers. Accordingly, if the structural integrity of subgrade and ABC layers is found to be adequate, maintenance measures can include simply resurfacing or treating the surface layer. However, in situations where the structural integrity of the ABC, the subgrade, or both, is found inadequate, extensive stabilization and soil improvement measures maybe needed and resurfacing alone will not be sufficient. The laboratory work on the subgrade materials was performed on three residual soil types taken from test sites in Davidson County, North Carolina. Testing included compaction of soil specimens in a 150 mm (6 in) mold, performing the CBR test on the prepared specimens, and then penetrating the specimens with the DCP probe. In parallel, the laboratory testing on the ABC materials included the preparation of thirty-two CBR specimens using material from two different sources. The field testing included work at seven sites with three CBR tests, seven DCP penetrations, three nuclear gauge measurements, three FWD tests and one bulk sample extraction conducted at each site. A second phase of field testing at three sites was also performed. Modeling work included development of correlation between the PR and CBR of subgrade soils, PR and CBR of the ABC material, and PR and compaction unit weight and moisture content of the subgrade soils. In addition, the coupled PR-subgrade and PR- ABC data were used to develop a pavement distress level that provided an indication of the test sites pavement's serviceability level.

Table of Contents

LIST OF TABLES 6

LIST OF FIGURES 7

1.0 INTRODUCTION 9

1.1 Research Objectives 11

1.2 Scope of Research 11

2.0 LITERATURE REVIEW 13

2.1 Development of Penetrometers 13

2.2 Mechanics of Dynamic Cone Penetration 14

2.3 Empirical Correlation of DCP and CBR 14

2.4 Independence of DCP - CBR Relationship 18
2.4.1 Dependency on Moisture/Unit weight 18
2.4.2 Vertical Confining Effect 20

2.5 Effects of Lateral Confinement 23

2.6 Other Factors Affecting Laboratory Correlation 24

3.0 MATERIALS AND METHODS 26

3.1 Subgrade Soil 27
3.1.1 Specimens Preparation 28
3.1.2 Laboratory Testing Procedure 29

3.2 ABC Material 30
3.2.1 Specimens Preparation 31

3.3 Laboratory Test Equipment 32

3.4 Field Testing Equipment 36

4.0 SUBGRADE SOILS AND COMPACTION PROPERITES 39

4.1 Moisture and DCP – CBR Relationship 40

4.2 Dry Unit weight and DCP – CBR Relationship 41

4.3 Soaking and DCP – CBR Relationship 42

4.4 Effect of Mold Diameter 44

5.0 SUBGRADE MODELS 48

5.1 PR-CBR Model 48

5.2 Laboratory Correlation for Field Use 49

5.3 PR-Moisture Correlation 50

5.4 PR/Unit Weight Correlation 51

5.4 Compaction Control Model Validation 53

6.0 ABC PR/CBR PROPERITES 56

6. CBR/DCP Correlation 59

7.0 FIELD TESTING 61

7.1 Field Testing Program 64

7.2 Field Material Properties 65

7.3 DCP Data 66

7.4 FWD Data and Correlation 68

7.5 PR/CBR Field Results 69

8.0 PAVEMENT DISTRESS MODEL 71

8.1 Model Validation 74

9.0 SUMMARY AND CONCLUSIONS 76

10.0 REFERENCES 80

APPENDIX A 84

List of Tables

Table 2.1 DCP – CBR Correlations (After Harison 1987)

Table 3.1 AASHTO (1992) Standard Specifications Used in Laboratory Testing

Table 3.2 Summary of Soil Classification

Table 3.3 Summary of Test Series on Subgrade Soils

Table 4.1 Summary of Moisture – Unit weight Relationships (T-99)

Table 7.1 Summary of Field Testing Program

Table 7.2 Summary of Test Site Information

Table 7.3 Summary of the Data Obtained By Means of the Nuclear Gage Device

Table 7.4 Summary of the DCP Findings as Synthesized from Figures A.1a through A.7c

Table 8.1 Summary of Test Sites Information, Phase II

List of Figures

Figure 2.1 General Dimensions of the Scala DCP (Kleyn 1975)

Figure2.2 Proposed Failure Mechanisms Adopted from Deep Foundation Theory for Conical Penetrometers (M. Livneh, Ishai, and N. Livneh c. 1993)

Figure 2.3 Relation between moisture content, dry unit weight, CBR, and DCP (PR) for MH soil (Harison 1989)

Figure 2.4 DCP test results for subgrade beneath granular structure (Livneh et al c.1993)

Figure 2.5 Correlation Between Confined and Unconfined DCP Within Clay Subgrades (Livneh, et al c. 1987)

Figure 2.6 CBR Results from Clay Subgrade Beneath 500 Mm (20 in) Thick Asphalt Structure (Livenh Et Al, 1993)

Figure 2.7 Effects of Asphalt Confinement on DCP Values in Granular Material (Livneh Et Al C. 1993)

Figure 3. Grain Size Distribution of the Test Soils

Figure 3.2 Grain Size Distribution for Virgin And Lab Assembled Materials

Figure 3.3 Automatic Compaction Hammer

Figure 3.4 Molds Used to Prepare Specimen

Figure 3.5 Specimen Penetrated by Scala DCP

Figure 3.6 Load Frame With CBR Specimen

Figure 3.7 DCP Performed at one of the Test Sites

Figure 4.1 T-99 Dry Unit Weight- Moisture Relationships for the Test Soils

Figure 4.2 CBR And PR Versus Moisture Content - Surratt Rd (Compaction Effort Held Constant at T-99)

Figure 4.3 CBR And PR Versus Percent Compaction - Surratt Rd (Moisture Content Held Constant at Optimum)

Figure 4.4 CBR And PR Versus Molding Moisture Content for Soaked And Unsoaked

Specimen - Poole Rd

Figure 4.5 Relationship Between CBR Estimated by Correlations Based Upon Soaked And Unsoaked Specimen (Harison 1989)

Figure 4.6 Comparison of Dry Density in 150 Mm (6 in) And 250 Mm (10 in) Molds

Figure 4.7 Comparison of PR Between 150 Mm (6 in) Mold And 250 Mm (10 in) Mold

Figure 4.8 Comparison of CBR Between 150 Mm (6 in) Mold And 250 Mm (10 in) Mold

Figure 4.9 Theoretical Shear Failure Surface of Bearing Capacity Failure Produced by CBR Piston in A 150 Mm (6 in) Mold (Black 1961)

Figure 5.1 CBR - PR Laboratory Data Shown With Several Correlations

Figure 5.2 Corrected Laboratory Data With Data From the 250 Mm (10 in) Mold

Figure 5.3 Comparison of Correlation Results for Piedmont Residual Soil

Figure 5.4 PR Versus Liquidity index

Figure 5.5 PR Versus Percent Saturation

Figure 5.6 Measured Versus Predicted Values: A) Moisture Content, And B) Dry Unit Weight

Figure 6.1 Compaction Desnity-Mositure Relationships, Thomasville Quarry, T99 And T180

Figure 6.2 CBR And PR Vs Moisture Content: A) Thomasville Quarry, And B) Gold Hill Quarry

Figure 6.3 CBR-PR Correlations for Gold Thomasville And Gold Hill Material - Lab Data

Figure 7. Serviceability Versus Age

Figure 7.2 Grain Size Distribution of ABC Material-Field Sites

Figure 7.3 Variation of FWD Deflection Data With PR-ABC And PR-Subgrade Values

Figure 7.4 Field CBR As A Function of PR-ABC: Predicted Versus Measured

Figure 8.1 Pavement Distress Model: Performance Boundary And Field Comparisons

Figure 8.2 Pavement Distress Model Validation: Three Sites

ABSTRACT

This report summarizes the findings of one-year research study sponsored by the North Carolina Department of Transportation on the use of the DCP to develop a pavement distress evaluation model. Work included laboratory and field testing programs as well as modeling effort. In this report, a method was proposed by which the DCP PR data were utilized to evaluate pavement distress state. Such evaluation is needed on regular basis in order to categorize the implementation of rehabilitation measures. The principle idea was to use the DCP data to discern the integrity of the subase and ABC layers. Accordingly, if the structural integrity of subgrade and ABC layers is found to be adequate, maintenance measures can include simply resurfacing or treating the surface layer. However, in situations where the structural integrity of the ABC, the subgrade, or both, is found inadequate, extensive stabilization and soil improvement measures maybe needed and resurfacing alone will not be sufficient. The laboratory work on the subgrade materials was performed on three residual soil types taken from test sites in Davidson County, North Carolina. Testing included compaction of soil specimens in a 150 mm (6 in) mold, performing the CBR test on the prepared specimens, and then penetrating the specimens with the DCP probe. In parallel, the laboratory testing on the ABC materials included the preparation of thirty-two CBR specimens using material from two different sources. The field testing included work at seven sites with three CBR tests, seven DCP penetrations, three nuclear gauge measurements, three FWD tests and one bulk sample extraction conducted at each site. A second phase of field testing at three sites was also performed. Modeling work included development of correlation between the PR and CBR of subgrade soils, PR and CBR of the ABC material, and PR and compaction unit weight and moisture content of the subgrade soils. In addition, the coupled PR-subgrade and PR- ABC data were used to develop a pavement distress level that provided an indication of the test sites pavement's serviceability level.

1.0 INTRODUCTION

Evaluation of in-situ flexible pavements has included performance of time-consuming and expensive in-situ tests such as the California Bearing Ratio (CBR) and more recently by nondestructive testing devices such as the falling weight deflectometer (FWD). Alternatively, the Dynamic Cone Penetration (DCP) device offers the potential of an inexpensive technique to evaluate the structural integrity of the pavement base/subbase and subgrade layers. The DCP, also known as the Scala Penetrometer, was originally developed in 1956 in South Africa and has been used in the past decade to evaluate the strength of the aggregate base course (ABC) and subgrade layers of pavement. Review of literature reveals that the Scala DCP has been used to estimate the CBR value of both ABC and subgrade layers and to estimate subgrade elastic modulus as well as soil strength parameters.

In pavement-related applications, past research has been performed to develop an empirical relationship between DCP penetration rate (PR) and the California Bearing Ratio (CBR) measurements. Examples of this work include research by Kleyn, (1975), Harison (1987), Livneh, M. (1987), McElvaney, and Bunadidjatnika (1991), Livneh, Ishai, and Livneh, (1992), Livneh, and Livneh (1994) and Dag et al (1995). The vast majority of this research has been performed using Scala's DCP, as it was originally developed, to estimate the CBR of subgrade soils. In general, many of the relationships presented in literature between DCP and CBR data seem to have converged to a correlation with the following form:

$$\log(CBR) = A + B\log(PR) \qquad (1)$$

where PR= DCP penetration rate in (mm/blow), A= a coefficient that ranged from 2.44-2.56 and B= a coefficient that ranged from 1.07 to 1.16.

In addition to CBR-PR correlations, several of the past studies attempted to define the DCP failure mechanisms, the impact of non-perpendicular penetration, or the impact of rod diameter to specimen diameter ratio in laboratory tests. One notable observation relevant to the research work presented in this report is that majority of past work was directed toward subgrade soils and not necessarily ABC material.

This report summarizes the findings of a one year research study sponsored by the North Carolina Department of Transportation on the use of the DCP to develop a pavement distress evaluation model with relative emphasis on the ABC material. In this report, a method is proposed by which the DCP PR data are utilized to evaluate the pavement distress state. Such evaluation is needed on a regular basis in order to prioritize the implementation of rehabilitation measures. The principle idea is to use the DCP data to discern the integrity of both, the sub-base and ABC layers. Accordingly, if the structural integrity of subgrade and ABC layers is adequate, required maintenance measures will involve the surface layer include resurfacing and treating the surface layer. However, in situations where the structural integrity of the ABC, and/or the subgrade, is inadequate, then stabilization and soil improvement measures will be needed before resurfacing, for long term enhanced performance.

Laboratory and field testing programs were performed on aggregate base course (ABC) and subgrade materials from seven sites in Davidson County, North Carolina. The laboratory program included compaction and CBR testing as well as penetrating soil and ABC specimens with the DCP device. Several series of tests were performed under various conditions representative of compactive efforts T-99 and T-180 (by AASHTO designation). Correlation patterns between the DCP penetration rate (PR) and the CBR were developed for both the subgrade and the ABC materials. The field testing program included performing CBR, DCP, Falling Weight Deflectometer (FWD), and nuclear gage tests on both, the ABC and the subgrade layers. A pavement distress model for determining the structural adequacy of the pavement layers, based on the relative strengths of the ABC and the subgrade soil, is proposed and discussed. The developed pavement distress model is demonstrated and validated using the results from additional field testing.

1.1 Research Objectives

The overall objective of this research was to develop and validate a procedure for utilizing the portable DCP device for the evaluation of the pavement distress level. Emphasis was placed on correlating the DCP data with the CBR values for the ABC layers, the compaction properties of the subgrade layers, and the level of the pavement distress as expressed by serviceability level. A systematic design procedure for evaluating the subbase and subgrade characteristics was developed. Specifically, the following objectives were achieved:

1) evaluate the dependence of the DCP – CBR relationship on the dry unit weight and moisture level of the subgrade soil,

2) determine the correlation between CBR and DCP for Piedmont residual soils and ABC material,

3) propose a step by step process for predicting the compaction parameters of the subgrade soils using the DCP data,

4) propose critical PR values for both ABC and subgrade whereby a decision regarding paving of the road can be made, and,

5) propose a method to evaluate the structural integrity and distress level of the subgrade and ABC pavement layers and their serviceability level.

1.2 Scope of Research

The laboratory work on the subgrade material is performed on three soil types taken from test sites in Davidson County, North Carolina. The laboratory program included compaction of soil specimens in a 150 mm (6 in) mold, performing the CBR test on the prepared specimens, and then penetrating the specimens with the DCP probe. In the case of the subgrade soils, several series of tests were performed under various conditions. In the first series of tests, the moisture content was varied while holding the compaction effort constant, forming a T-99 moisture - unit weight relationship. In the second series of tests, the compaction effort was varied while the moisture content was held at optimum. For the third series, pairs of specimens are compacted at equal moisture contents, then one of each pairs was soaked 96 hours prior to performing the CBR and DCP tests. Finally, a fourth series was performed by compacting specimens at equal moisture contents in two different diameter molds to evaluate the confining effect of the mold on the measured DCP and CBR values.

In parallel, the laboratory testing on the ABC materials included the preparation of thirty-two CBR specimens using material from two different sources. A total of sixteen specimens for each material were prepared and both materials were tested in the same manner. Three specimens for each target water content, compacted at the AASHTO T180 designation, were prepared and both CBR and DCP were performed on the specimens. One specimen per water content compacted at the AASHTO T99 designation was prepared and both CBR and DCP were performed on each specimen.

The field testing program included work at seven sites with three CBR tests, seven DCP penetrations, three nuclear gauge measurements, three FWD tests and one bulk sample extraction conducted at each site. A second phase of field testing at three included DCP, moisture, and in-situ CBR measurements on the ABC as well as DCP, moisture and in-situ CBR measurements on the subgrade soil. Modeling work included development of correlations between the PR and CBR of subgrade soils, the PR and CBR of the ABC material and the PR and compaction unit weight and moisture values of the subgrade soils. In addition, the coupled PR-subgrade and PR- ABC data were used to develop a pavement distress model that can be used to provide an indication of the pavement's serviceability level.

2.0 LITERATURE REVIEW

2.1 Development of Penetrometers

Several dynamic cone penetrometers have been used to evaluate the consistency and strength of soils. The most common dynamically driven penetrometer is the split spoon penetrometer operated from a drill rig. In the late fifties, Scala developed his penetrometer, shown in Figure 2.1, to evaluate flexible pavement subbases and subgrade soils, and Sowers developed a handheld penetrometer to be used for field exploration and verification of soil conditions of individual footings during construction. Sowers' penetrometer was not intended to replace traditional exploration and laboratory testing.

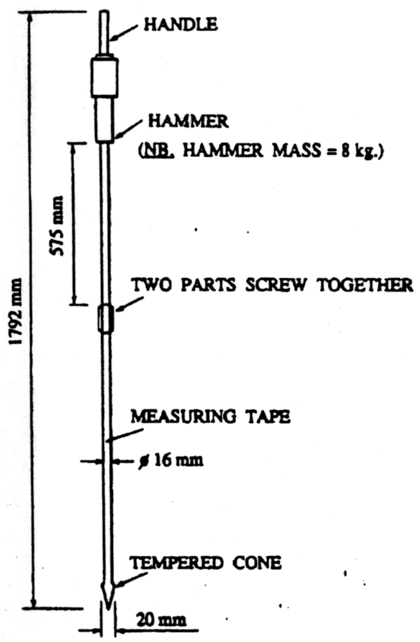

Figure 2.1 General Dimensions of the Scala DCP (Kleyn 1975)

Rather, the penetrometer was intended to supplement traditional exploration by verifying soil conditions at individual footings and to test soil conditions where a drill rig could not reach (Sowers and Hedges 1966).

All penetrometers, including Sower's and Scala's, were based upon the same principal of probing soil strength through developing a shear failure zone and measuring corresponding penetration resistance. Several material properties have been correlated to penetration resistance including friction angle, unconfined compressive strength, elastic modulus, and relative density as presented by Tolia (1977) and Marcu et al (1982).

2.2 Mechanics of Dynamic Cone Penetration

Durgunoglu and Mitchell (1974) proposed three failure mechanisms for deep foundations that have been adopted to describe the theoretical failure surfaces for penetrometers. Figure 2.2 shows these mechanisms. Nowatzki and Karafiath used the failure surface Figure 2.2c to model the failure mechanism in cohesionless soils due to probe insertion. Because the exact failure mechanism employed during the dynamic cone penetration is difficult to predict, many researchers have developed empirical correlations between penetration resistance and the parameter of interest. Figure 2.2 shows proposed

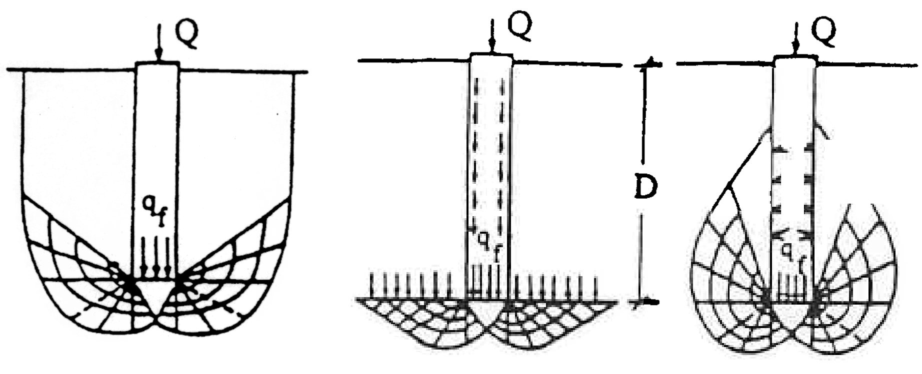

Failure Figure 2.2 Mechanisms Adopted from Deep Foundation Theory for Conical Penetrometers (M. Livneh, Ishai, and N. Livneh c. 1993)

2.3 Empirical Correlation of DCP and CBR

Extensive research has been performed to develop empirical relationships between

DCP resistance and CBR measurements. The vast majority of this research has been performed using Scala's DCP, as it was originally developed, to estimate the CBR of subgrade soils under flexible pavements. Kleyn (1975) performed DCP and CBR tests on 2000 specimens to develop a laboratory based correlation between DCP data and CBR. Kleyn varied the moisture content while holding the compaction effort at a standard proctor effort (T-99) for a sandy soil, clay soil, and gravel. The tests were conducted in various size molds (150 mm, 200 mm, and 200mm) in order to investigate the effect of the mold size on the DCP results. Kleyn found that the DCP data varied in a manner similar to the CBR data with respect to the moisture content for a given soil. Accordingly, he concluded that the DCP-CBR relationship was independent of moisture content. His data also indicated that as the size of the mold was decreased, an increase in the DCP penetration rate (PR) was observed.

Harison (1987) performed a study to establish whether a correlation existed between CBR data and penetration rate of the DCP for clay-like soils, well-graded sand, and gravel. It was concluded that a strong correlation between CBR and DCP data existed for each of the materials tested with an accuracy of +/- 10%. In addition, soaking processes were found to have an insignificant effect on the CBR/DCP relationship. Livneh (1987) performed DCP and in-situ CBR tests at two airfields and one road. The DCP tests were performed inside and outside test pits to evaluate the combined effect of vertical confinement and friction. Livenh indicated that at these sites, the combined effect of overburden and friction was negligible. In addition, profile measurement from the DCP test can be used to determine in situ layer thicknesses. McElvaney and Bunadidjatnika (1991) used the DCP to evaluate the strength of lime-stabilized pavement subgrade. Results from these tests indicated that the DCP can be used to provide a reasonable estimate of the unconfined compressive strength (UCS) of soil-lime mixtures and that the correlation obtained was primarily a function of strength level.

Livneh, Ishai, and Livneh (1992) conducted a comparative study of the Automated DCP (ADCP) and the Manual DCP (MDCP) and their correlation with California bearing ratio (CBR) values. The tests were conducted on materials ranging from low strength natural clay to high strength sub-base (granular) material. It was concluded that the CBR values derived from the ADCP should be reduced by a factor equal to 0.86 and that the use of the ADCP was recommended over the use of the manual DCP based upon improved precision and accuracy.

Ese el al (1995) conducted a comprehensive study on the use of DCP for road strengthening design in Norway. Conclusions from this study indicated that a correlation existed between the DCP data and the stability of the ABC with a PR of 2.6mm/blow being the maximum cutoff value between a good or fair roads. Values higher than 2.6mm/blow indicated poor roads. The following procedure for using the DCP as a tool for pavement evaluation was suggested:

a) Road sections that have decreased in serviceability are evaluated by a pavement management system.

b) DCP measurements are carried out on roads identified as having decreased serviceability.

c) Improved drainage is attempted to improve the base layer. If the DCP indicated that during the thaw period of the frost-thaw cycle that the base layer had been sufficiently improved, the road will simply be resurfaced. If sufficient improvement of the base course is not achieved through better drainage, then strengthening has to be carried out before resurfacing may take place.

A summary of different relationships presented in the literature between DCP and CBR data are presented in Table 2.1.

Table 2.1 DCP – CBR Correlations (After Harison 1987)

Researcher(s)	Correlation Equation	No. of Data Points, N	Field or Lab Based Study	Material Tested	Year of Work
Livneh	log(CBR) = 2.56 - 1.16 log(DCP)	76	lab	granular and cohesive	1991
Livneh, Ishai, and Livneh	log(CBR) = 2.45 – 1.12 log(DCP)	135	field and lab	granular and cohesive	c.1993
Harison	log(CBR) = 2.55 – 1.14 log(DCP)	72	lab	granular and cohesive	1987
Smith and Pratt	log(CBR) = 2.56 – 1.16 log(DCP)	unknown	field	unknown	1983
Kleyn	log(CBR) = 2.62 – 1.27 log(DCP)	2000	lab	unknown	1975
NCDOT	log(CBR) = 2.6 – 1.07 log(DCP)	unknown	adaptation on field, and lab	ABC and cohesive	c.1989, Shin et al
Norwegian Road Research	log(CBR) = 2.44 – 1.07 log(DCP)	79	both	ABC	1995

2.4 Independence of DCP - CBR Relationship

Past research has been performed to determine if the relationship between DCP and CBR depends upon factors such as vertical confinement, soil type, grain size, soil plasticity, dry unit weight, and moisture content. Such research has raised additional questions as to the effect of the diameter and depth of the mold used in laboratory- based correlations as well as the likelihood of any effect created by the unit weight gradient with depth in laboratory compacted specimens. Further issues were related to field testing and included the vertical confining effect on clay, silt and granular materials by rigid, flexible, and granular layers.

2.4.1 Dependency on Moisture/Unit weight

Harison (1989) showed that the DCP-CBR relationship was independent of moisture content and dry unit weight. Harison performed a testing program by compacting material in standard 150 mm (6 in) molds, performed a DCP test on one specimen and a CBR test on the other. Figure 2.3 shows how the DCP and CBR values varied with moisture content and dry unit weight for a silty soil. Figure 2.3a shows the compaction curve for the test soil. These results then generated Figure 2.3c that showed the DCP and CBR exhibited the same strength response to changes in moisture content, similar to Kleyn's results. In like manner, DCP and CBR responded in the same manner to changes in dry unit weight as shown in Figures 2.3c. Figure 2.3b shows that the DCP and CBR also responded to changes in dry unit weight in the same manner. Accordingly, Harison concluded that the DCP – CBR relationship was independent of moisture content and dry unit weight.

Material	LL	PL	PI	
MH	54%	40·5%	13·5	● 10 blows, ○ 25 blows, △ 40 blows, × 56 blows } soaked; ■ 10 blows, □ 25 blows } unsoaked

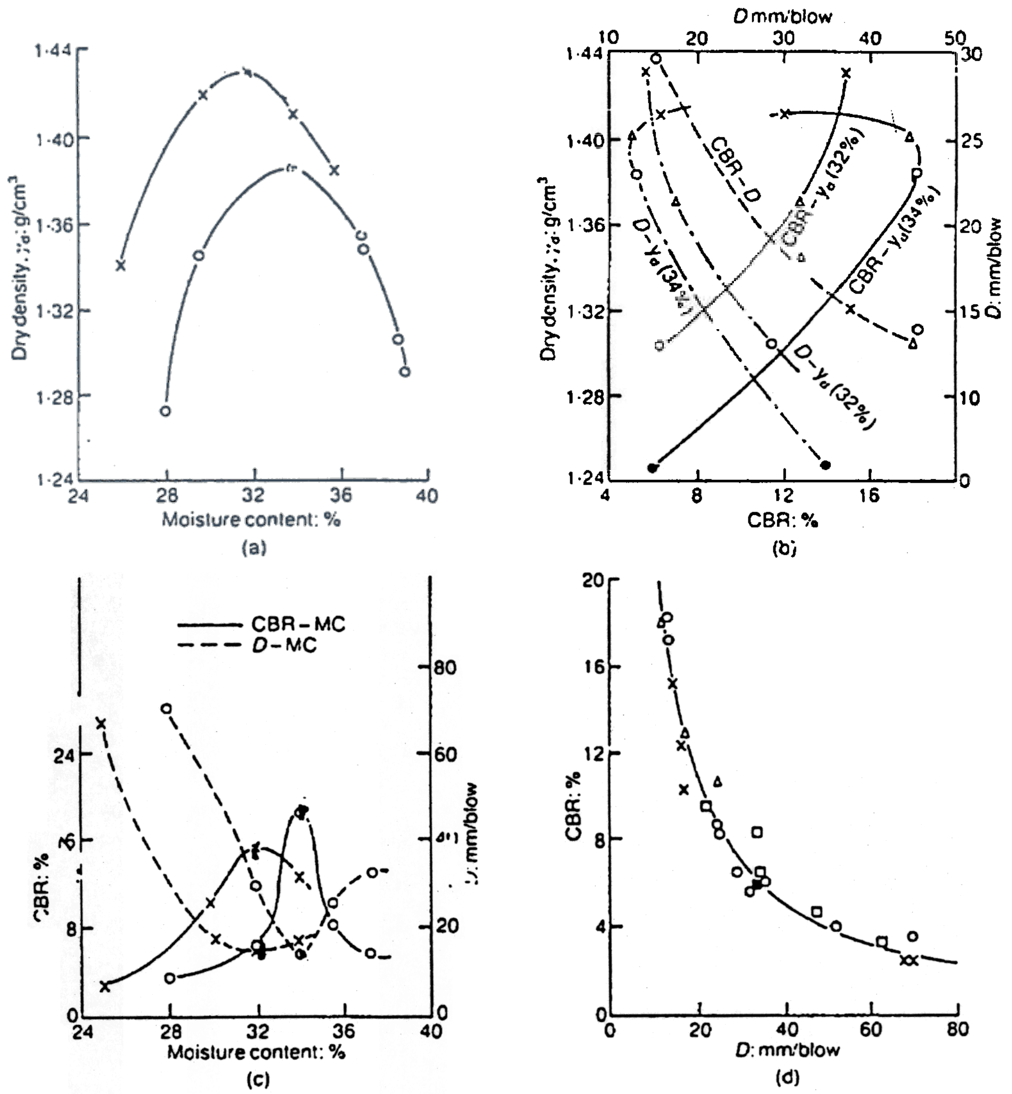

Figure 2.3 Relation between moisture content, dry unit weight, CBR, and DCP (PR) for MH soil (Harison 1989)

2.4.2 Vertical Confining Effect

M. Livneh, Ilan, and Livneh (c. 1993) studied the vertical confining effect of granular layers on silt and clay subgrades by coring 11 holes through the asphalt pavement and penetrating the DCP through the ABC and into the silt and clay subgrade soils. A test pit was then excavated at each of the 11 sites exposing the subgrade. The DCP was then penetrated into the silt and clay subgrade soil without the vertical confinement of the ABC layer. A linear regression, see Figure 2.4, showed that the DCP penetration rate (PR) of the silt and clay subgrade confined by the ABC was on the average 34% lower (stronger) than the PR value in the unconfined condition. Two of the sites involving a silt subgrade soil showed that the silt exhibited a larger change in the DCP readings.

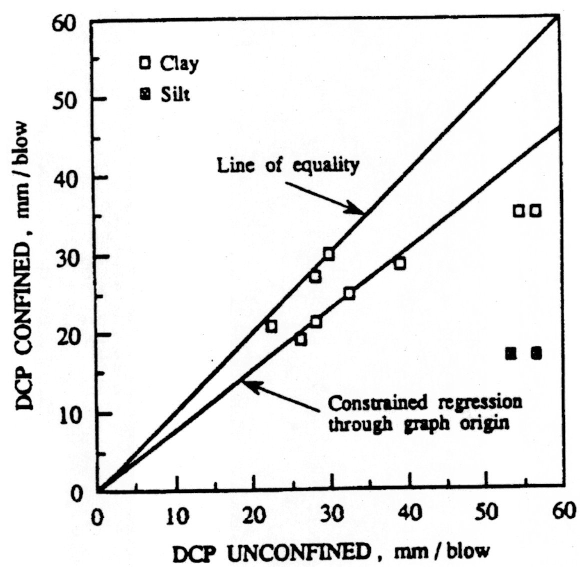

Figure 2.4 DCP Test Results for Subgrade Beneath Granular Structure (Livneh et al c.1993)

The vertical confining effect on clay subgrade was determined by penetrating the DCP from the surface to a depth of at least 500 mm at 27 locations, then excavating to a depth of 500 mm at each location and again penetrating the DCP into the exposed clay.

Figure 2.5 shows the results of this work. The confined DCP data yielded PR from 500 to 700 mm below the surface, while the unconfined DCP data yielded PR from 0 to 200 mm below the exposed surface of the 500 mm deep test pit excavations. The statistical analysis showed that there was no difference between the confined and unconfined PR for clay subgrade with a clay soil providing the vertical confinement (Livneh et al c. 1993).

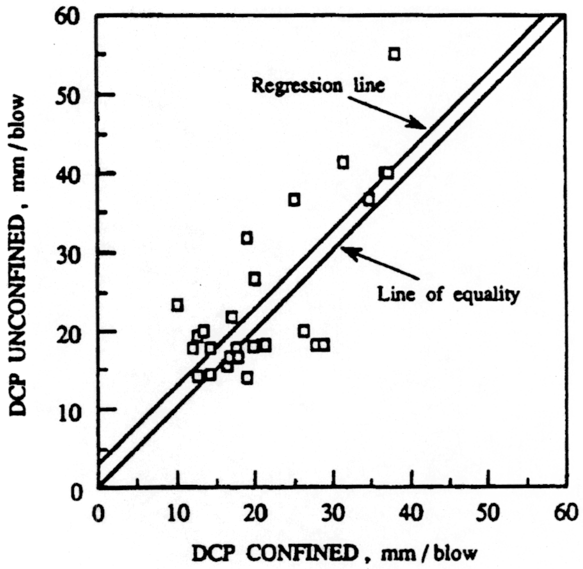

Figure 2.5 Correlation Between Confined and Unconfined DCP Within Clay Subgrades (Livneh, et al c. 1987)

To determine the vertical confining effect of an asphalt pavement on the predicted CBR values, the clay subgrade soil was penetrated with the DCP. The CBR value predicted by the DCP was then compared with the actual CBR measurement made in-situ through the cored asphalt pavement. Figure 2.6 shows that the CBR values predicted were 75 percent higher than the measured CBR values. To determine if the 75 percent increase was caused by the vertical confinement of the asphalt pavement on the clay subgrade or if the difference could be attributed to friction of the DCP against the asphalt layer from accidental tilting of the DCP, a series of laboratory tests were performed. CBR tests were performed with and without a confining plate on the clay subgrade soil compacted in a standard 150 mm (6 in) mold.

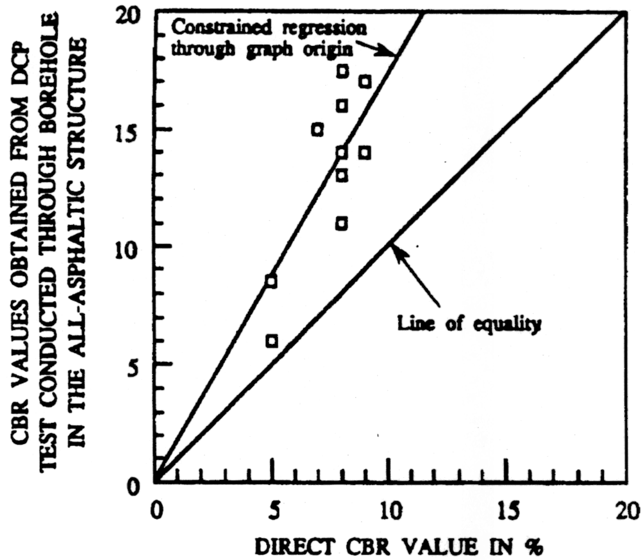

Figure 2.6 CBR Results from Clay Subgrade Beneath 500 Mm (20 in) Thick Asphalt Structure (Livenh et al, 1993)

The results indicate that vertical confinement of the clay subgrade did not cause the 75 percent strength difference. The authors concluded that this difference was likely caused by friction between the DCP rod and the asphalt layer during penetration, thereby decreasing the PR and predicting a higher CBR value.

The effect of vertical confinement on a granular layer from the overlying asphalt pavement layer was tested by coring a small diameter hole through the asphalt pavement, penetrating the granular layer with the DCP, then removing a wide strip of pavement and penetrating the same exposed granular layer with the DCP. The results are shown in Figure 2.7. Livneh et al (c. 1993) found that the confined granular layer had an 84 percent lower PR than the unconfined. This is the expected result for a granular ($\phi > 0$)

material. Because the true state of the granular layer during service includes the vertical confinement of the asphalt pavement, M. Livneh, Ilan, and N. Livneh recommend evaluating the quality of the ABC using the DCP through a small diameter core to maintain the vertical confinement of the asphalt pavement.

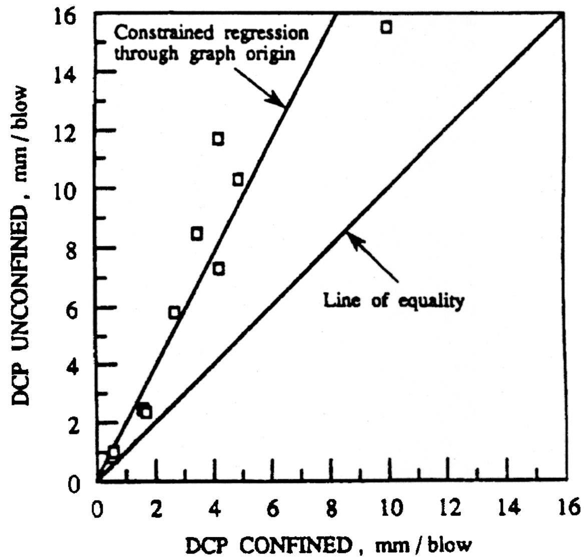

Figure 2.7 Effects of Asphalt Confinement on DCP Values in Granular material (Livneh et al c. 1993)

2.5 Effects of Lateral Confinement

Kleyn (1975) conducted a study to investigate several scenarios affected the readings of the DCP. One of the scenarios included performing the DCP in a 150 mm (6 inch) mold and comparing the results to those obtained in 200 mm and 250 mm diameter molds. The soils tested included fine and granular materials. Kleyn concluded that DCP laboratory readings from 150 mm (6 inch) mold must be corrected by means of a log-log linear plot in order for the laboratory readings to correspond with field values. The confining effect on PR was negligible between the 200 mm (8 in) and 250 mm (10 in) molds. Kleyn also concluded that the confining effect was proportional to the quality of the material with higher correction factor as the shear strength of the material is increased.

Based on Kleyn's data, an average correction factor of 1.2 needs to be applied to the PR reading from the 150 mm mold in order to obtain the reading form the 250 mm mold (or what can be defined the PR value to be obtained in the field.)

Harison (1987) used a confining correction factor to adjust his laboratory-based DCP-CBR correlation. Harison recommended decreasing the CBR values computed from laboratory-developed relationship by a factor of 0.7 in order to account for the confinement effect and obtain field-comparable CBR values. The equation used by Harison to represent the CBR-PR relationship with accounting for the confining effect was:

$$\text{Log}(CBR(1 + A)) = 2.70 - 1.12\text{Log}(PR). \quad \text{Where } A = 0.43 \qquad (2)$$

2.6 Other Factors Affecting Laboratory Correlation

In addition to mold diameter, Kleyn (1975) considered mold height and unit weight gradient as possible influences on a laboratory DCP – CBR based correlation. Kleyn (1975) examined mold height by bolting two molds together and then comparing the PR of the upper half of the bolted double high mold with the PR from the full depth of a single mold. Kleyn found that mold height did not affect PR. However, Kleyn observed that unit weight gradient influenced PR.

The bottom layer of a dynamically compacted laboratory specimen had a higher unit weight than subsequent layers, forming a unit weight gradient. The CBR was performed on the bottom of the inverted specimen and then correlated with the average PR of the full depth of the specimen. Kleyn compared the PR from the bottom layer (30 mm) to the average PR for the full depth. Kleyn alternated penetrating the specimen from the top and bottom to ensure that any difference measured in the bottom layer would not be due to friction. Kleyn found that the PR in the bottom layer was 10 to 25 percent lower (stronger) than the PR obtained from the full depth with the difference being proportional to the quality of the material.

3.0 MATERIALS AND METHODS

Laboratory and field testing programs were performed on aggregate base course (ABC) and subgrade materials from sites in Davidson County, North Carolina (NC). The laboratory program included performing series of tests under conditions representative of a range of compactive efforts. These tests were conducted in accordance with methods described in the American Association of State Highway and Transportation Officials (AASHTO) manual. Table 3.1 summarizes test designations used in the laboratory experimental program. Physical properties tests included sieve analysis by washing (T 11), determination of the liquid limit (T 89-96), and determination of the plastic limit and plasticity index (T 90-96). In addition to the tests shown in Table 3.1, the laboratory-prepared specimens were also penetrated with the DCP device with the PR measured for each test specimen. The field experimental program included CBR, DCP, FWD, and nuclear gage tests.

Table 3.1 AASHTO (1992) Standard Specifications Used in Laboratory Testing

AASHTO Designation	Standard Specification
T2	Aggregate Sampling
T27	Sieve Analysis of Fine and Course Aggregates
T87	Dry Preparation of Disturbed Soil and Soil Aggregate Samples for Test
T99	The Moisture-Density Relations of Soils Using a 2.5-kg (5.5-lb) Rammer and a 305-mm (12-in.) Drop
T180	Moisture-Density Relations of Soils Using a 4.54-kg (10-lb) Rammer and a 457-mm (18in.) Drop
T193	The California Bearing Ratio
T255	Total Moisture Content of Aggregate by Drying

3.1 Subgrade Soil

Three fine-grained Piedmont residual soils were chosen for this laboratory testing program and were obtained from sites in Davidson County, NC. Figure 3.1 shows the grain size distribution of the test soils.

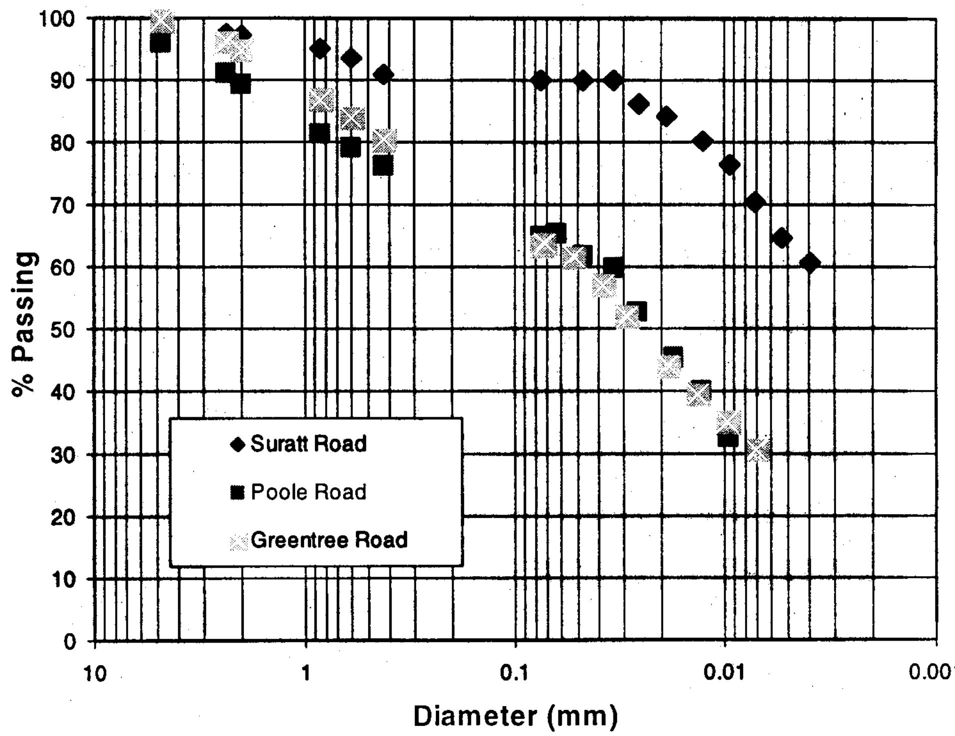

Figure 3.1 Grain Size Distribution of the Test Soils

The Piedmont region of North Carolina from which soil samples were retrieved lies between the Blue Ridge mountains and the Coastal Plain region. The test soils were clay of residual origin. These soil samples were taken from sites that will be referred to as Surratt Road, Poole Road, and Greentree Road. The residual clay at the three test sites was formed by the chemical weathering of the in-place rock, leaving behind a soil with similar structure to that of the parent material. The Poole Road and Greentree Road test sites are 5 km (3 mi.) apart. Both lie on the border between the Charlotte Belt and the Carolina Slate Belt geologic regions. Surratt Rd site is on the southern end of Davidson

County, 35 km (21 mi.) south of Surratt and Greentree Roads. Surratt Road lies in the Carolina Slate Belt, which is characterized by deformed volcanic and sedimentary rocks.

3.1.1 Specimens Preparation

In order to prepare test specimens for compaction, CBR, and DCP testing, the soil samples were air dried to moisture content below that of the desired moisture content. The moisture content was then determined for the air-dried soil. Water was then added to bring the soil to the desired moisture content and the soil was mixed thoroughly until a uniform color was achieved indicating uniform distribution of the moisture within the sample.

Soil specimens were then compacted in the 150 mm (6 in) mold using an automatic compaction hammer. Tests performed for comparison of size effect (150 mm versus 250 mm diameter molds) were manually compacted with a Proctor hammer because the 250 mm (10 in) diameter mold could not be placed in the automatic compaction hammer frame. After compaction, the top of each specimen was carefully trimmed and the CBR test was performed before inverting the specimens and the DCP test was performed. The first blow and the penetration of the first blow were not used in determining the penetration rate (PR).

The test soils were classified per AASHTO M 145-91. Table 3.2 shows a summary of the results of physical properties tests and the associated soil classification. Specimens from Poole and Greentree sites yielded relatively similar values of liquid limit (33% and 30%, respectively) and PI of 13% and 12%. These two soils were classified as A-6 (CL). On the other hand, the soil from Surratt road site exhibited a more plastic behavior and was classified as A-7-6 (CH) with a liquid limit of 55% and PI of 27%.

Table 3.2 Summary of soil classification

Soil Sample	Liquid Limit (%)	Plastic Limit (%)	Plasticity Index (%)	Percent Finer 0.075mm	Classification	
					AASHTO	ASTM
Surratt Rd	55	28	27	90	A-7-6	CH
Poole Rd	33	20	13	65	A-6	CL
Greentree Rd	30	18	12	63	A-6	CL

3.1.2 Laboratory Testing Procedure

Four series of tests were performed to determine the dependence of the DCP – CBR relationship on four different parameters. Table 3.3 shows a summary of the material tested, the independent variable, and the dependent variable examined for each test series.

Table 3.3 Summary of Test Series on Subgrade Soils

Test Series	Material Tested	Independent Variable	Dependent Variables
1	Surratt Rd	moisture content	CBR, DCP
2	Surratt Rd	compaction effort	CBR, DCP
3	Poole Rd	(un)soaked	CBR, DCP
4	Greentree Rd	mold size	CBR, DCP

Specimens in test series 1 through 3 were then compacted in the 150 mm (6 in) mold using the automatic compaction hammer. Specimens in test series four were compacted manually using a standard proctor hammer (T-99). The 250 mm (10 in) diameter mold could not be placed in the automatic compaction hammer, therefore, both the 150 mm (6 in) and 250 mm (10 in) diameter molds were manually compacted. After the specimens were prepared, they were penetrated to a depth of 7.62 mm (0.3 in) with the CBR piston. The CBR test was performed per AASHTO T-193. The specimen was then removed from the load frame, inverted, and placed on the concrete floor and the DCP test was run. The 44 N (10 lb.) surcharge weight used in the CBR test was also placed on the specimen during DCP penetration. A zero tick mark was made prior to penetrating the DCP probe. A tick was then marked after each blow of the hammer. The PR in the 150 mm (6 in) mold specimen was the average penetration rate after the first blow to the bottom of the 116 mm (4.58 in) specimen. The first blow and the penetration of the first blow were not used in determining the PR. The PR in the 250 mm (10 in) diameter mold was determined from the PR in the top 200 mm (4 in), not counting the first blow.

3.2 ABC Material

The materials tested were aggregate base course (ABC) samples obtained from two different rock quarries. One ABC sample was obtained from the Martin Marietta rock quarry located in Thomasville, NC, while the other sample came from Vulcan Materials located in Gold Hill, NC. The Gold Hill material was more angular and linear with a slatey cleavage, while the Thomasville material was more rounded with a uniform diameter. Figure 3.2 shows a plot of the grain size distribution of the two materials in their virgin states as well as the grain size distribution for both materials as tested in the lab. The virgin state was the state of the material as it sits in the rock quarry.

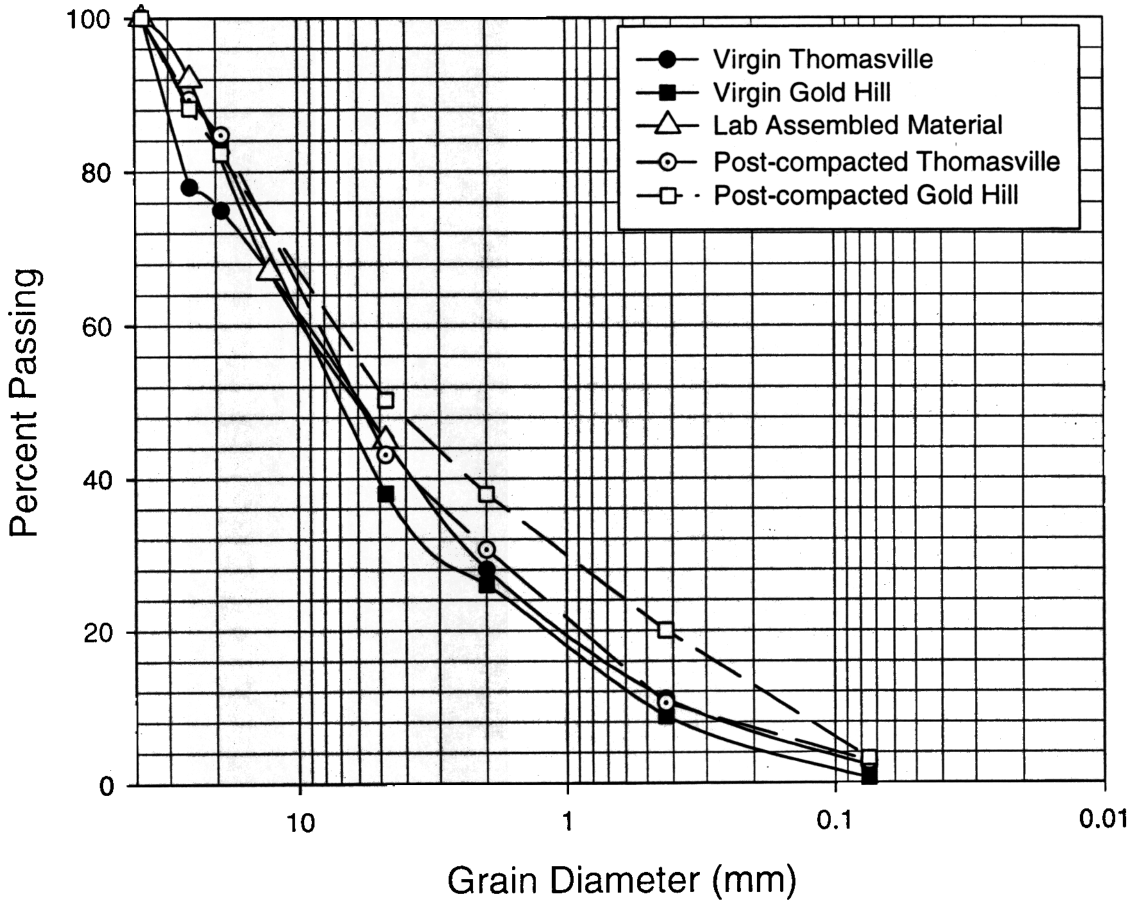

Figure 3.2 Grain Size Distribution for Virgin and Lab Assembled Materials

The materials represented in this Figure 3.2 were properly extracted from the quarry following AASHTO T2 specifications. The ABC material was dumped by a front-end loader and then leveled. Afterwards, ten spaced-out specimens were hand-shoveled from the leveled dump into ten separate canvas bags. Each grain size plot represents the content of one canvas bag.

3.2.1 Specimen Preparation

The lab-assembled state was the same for both ABC materials. Each aggregate base course was assembled to meet specific percentages of certain grain sizes; therefore, both aggregates have the same distribution. Notice that the lab-assembled distribution is defined only for grains sized 4.75 mm (number 4) and larger. This is because specifications only apply to 1 inch, ½ inch and the number 4 sieve sized grains. As shown in Figure 3.2, approximately 42 percent of the material was smaller than the No. 4 sieve and therefore was not subject to specification assembly. The coefficient of uniformity of the virgin material from the two quarries was estimated equal to 25 and the coefficient of curvature was approximately equal to 0.75.

The data plotted Figure 3.2 also include the grain size distribution for the two testing materials after the testing procedure has been completed. Comparing the before and after compaction distributions indicated no significant changes in the grain sizes were induced by compaction and handling for the Thomasville material, as shown in Figure 3.2. On the other hand, the Gold Hill material seems to have slightly broken down due compaction which resulted in a finer material distribution, especially for grain sizes smaller than 10 mm. The post compaction coefficient of uniformity of the Gold Hill material was estimated equal to 85 and the coefficient of curvature was approximately equal to 0.85.

3.3 Laboratory Test Equipment

Laboratory equipment included an automatic compaction hammer, two different sized molds, the Scala DCP, and a load frame for CBR. Laboratory testing was performed at the North Carolina Department of Transportation Materials and Tests Unit in Raleigh, NC.

The automatic compaction hammer is a Mechanical Compactor M100-2 with a solid state counter and a hammer weight of 41 kg. Figure 3.3 is a photograph of the compaction hammer used to compact the specimen in this program. Two molds were used to prepare laboratory specimen in this program. The smaller mold, 150 mm (6 in) in diameter was a standard CBR mold as designated by AASHTO T 193-93, *Standard Specification for the California Bearing Ratio*. The larger mold was 250 mm (10 in) in diameter and 253 mm (10.1 in) in height. Figure 3.4 is a photo of the two molds used. The larger, 250 mm (10 in) diameter mold is shown with a 12 in (305 mm) ruler.

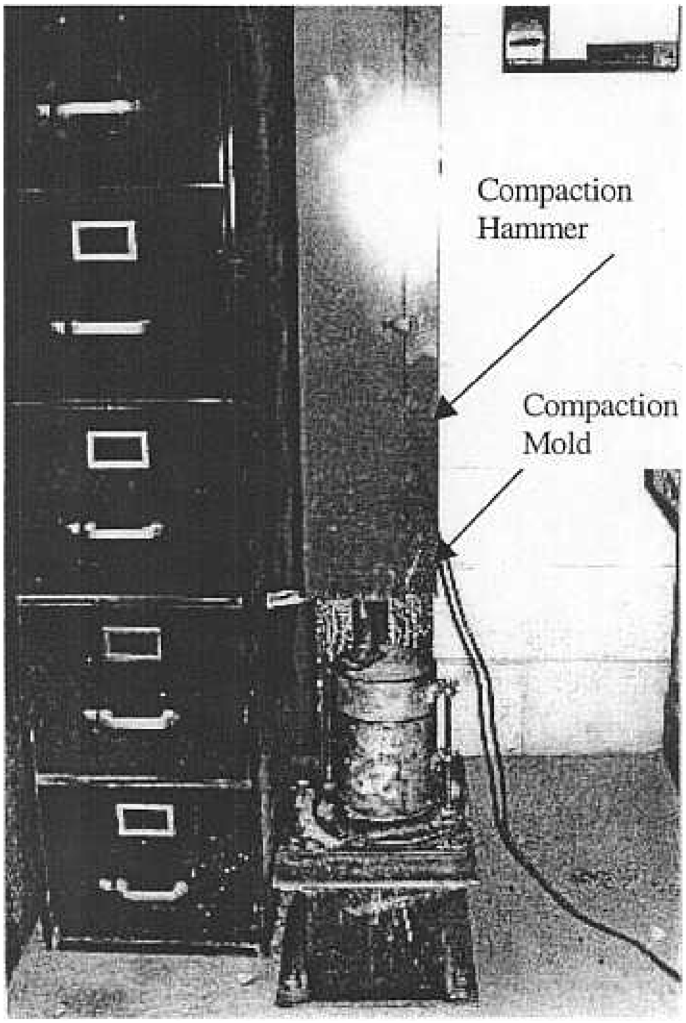

Figure 3.3 Automatic compaction hammer

The Scala DCP was shown in Figure 2.1 and consists of an 8 kg (17.6 lb.) sliding doughnut weight falling 575 mm (22.6 in). The conical tip is 20 mm (0.79 in) in diameter and angled at 30° from vertical. The lower rod, the penetrating portion with the conical tip, is 16 mm (0.63 in) in diameter and 800 mm (31.5 in) in length. Figure 3.5 is a photograph of a penetrated specimen cut in half to show the cross-section. (The rod remains straight during penetration. The specimen was slightly distorted when cut in half.)

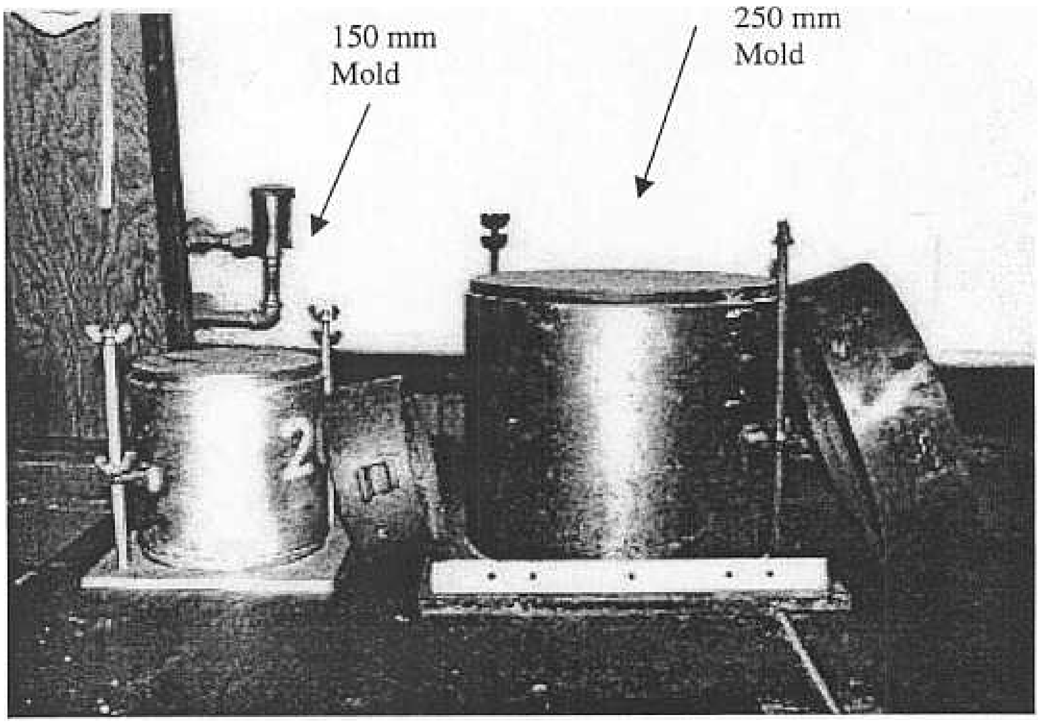

Figure 3.4 Molds used to prepare specimen

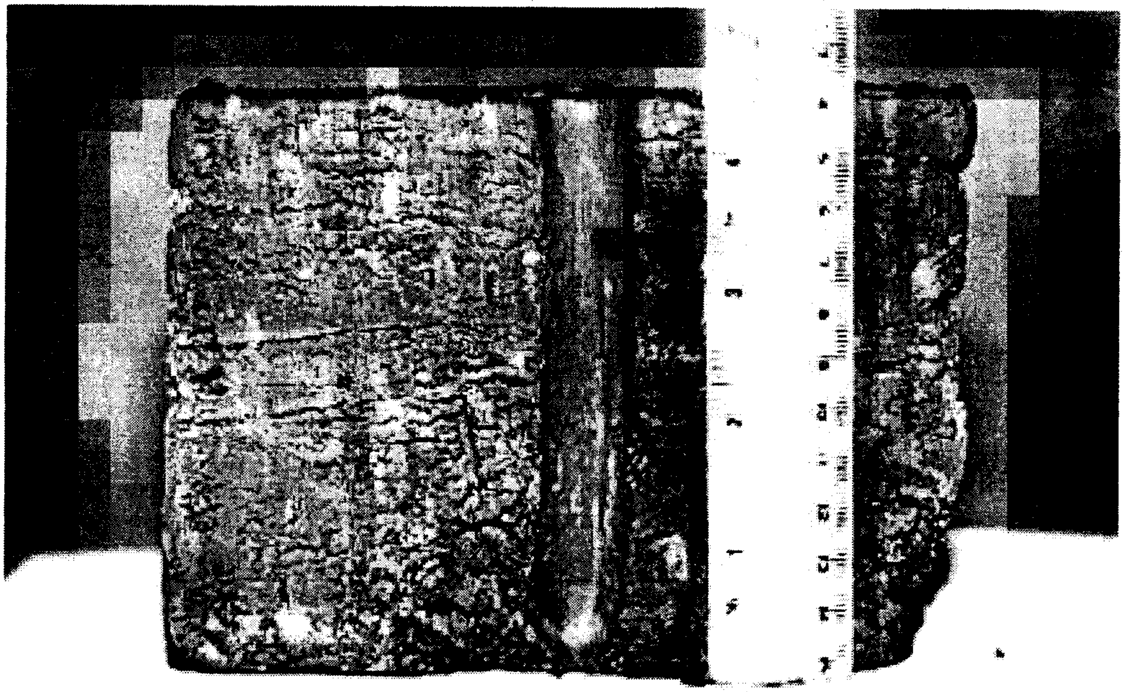

Figure 3.5 Specimen penetrated by Scala DCP

The loading frame used for CBR testing was an HM2000 Master Loader Compression Tester manufactured by Humboldt. The frame was bench mounted with a 5 ton capacity. Figure 3.6 is a photograph of a CBR specimen in the load frame. The load was measure with an H-1339PR 44.48 kN (10,000 lb.) proving ring. The deflection was measured with a linearly variable differential transducer (LVDT). A data acquisition device was used to collect the load and deflection readings every 6 seconds or 0.127 mm (0.005 in) of deflection at the CBR loading rate of 1.27 mm (0.05 in) per minute.

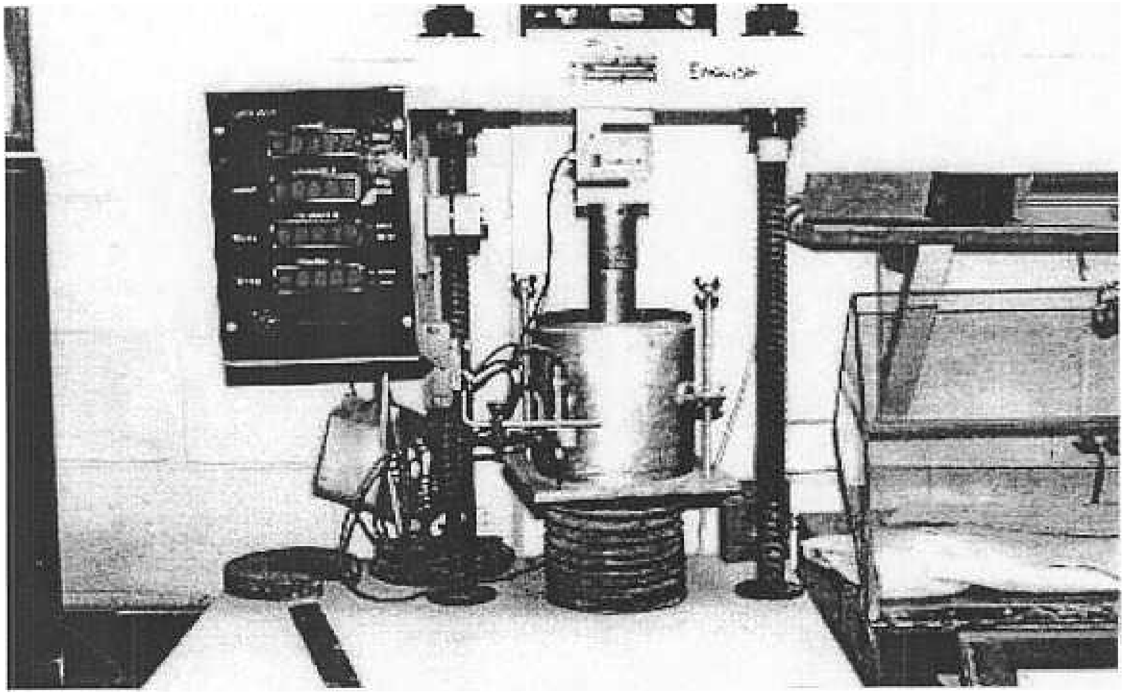

Figure 3.6 Load frame with CBR specimen

3.4 Field Testing Equipment

Field testing equipment included the nuclear moisture/density gage, DCP, FWD, and CBR loading truck. The field testing equipment was provided by the North Carolina Department of Transportation. Figure 3.7 shows a photograph of the DCP being driven continuously through the bituminous asphalt pavement (BST) and into the ABC and subgrade layers.

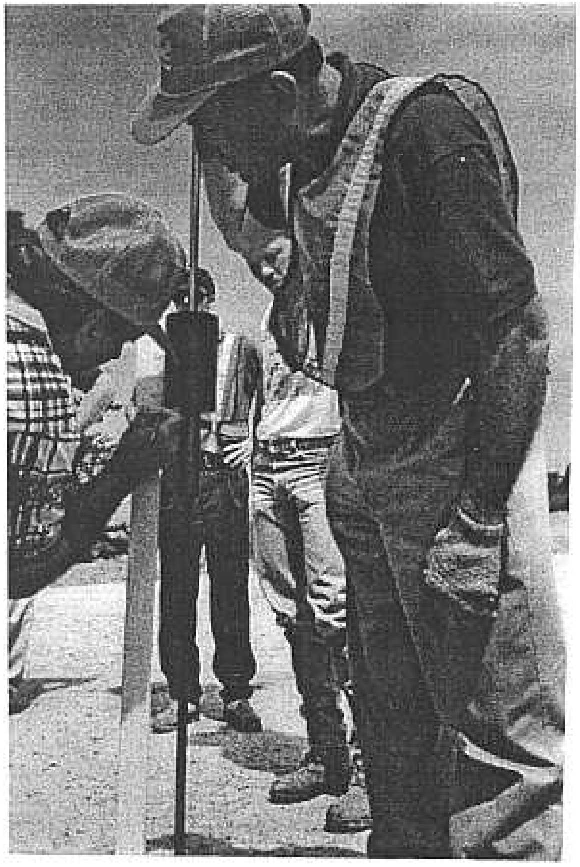

Figure 3.7 DCP Performed at One of the Test Sites

The FWD is a nondestructive testing device used to determine modulus of the various pavement layers. An impact loading was generated by dropping a weight from a height on a round rubber plate that impacts the pavement. The deflection was measured using seismometers measuring deflections from 0 to 5080 microns (0 to 200 mils). The deflection sensors were located at 0, 200 mm (8 in), 300 mm (12 in), 450 mm (18 in), 600 mm (24 in), 900 mm (36 in), 1200 mm (48 in), 1500 mm (60 in), and 1800 mm (72 in) beyond the point of impact. The model used in this testing was Kuab 2m. This deflection curve (bowl) data can be processed in combination with layer thickness information in order to calculate the resilient modulus for each layer of the pavement structure.

The CBR truck was a single axle dual wheeled Ford truck. The truck was weighted in the rear with a large capacity water tank. The truck had a hydraulic jack in the front and two hydraulic jacks in the rear to level the truck and provide stability during testing. The in-situ CBR was performed using a 44.5 kN (10,000 lb.) proving ring to measure load and LVDT to measure deflection. The truck was fitted with a data acquisition system to collect the CBR data. A variable-speed hydraulic pump drove the CBR piston at the specified penetration rate, 1.27 mm (0.05 in) per minute.

4.0 SUBGRADE SOILS AND COMPACTION PROPERITES

The dry unit weight and moisture content were determined for each soil compacted with standard Proctor (T 99) effort. Figure 4.1 shows the moisture – unit weight relationships for the three soils and Table 4.1 summarizes the results. Poole Rd and Greentree Rd were classified as A-6 soils from the same geologic area. The optimum moisture content and dry unit weight for Poole Rd and Greentree Rd are relatively similar as shown in Table 4.1.

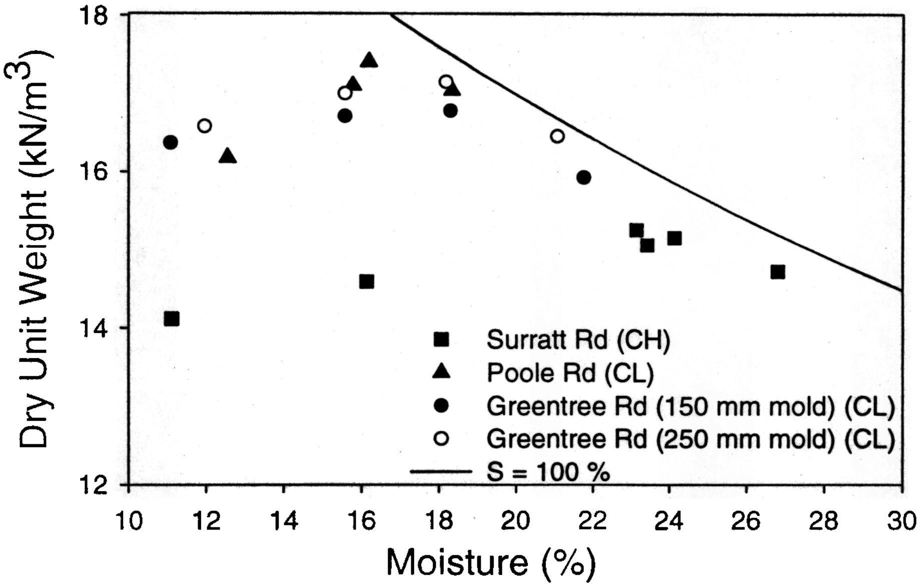

Figure 4.1 T-99 Dry Unit Weight- moisture relationships for the Test Soils

Table 4.1 Summary of Moisture – Unit weight Relationships (T-99)

Soil Sample	Optimum Moisture Content (%)	Dry Unit weight (kN/m^3)
Greentree Rd	18.5	16.8
Poole Rd	17.5	17.5
Surratt Rd	23.5	15.3

The range of the optimum moisture content for the test soils was 17.5% to 23.5% with a maximum dry unit weight of approximately 17.5 to 15.3 kN/m^3. There was no significant effect of the mold size on the moisture-unit weight data as can be seen from results on soil specimens from Greentree road for which some of the tests were performed in 150mm mold and then repeated in the 250 mm mold.

4.1 Moisture and DCP – CBR Relationship

The effect of moisture content on the DCP – CBR Relationship was determined by varying moisture content while holding the compaction effort constant at standard proctor (T –99). Figure 4.2 shows the CBR and PR versus moisture content for Surratt Rd soil. The moisture content of the soil was varied from 11 to 27%. This resulted in CBR values varying from 28% at 11% moisture content to 4% at 27% moisture content. The PR varied from 4 mm/blow at 11% moisture content to 75 mm/blow at 27% moisture content.

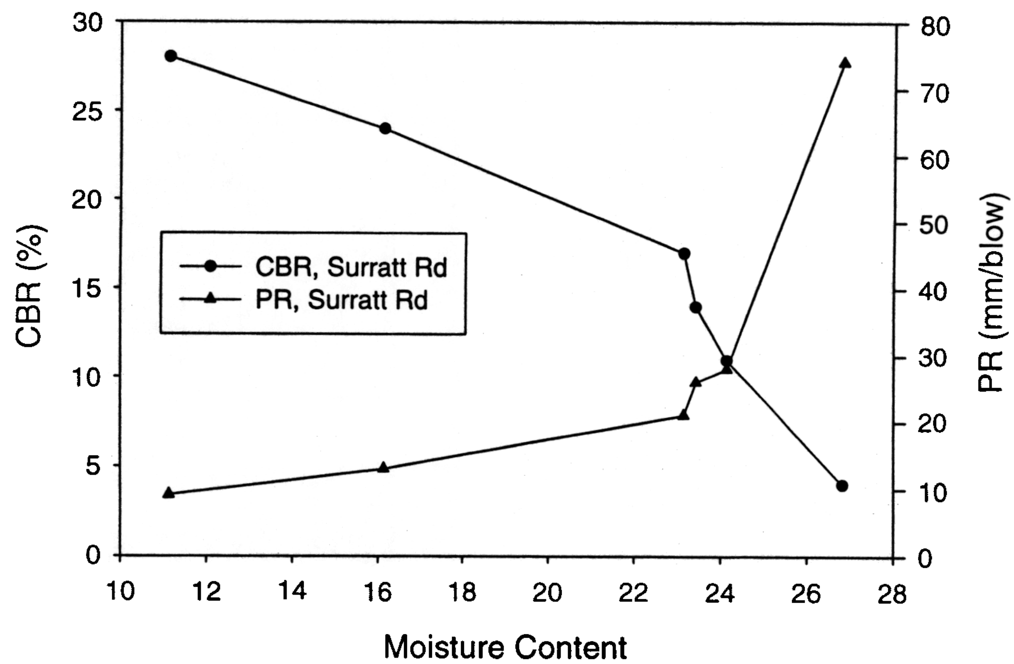

Figure 4.2 CBR and PR versus moisture content - Surratt Rd
(compaction effort held constant at T-99)

The CBR and PR values showed a consistent inverse relationship and reflected the same strength response to changes in moisture content of the test specimens. Since the dry unit weight varied as the moisture content varied, an experiment was performed to determine the dependence of the DCP – CBR relationship upon dry unit weight alone.

4.2 Dry Unit weight and DCP – CBR Relationship

To determine the dependence of the DCP – CBR relationship on dry unit weight, Surratt Rd specimens were formed at varying compaction effort while holding the moisture content constant at the optimum value of 23.5%. Figure 4.3 shows that CBR and PR reacted to changes in percent compaction (percentage of the maximum dry unit weight based upon standard proctor effort T-99) in an inverse manner. The CBR varied from 4% at 83% compaction to 10.5 % at 100 % compaction.

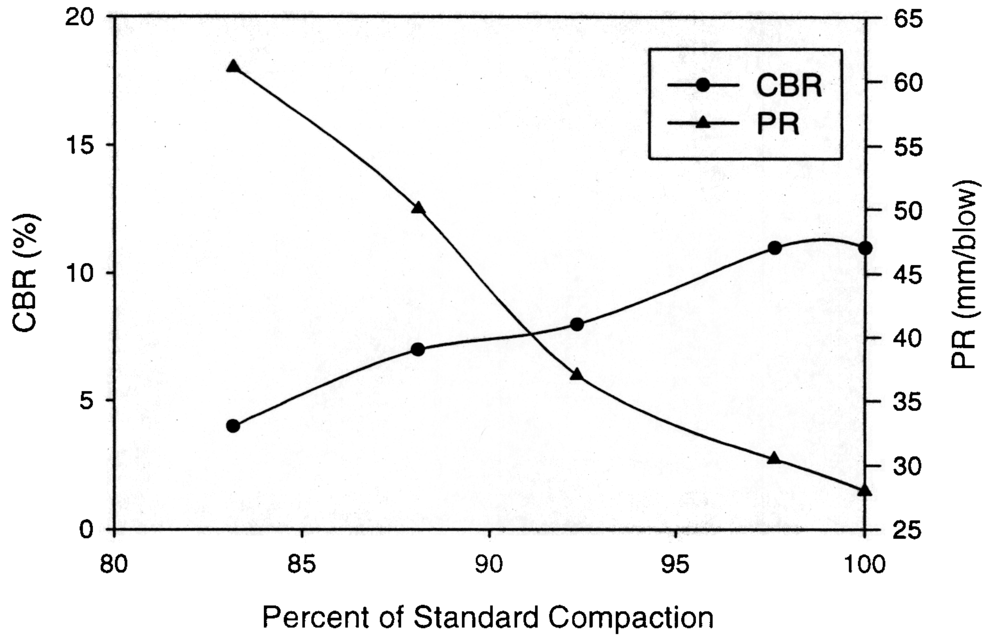

Figure 4.3 CBR and PR versus percent compaction - Surratt Rd
(moisture content held constant at optimum)

The PR varied from 18 mm/blow at 83 % compaction to 3 mm/blow at 100 % compaction. The percent compaction was chosen as the independent variable rater than dry unit weight to give a more general presentation of the behavior of CBR and PR with respect to varying dry unit weight. Although CBR and PR responded to changes in percent compaction in an inverse manner, each reflected a strength trend that was similar in response to changes in percent compaction.

4.3 Soaking and DCP – CBR Relationship

To determine the dependence of the CBR – DCP relationship on soaking, pairs of specimen were compacted at the same initial moisture content, then one of each of the pairs was soaked for 96 hours. Figure 4.4 shows the results of this set of experiments. Note that the open symbols denote the unsoaked state. The PR data for the unsoaked specimens behaved similar to the PR data for the unsoaked specimens. The unsoaked specimens exhibited the highest CBR and lowest PR in the driest state (this was due to the undrained shear strength caused by negative pore pressure). The unsoaked CBR varied from 14.5% at 12.5% moisture content to 5% at 18.5% moisture content. The soaked CBR ranged from 1% at a moisture content of 12.5% to 5% at 16% moisture content, and then decreased to 4% at 18.5% moisture content.

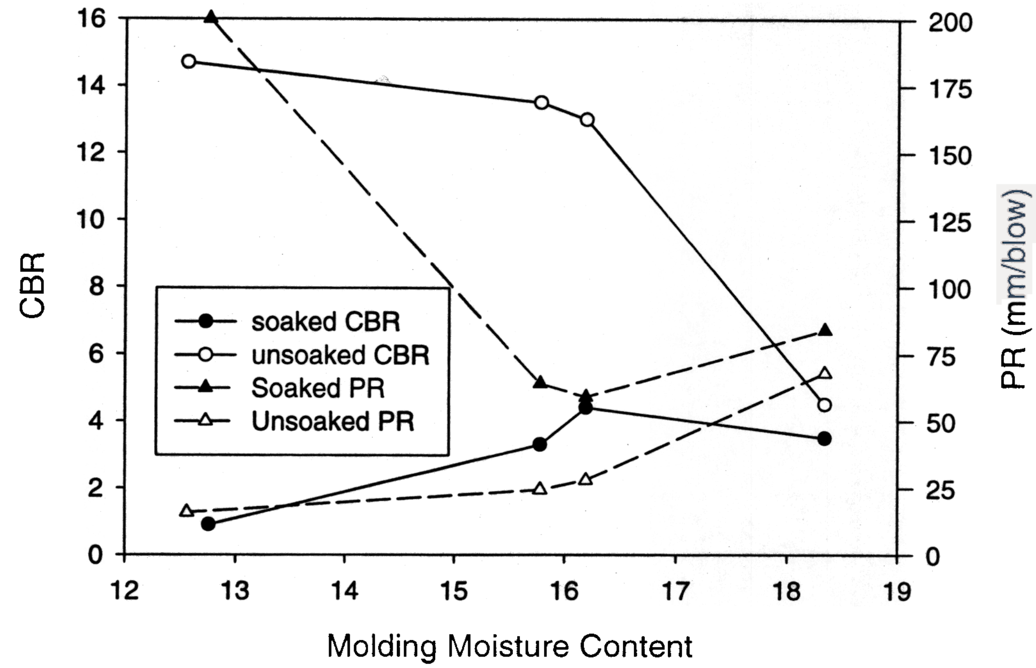

Figure 4.4 CBR and PR versus molding moisture content for soaked and unsoaked specimen - Poole Rd

The unsoaked PR varied from 15 mm/blow at 12.5% moisture content to 70 mm/blow at 18.5% moisture content. The soaked PR ranged from 200 mm/blow at 12.5% moisture content to 60 mm/blow at 16% moisture content, and then up to 85 mm/blow at 18.5 % moisture content. The soaked specimen showed great strength loss due to soaking when dry of optimum with a decreased effect as the molding moisture content neared the optimum moisture value (T-99).

While soaking changed the strength, as measured by the DCP and CBR, the DCP – CBR relationship was relatively independent of moisture changes due to soaking. For example, and referring to Figure 4.4, the CBR values corresponding to PR = 75 mm/blow was approximately 4% for both soaked and unsoaked specimens. Such a conclusion was also reported by Harison (1989) who indicated that soaking had only a slight effect on the

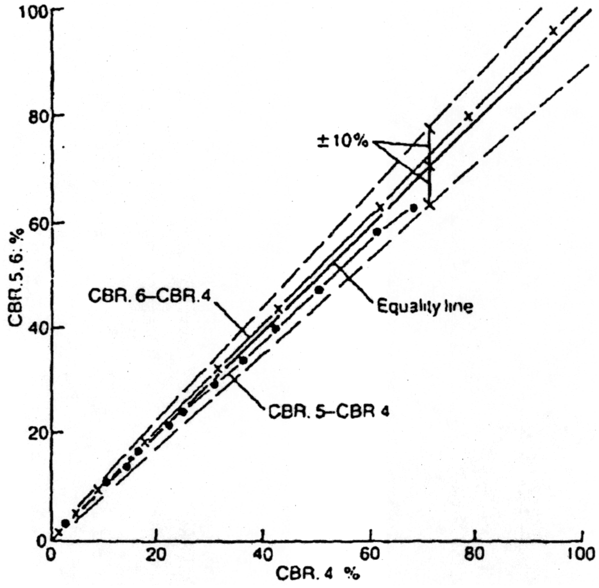

CBR.4 = CBR values from equation of *combined data*.
CBR.5 = CBR values from equation of *soaked samples*.
CBR.6 = CBR values from equation of *unsoaked samples*.

Figure 4.5 Relationship between CBR estimated by correlations based upon soaked and unsoaked specimen (Harison 1989)

DCP–CBR relationship. Figure 4.5 compares CBR values estimated from two DCP – CBR correlations, one developed using soaked specimens and the other using unsoaked specimen, with CBR values estimated from a combined correlation. Figure 4.5 shows that the DCP - CBR correlations derived from soaked and unsoaked specimen do not fall on the unity line when compared with the CBR estimates from the combined correlation. The difference, however, was less than 10 %. Further study may be needed to show with statistical significance that soaking has a slight effect on the DCP – CBR relationship.

4.4 Effect of Mold Diameter

To determine the effect of using 150 mm (6 in) on the data to correlate DCP PR values and CBR, pairs of specimen were compacted into 150 mm (6 in) and 250 mm (10 in) molds. The moisture content of each pair was varied and the compaction effort was held constant at standard proctor (T-99). Figure 4.6 shows that the dry unit weight for the

250 mm mold was slightly higher than the dry unit weight in the 150 mm with an average difference of 2%.

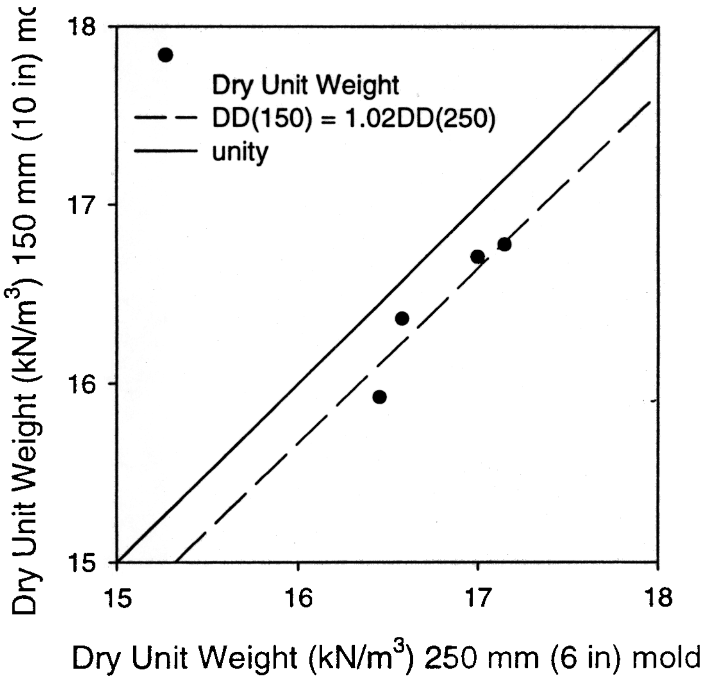

Figure 4.6 Comparison of dry density in 150 mm (6 in) and 250 mm (10 in) molds

The difference in dry unit weight may be due to differences in the ratio of the plunger diameter and the mold diameter causing different confining states within each mold during compaction.

Mold diameter did not appear to significantly affect PR data. Figure 4.7 shows that the 2 data points for the stronger specimen, 10 < PR < 25 mm/blow, were not affected by the mold diameter. The data point from the softer specimen had approximately 20 % decrease in PR values when tested in the 150 mm (6 in) mold as compared to the 250 mm (10 in) mold.

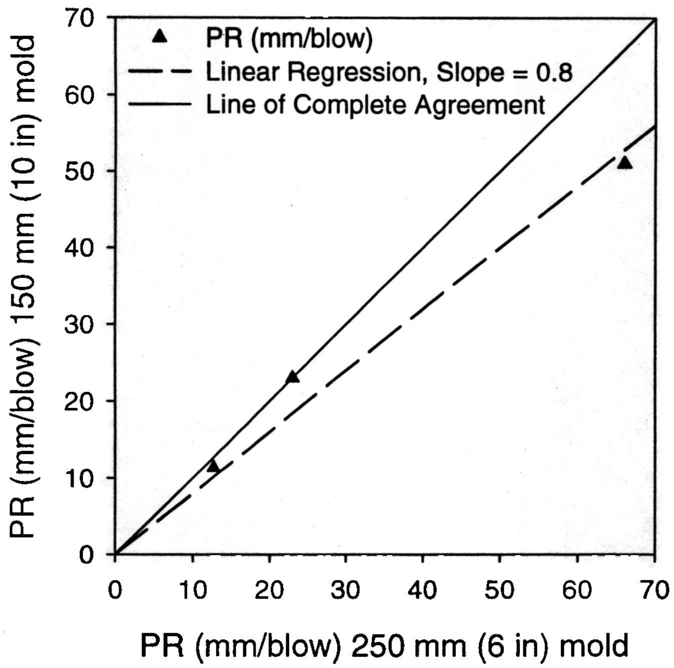

Figure 4.7 Comparison of PR between 150 mm (6 in) mold

In addition, the CBR data showed a greater difference in each mold as shown in Figure 4.8. Approximately 63 % higher CBR values were found in the 150 mm (6 in) mold. The confining effect of the 150 mm (6 in) mold caused the CBR reading to be higher than in the 250 mm (10 in) mold. Figure 4.9 illustrates that the theoretical shear failure surface of a bearing capacity failure produced by penetrating the CBR piston can intersect the sides of a 150 mm (6 in) mold. The confining effect of the 150 mm (6 in) mold caused higher CBR readings in the 150 mm (6 in) mold when compared with the 250 mm (10 in) mold.

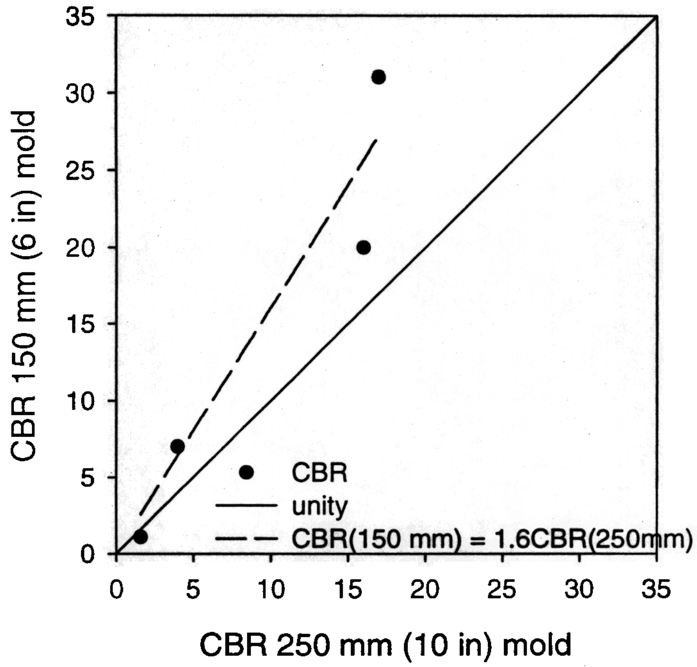

Figure 4.8 Comparison of CBR Between 150 mm (6 in) Mold and 250 mm (10 in) Mold

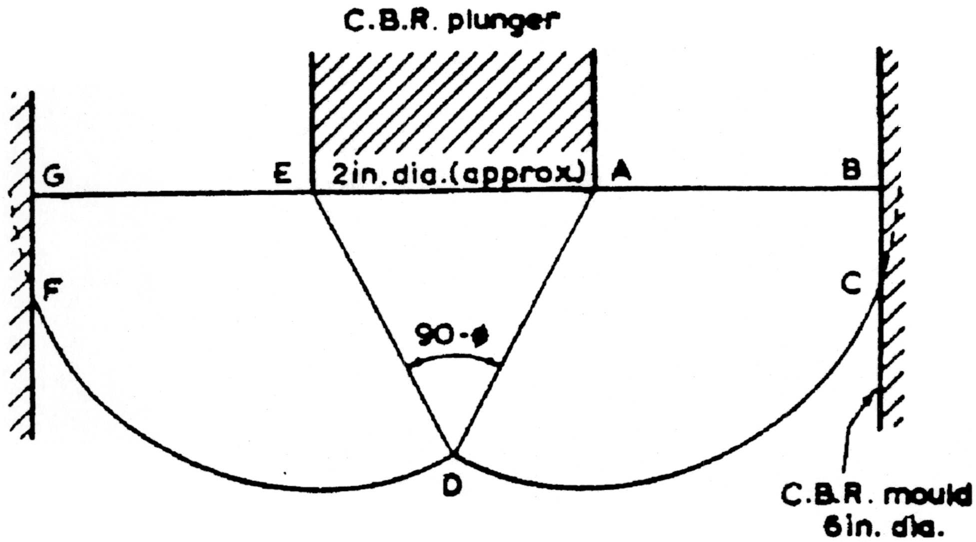

Figure 4.9 Theoretical shear failure surface of bearing capacity failure produced by CBR piston in a 150 mm (6 in) mold (Black 1961)

5.0 SUBGRADE MODELS

5.1 PR-CBR Model

All penetration and CBR laboratory data measured in this study are shown in Figure 5.1 along with predictions from PR – CBR correlations published in literature. The test results from this research appear to lie above the trends obtained from previous correlations. At this point, it is possible that the difference between the measured data and previous correlations can be attributed to the confining effect of the 150 mm (6 in) mold used in this study. Livneh et al (1993) based their correlation on field and lab data and Smith and Pratt based their correlation on field data alone.

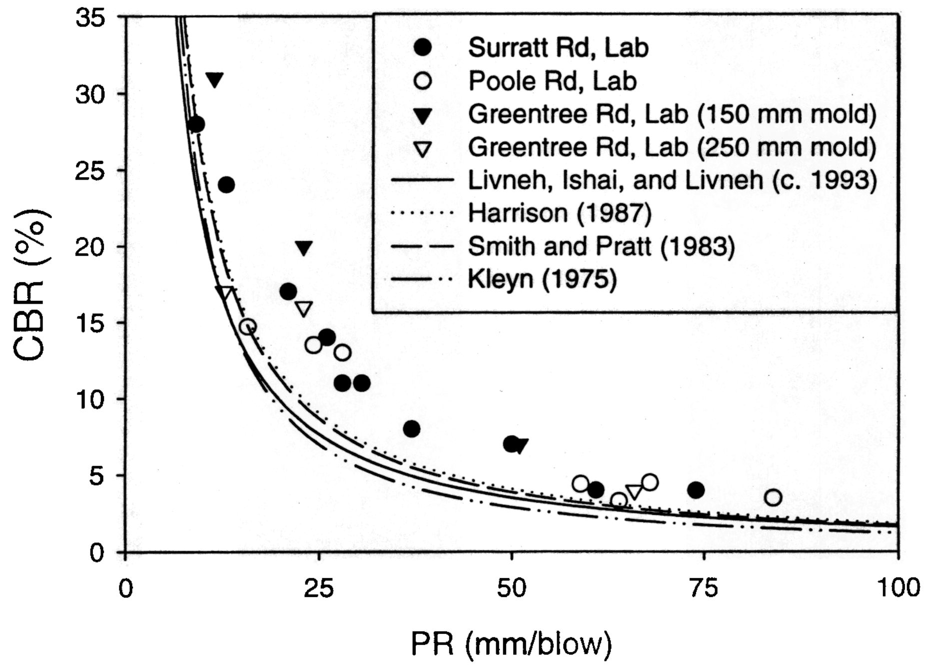

Figure 5.1 CBR - PR laboratory data shown with several correlations

5.2 Laboratory Correlation for Field Use

Figure 5.2 shows a "best-fit" correlation based upon corrected data from the 150 mm (6 in) laboratory specimens as well as uncorrected 250 mm results. To correct the data from the 150 mm (6 in) test specimens for confinement, the CBR values were multiplied by 0.63 (see results from the confinement effect study).

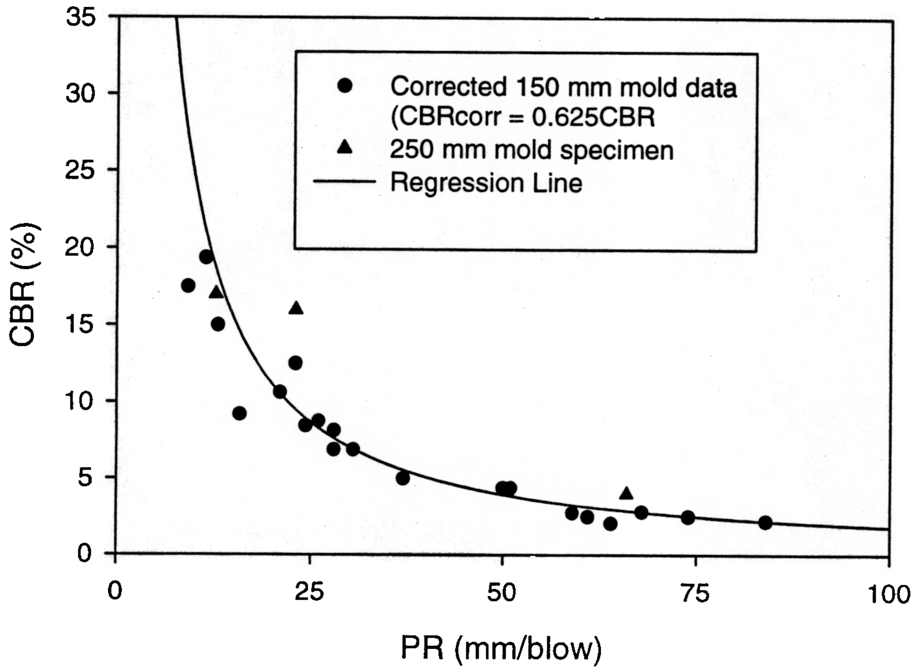

Figure 5.2 Corrected laboratory data with data from the 250 mm (10 in) mold

The 250 mm (10 in) mold data were not corrected for confinement. A log–log regression analysis was performed on all of the data and the most proper log-log equation to fit the data range was developed as:

$$\text{Log(CBR)} = 2.53 - 1.14\ \text{Log(DCP)} \qquad (3)$$

Figure 5.3 shows the fit of equation (3) to the corrected laboratory data in conjunction with other correlations reported in literature. Note that results from equation (3) are nearly identical to Smith and Pratts' model, which was based upon field data.

5.3 PR-Moisture Correlation

Liquidity index (LI) is often used to normalize undrained shear strength for clays (Lambe and Whitman,1969). Figure 5.4 shows the PR values for the three soil types versus liquidity index (LI) as measured in the laboratory. In this case, as LI increased from –0.7 to 0.2,

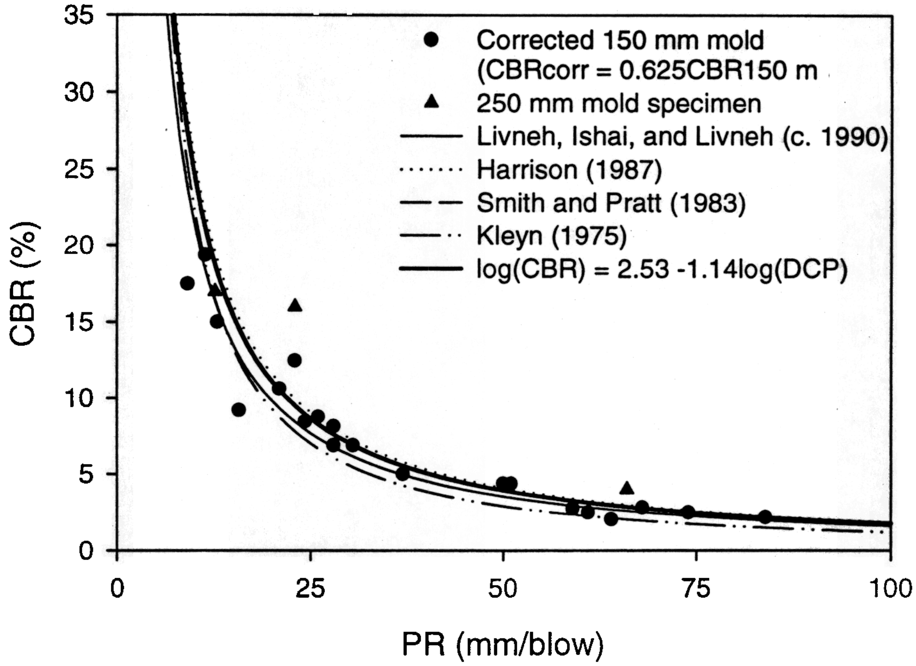

Figure 5.3 Comparison of correlation Results for Piedmont Residual Soil

PR increased from approximately 10 to 200 mm/blow. Based on the data shown in Figure 5.4, the following relationship was developed for determining the LI from the PR data:

$$LI = A \, Log \, PR - B \qquad (4)$$

where LI= Liquidity Index, PR = penetration rate in mm/blow. In this case, the A coefficient is equal to 0.65 and the B coefficient is equal to 1.15. If the PR data measured in the 150 mm mold were modified by a correction factor of .2 in order to account for the boundary effect, the A coefficient remains at 0.65 while the B coefficient is modified to be (B_m) = 1.2. The coefficient of determination R^2 for this relationship is 0.86. Based on estimating the LI from the PR data and knowing the liquid limit and the plastic limit values of the soil, the in-place moisture content (w_{insitu}) can be evaluated as:

$$w_{insitu} = PL + (LI * PI) \qquad (5)$$

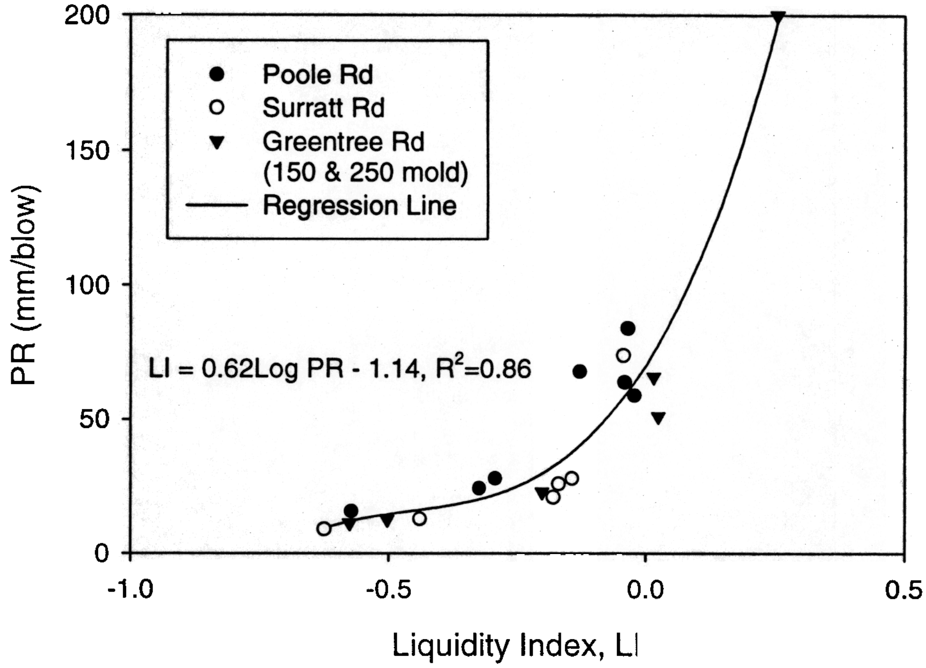

Figure 5.4 PR versus liquidity index

where w_{insitu} = in situ moisture content, PL = plastic limit, LI = liquidity index, and PI= plasticity index. Accordingly, the in situ water content can be evaluated as follows:

$$w_{insitu} = PL + [(A * \text{Log PR} - B_m) * PI] \qquad (6)$$

In the case of the three tested residual soils, A = 0.65 and B_m=1.2.

5.4 PR/Unit Weight Correlation

Data correlating the PR with the unit weight of the compacted soils indicated that the PR values were not sensitive to the variation in the dry unit weight of the test soils. In this case, a direct correlation was not favored. Alternatively, and since in partially saturated cohesive soil negative pore pressure is usually a dominate factor controlling shear strength, percent saturation was used to represent the negative pore pressure state. Figure 5.5 shows the correlation between the PR data and the degree of Saturation (S). The degree of saturation ranged from 35% to 95% in this testing program. The PR values increased with increasing degree of saturation and the correlation was developed as:

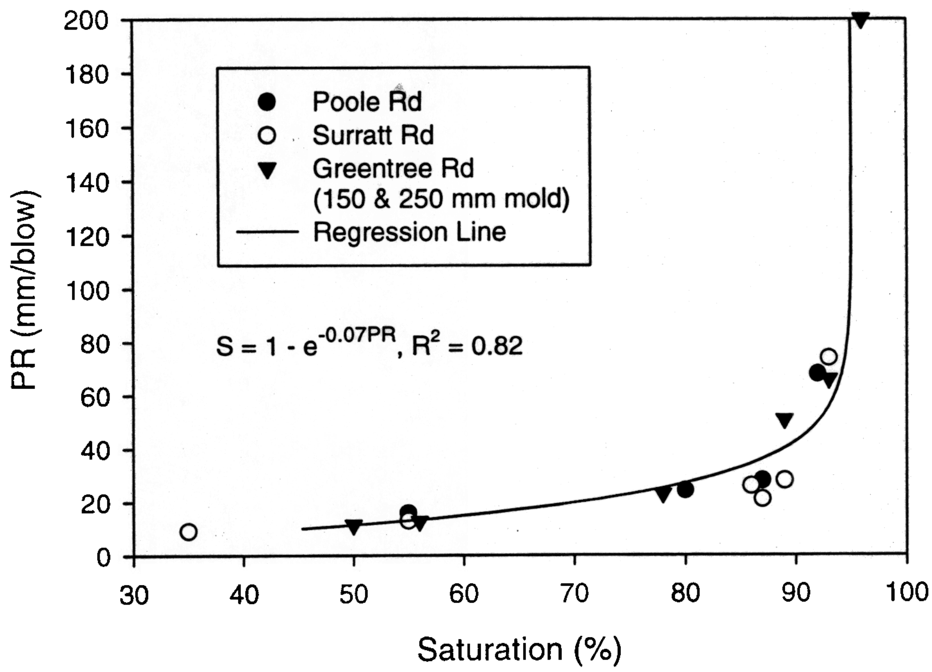

Figure 5.5 PR versus percent saturation

$$S = 1 - e^{(C*PR)} \tag{7}$$

Where S= degree of Saturation in (%). The C coefficient is equal to negative 0.07 (-0.07) for the three test soils used in this study.

If the PR data were modified by a factor of 1.2 to account for the confinement effects as discussed before, the modified C constant (C_m) is determined to be negative "– "0.065. The coefficient of determination R^2 for this relationship is 0.82. Once the degree of saturation (S), and the water content (w) were evaluated, the in situ dry unit weight can be computed as follows:

$$\gamma_{dry} = \frac{\gamma_w * \left[1 - e^{(Cm*PR)}\right]}{w + \dfrac{1 - e^{(Cm*PR)}}{Gs}} \tag{8}$$

Where γ_{dry}= dry unit weight, w = moisture content, S=degree of saturation, and Gs=specific gravity.

5.4 Compaction Control Model Validation

Six tests conducted using the Greentree soil were used to validate the models developed for estimating the moisture and dry unit weight. Three of the tests were conducted in the 150 mm mold and thee were conducted in the 250 mm molds. The boundary effects on the three tests that were conducted on the 250 mm mold can be considered minimal as presented by Kleyn (1975). The results from the three tests conducted in the 150 mm mold were predicted using the A,B, and C coefficients while the results from the three tests in the 250 mm mold were predicted using the A, B_m and C_m coefficients.

Figure 5.6a shows the measured versus predicted moisture contents. The average of the measured moisture contents was 15.1% with a coefficient of variation equal to 0.2 versus an average of 14.9% and a coefficient of variation of 0.14 for all predicted values. Figure 5.6b shows the comparison for the dry unit weights. The average measured dry unit weight was 16.8 kN/m^3 with a coefficient of variation equal to 0.02 versus an average of 17.1 kN/m^3 and a coefficient of variation equal to 0.04 for all predicted values.

These results are perhaps not surprising since the models were applied to one of the soils originally used as a part of the models' development. At the same time, these results illustrated the feasibility of using the DCP device for compaction control applications. However, the models presented in this paper are only applicable in fill situations where the Piedmont residual soils have an appreciable fine content (>60%) are used and were compacted at the T-99 energy level. The model coefficients should be expected to vary with soil type.

At this point of development, the DCP can be used as a secondary tool for compaction control. Normally, a compaction curve is developed in the laboratory for soils to be potentially used as fill material. It is proposed that in conjunction with the "traditionally" performed compaction tests, the DCP test is also performed in the manner described in this study. Accordingly, the A, B_m, and C_m coefficients in equations 4 and 6 can be determined for a specific fill type. In addition, a field calibration procedure should be implemented in which moisture content and dry unit weights are evaluated in the field by alternative means such as the sand cone device. Accordingly, moisture contents and unit weight values based on the DCP data can be adjusted if needed.

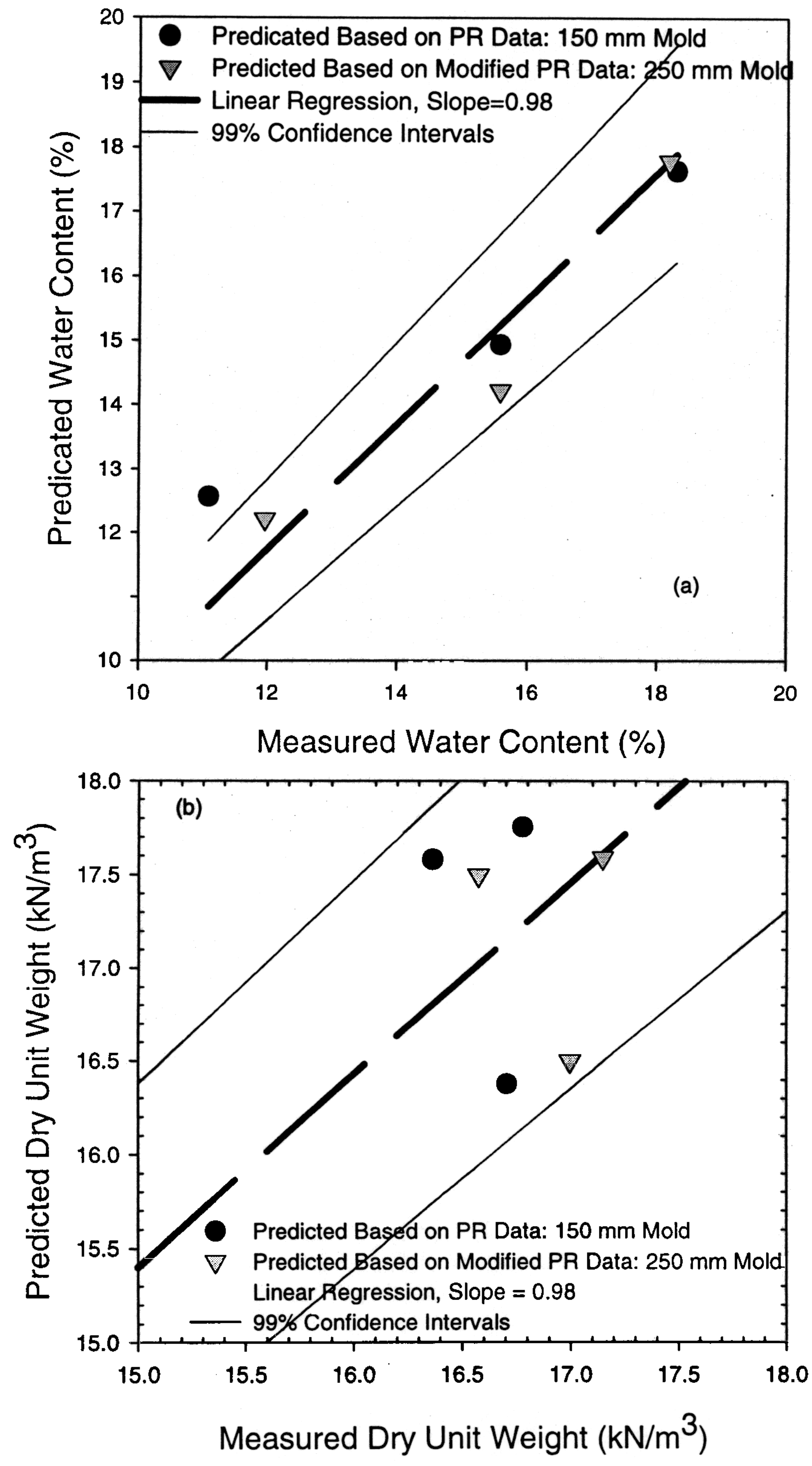

Figure 5.6 Measured Versus Predicted Values: a) Moisture Content, and b) Dry Unit Weight

6.0 ABC PR/CBR PROPERITES

Figure 6.1 shows the moisture-dry unit weight relationships for the two samples of ABC material used in this study; measured under compactive efforts corresponding to both the T99 and T180 specifications. The ABC from Thomasville had γdry increase as the moisture content was increased from 4% to 6.5%. At 4% moisture content, γdry at T99 was 21.5 kN/m^3 versus 22.5 kN/m^3 for T180 compaction effort. At 6% moisture content, γdry at T99 was 22.8 kN/m^3 versus 23.5 kN/m^3 for the T180 compaction effort. In comparison, relatively lower dry unit weights were achieved for the ABC from Gold Hill quarry. As shown in Figure 6.1, γdry at T99 was 20.5 kN/m^3 for ABC from Gold Hill quarry versus 21.5 kN/m^3 for Thomasville ABC and, at T180, was 22 kN/m^3 versus 22.5

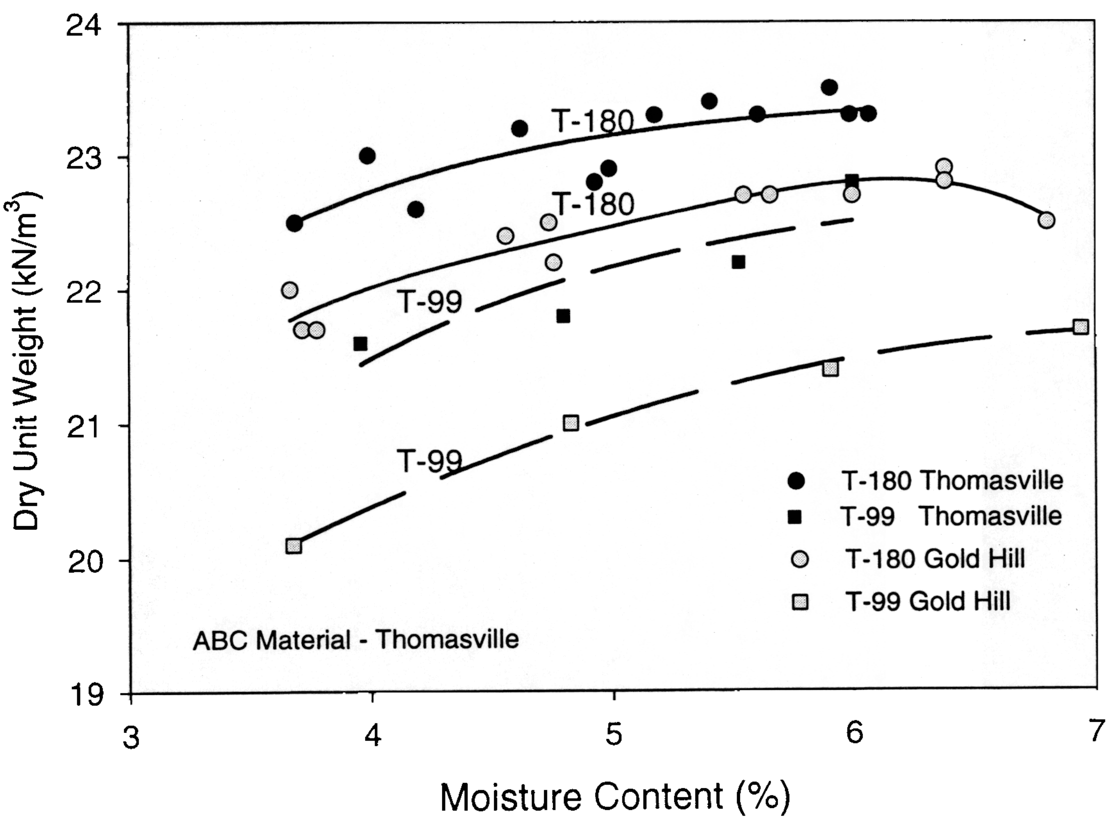

Figure 6.1 Compaction Desnity-Mositure Relationships, Thomasville Quarry, T99 and T180

kN/m^3, respectively. At 6% moisture content, the measured γdry values for the Gold Hill ABC were 21.5 kN/m^3 and 22.8 kN/m^3 for T99 and T180, respectively. These data did not reach maximum γdry for the tested w (%) range.

Figure 6.2 shows the variation of the PR and CBR values, as measured in the laboratory, with the moisture content for both types of ABC materials. A consistent trend of decrease in the CBR value as the PR is increased was observed at both compactive energy levels. In case of Thomasville's ABC material and as the moisture content was increased, the CBR slightly increased and the PR decreased up to moisture content of 5.4%. In the case of T180 data, and as the moisture content was increased from 5.4% to 6%, the PR increased from 3.8mm/blow to 11mm/blow with the CBR decreasing from 130% to 70%. Similar behavior was measured for T99 energy level.

In the case of the Gold Hill ABC material, the CBR values at the T99 energy level were significantly lower (50%-33%) of the values measured at the T180 energy level. As the moisture content increased from 4 % to 6%, the CBR values for the Gold Hill material decreased from approximately 100 to 50% at T 180 energy level and from 40 to 27% at T 99 energy level. The PR value corresponding to CBR of 100% was approximately 4-5 mm/blow while the PR value corresponding to CBR of 40% was approximately 8-9 m/blow.

In comparison to the Thomasville material where material with CBR of 100% yielded a PR value of 7 mm/blow with the lowest achieved CBR value for the range of moisture contents tested being on the order of 90%. It is of interest to note that the CBR values of the Gold Hill material at T99 energy level were on the same order of magnitude as that of sand material and not necessarily aggregate or stone.

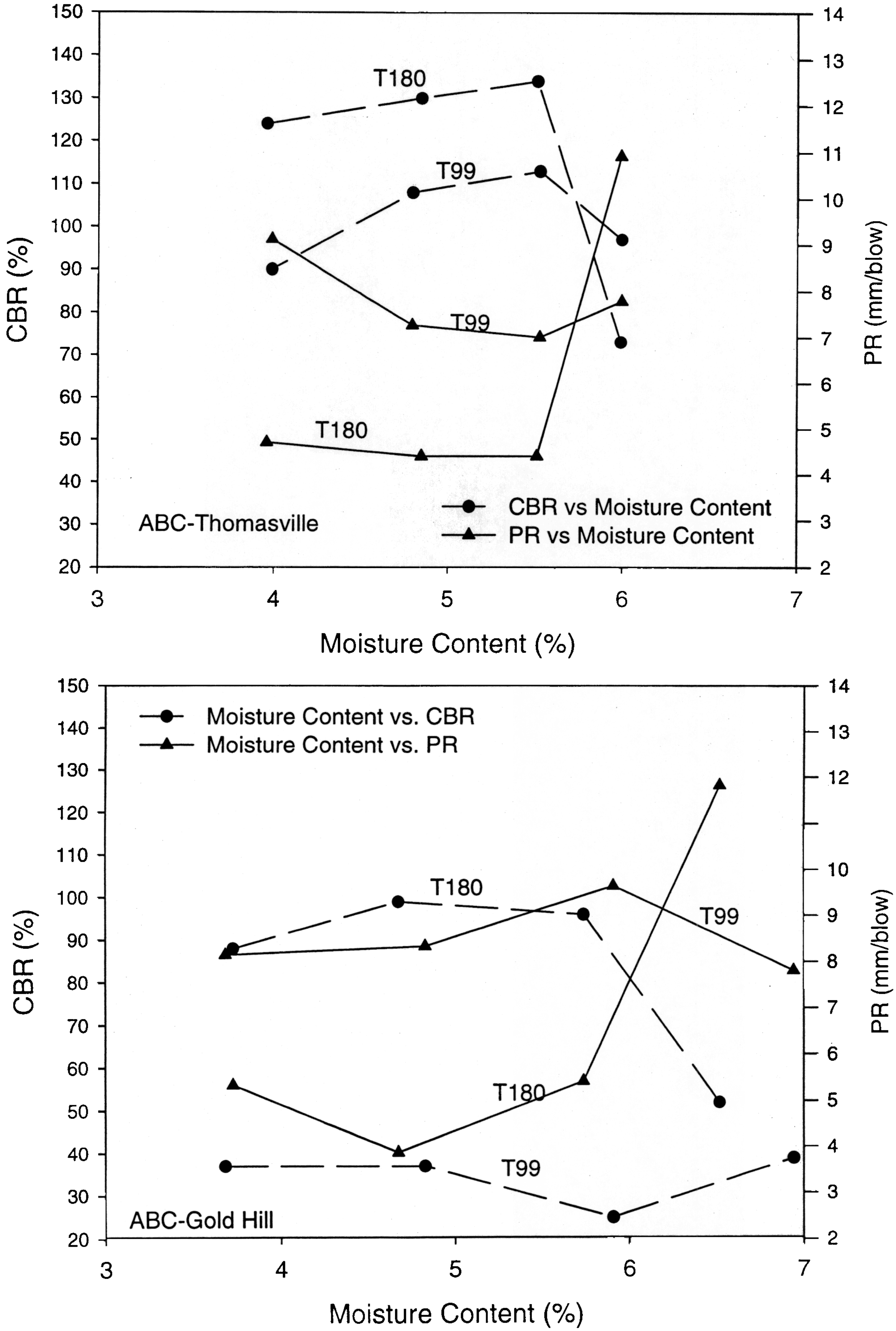

Figure 6.2 CBR and PR vs Moisture Content: a) Thomasville Quarry, and b) Gold Hill Quarry

6.1 CBR/DCP Correlation

Figure 6.3 shows the variation of the CBR of the ABC as a function of the PR (mm/blow) data as measured in the laboratory. The laboratory data included results from both T180 and T99 tests; only the averages of the triplicate tests performed for the T180 energy level are presented on the figure. Performing linear regression on the laboratory data, the following correlation for Thomasville ABC was developed between PR and CBR values:

$$\text{Log (CBR)} = 2.5 - 0.57 \text{ Log (PR, in mm/blow)} \qquad (9)$$

The coefficient of determination R^2 for this relationship is 0.82 and the form used for the equation was the same as previously published in the literature (e.g. Ese, 1995).

Similarly, for the Gold Hill Material

$$\text{Log (CBR)} = 2.7 - 1.14 \text{ Log (PR, in mm/blow)} \qquad (10)$$

At this point, it customary to apply a correction factors in order to adjust the laboratory-developed correlation to match the field data. A reduction factor of 30% was applied to the CBR values predicted from the laboratory-developed correlation as was recommended by Harison (1987). However, since both laboratory and field CBR data were obtained in this study, the correction of equations 9 and 10 will be introduced along with the field data in the next chapter.

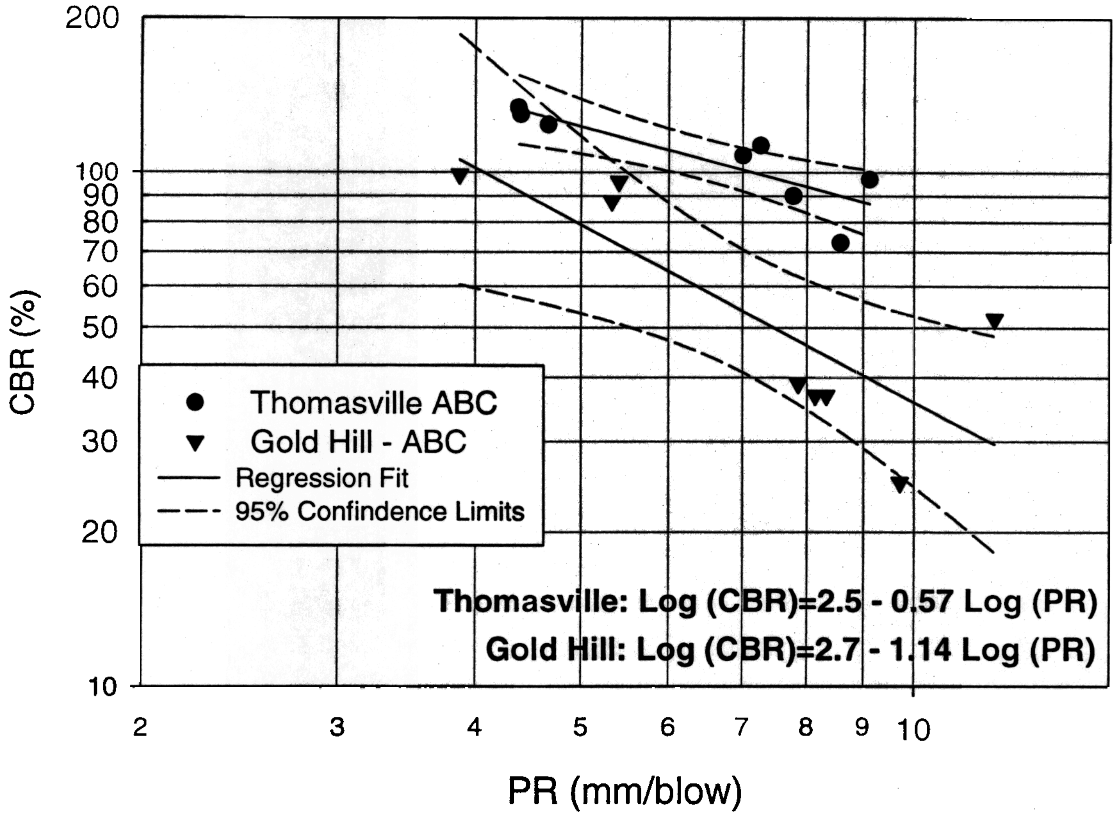

Figure 6.3 CBR-PR Correlations for Gold Thomasville and Gold Hill Material - Lab Data

7.0 FIELD TESTING

Seven secondary roads were selected for the first phase of the field testing program. The sites were low traffic volume BST roads and each road was constructed with varying depth of ABC stone. Six maps, showing the location of each of the seven test sites, are given in Appendix A. These maps are labeled Map A.1 through A.6. Map A.1 shows the location of SR 2111 and 2117. Map A.2 shows the location of SR 2352. Map A.3 shows the location of SR 2487. Map A.4 shows the location of SR 2529. Map A.5 shows the location of SR 2751 and Map A.6 shows the location of SR 2572. All test sites are located within Davidson County. Table 7.1 provides a summary of tests performed at each site.

Table 7.1 Summary of Field Testing Program

Road Name	Unconfined DCP	Confined DCP	CBR on ABC	Bulk Sample	Nuclear Gauge	Precut FWD	Postcut FWD
2111 (Poole Rd.)	3	4	3	1	N/A	3	0
2117 (Carter Rd.)	3	4	3	1	3	3	3
2352 (Newsome)	3	4	3	1	3	3	0
2487 (Frontier Rd.)	3	4	3	1	3	3	0
2529 (Surratt Rd.)	3	4	3	1	3	3	0
2572 (Lee Wilson)	3	4	3	1	3	3	0
2751 (Greentree Rd.)	3	4	3	1	3	3	0

Information collected at each test site included the pavement and ABC thickness, data from geotechnical investigation, the pavement age, and traffic load information. A summary of the site information as was provided by the North Carolina Department of Transportation (NCDOT) is presented in Table 7.2.

Table 7.2 Summary of Test Sites Information

Road	Asphalt Depth (inches) and Serviceability	ABC Quarry and Depth (inches) (mm)	Average Daily Traffic[1]	Road Type	Other Information
2111 (Poole Rd.)	½ 4	TV[2] 9.4 (239)	40	Dead End	Residential traffic, test section was at grade, paved October 1997
2117 (Carter Rd.)	5/8 3	TV 6.7 (170)	114	Thru Road	Residential traffic, fill section, paved in 1995 and resurfaced in 1996
2352 (Newsome Rd.)	1.5 1	GH[3] 5.5 (140)	122	Dead End	Residential and commercial traffic, fill section, road was paved in 1980, no resurfacing
2487 (Frontier Rd.)	1.39 1	TV 3.5 (89)	219	Dead End	Residential traffic, fill section, road was built by contractor, then taken over by state for maintenance, built prior to 1991 and possibly resurfaced in 1996
2529 (Surratt Rd.)	1 4	GH 5.5 (140)	107	Thru Road	Residential and commercial traffic, cut section, built in 1994 and resurfaced in 1996
2572 (Lee Wilson Rd.)	5/8 3	GH 7.9 (201)	337	Dead End	Residential traffic, fill section, paved in May 1996
2751 (Greentree Rd.)	1.39 2	TV 3.5 (89)	174	Dead End	Residential traffic, fill section, built by contractor prior to 1991 and resurfaced in 1996 and 1998

[1] Average daily traffic counts taken January 27, 1999.,
[2] TV = Thomasville Quarry
[3] GH = Gold Hill Quarry

Serviceability rating of the test sites was excellent to poor. Serviceability in this case is a numerical rating assigned to each road by means of visual inspection with only rutting considered in the ranking system.

This process was conducted in conformance with NC DOT pavement condition survey manual (1998). The highest-ranking road received a serviceability rating of 4, and the poorest-ranking road received a serviceability rating of 1. Figure 7.1 shows that as the pavement age was increased the serviceability tended to decrease. Pavements with serviceability levels less than 2 were generally older than 8 years in age.

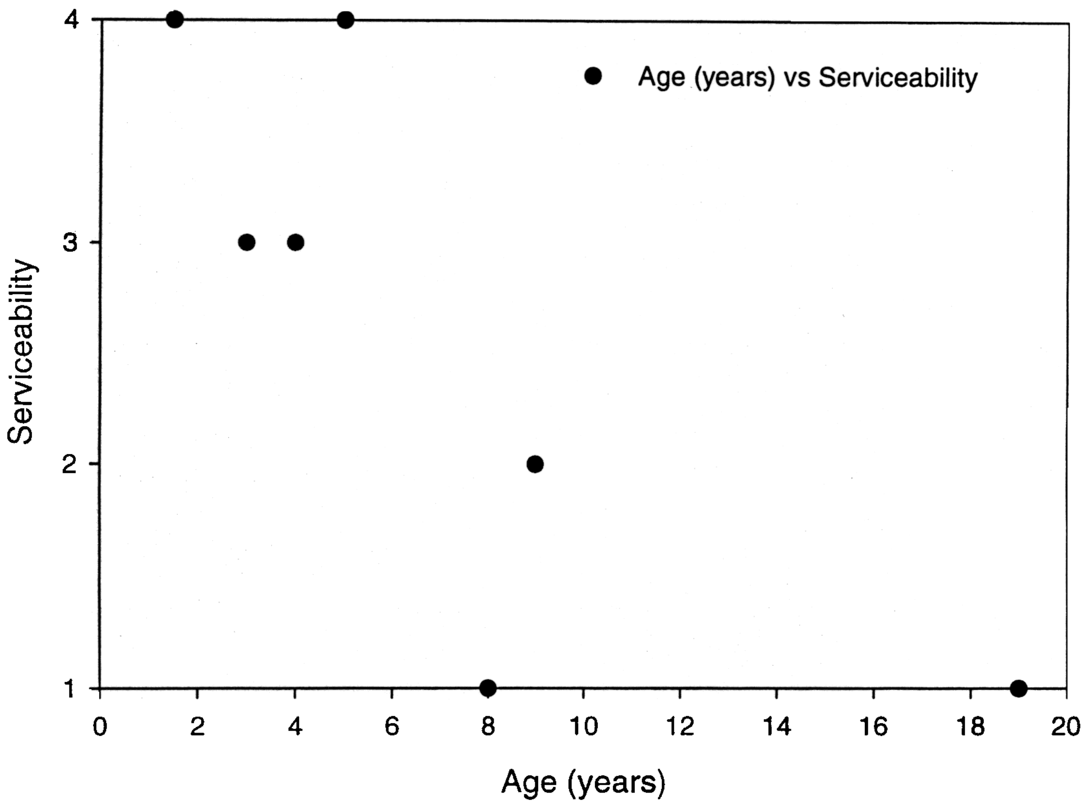

Figure 7.1 Serviceability versus Age

7.1 Field Testing Program

At each of the seven test sites, the pavement was removed over 600 mm (2 ft) x 600 mm (2 ft) squares at three locations spaced 1.2 m (4 ft) on center and cut within the wheel path of the road. The DCP test was performed in each square and on the side of each of the squares, through the pavement. In-situ CBR tests were only performed within each square. Nuclear gage density measurements were made on the ABC layer at each site. In addition, FWD tests were performed at each site. ABC moisture samples and bulk samples of the subgrade were taken for laboratory testing.

Once the test sites were identified, the twenty-one 600 by 600 mm areas, that were to have the pavement removed, were marked. Using a large wooden stencil, the areas were outlined in spray paint. Beginning with SR 2117, FWD tests were conducted at the three marked stations prior to and following cutting the asphalt along the painted lines. This was the only road for which this procedure was conducted. All of the other roads had FWD taken prior to asphalt cutting only. After the FWD test was completed, the asphalt from the three marked stations was removed and in-situ CBR measurements were made. Following CBR and nuclear gauge tests, the DCP test was then conducted.

The DCP test was performed both inside the three marked areas as well as on both sides of the marked areas. (For future reference, tests that were performed outside of the asphalt-free marked areas will be referred to as confined, and tests performed inside the asphalt-free marked areas will be referred to as unconfined) The DCP was penetrated to the full length of the shaft (1m). The penetration rate was recorded by markings made on a tomato stake. Penetration blows were recorded in increments of five.

After all of the tests had been conducted, a steel circular collar was placed on the exposed ABC and a sample was extracted. The extracted sample was then taken to the NCDOT materials laboratory for grain-size analyses.

7.2 Field Material Properties

The grain size distributions of ABC specimens retrieved during the field testing program are shown in Figure 7.2. Comparing these distributions to the results obtained in the laboratory indicated that both materials have a similar grain size distribution with the construction activities not affecting the original grain size distribution.

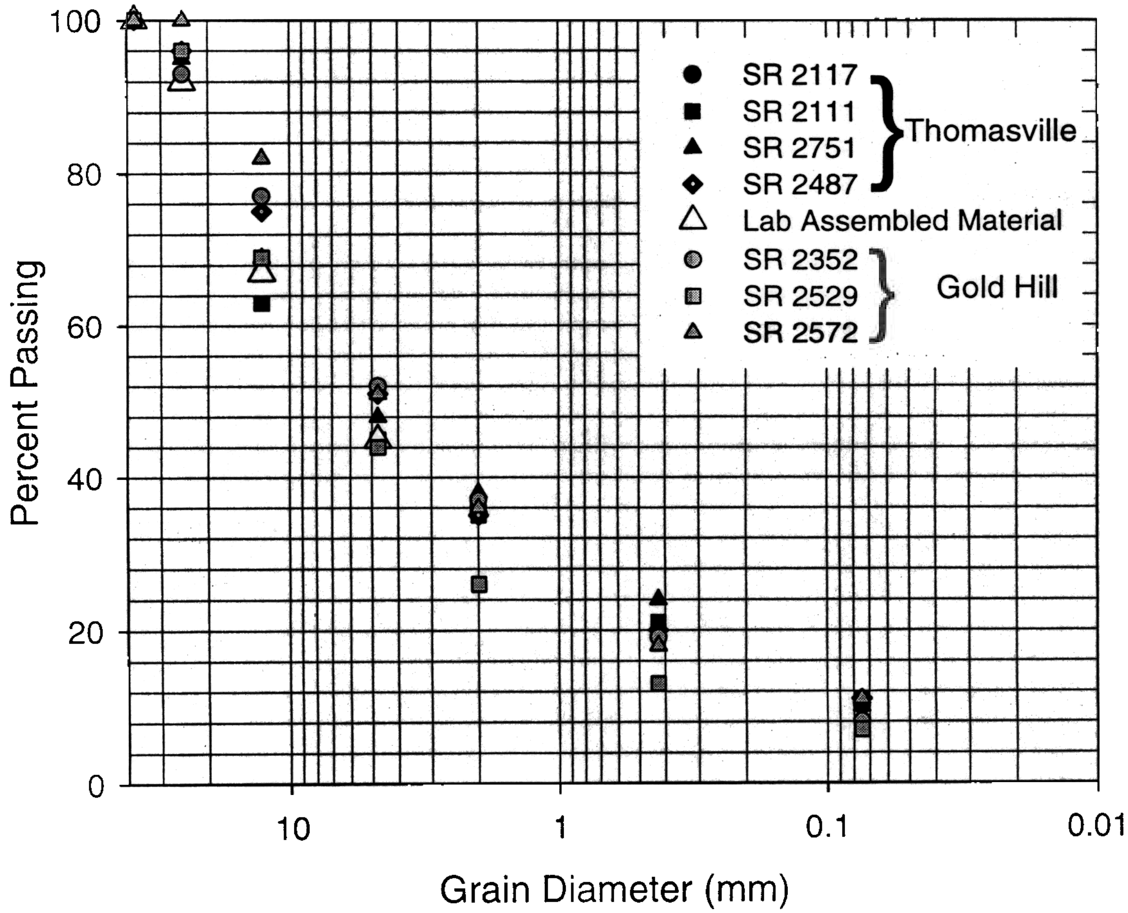

Figure 7.2 Grain Size Distribution of ABC Material-Field Sites

Table 7.3 presents the results of the nuclear density gage tests on the ABC at the test site. At the time of testing, the moisture content of the ABC material averaged 4.7% . The dry unit weight of the ABC material in the field ranged from 21.3 to 22.5 kN/m^3. In the case of the four sites constructed with the Thomasville ABC material, these values were comparable to the T99 values obtained in the laboratory. In the case of sites constructed with the Gold Hill ABC material, these values were comparable to those obtained under T180 compaction energy level in the laboratory.

Table 7.3 Summary of the Data Obtained By Means of the Nuclear Gage Device

Road	Dry Density kN/m^3	Moisture Content (%)
2117 (Carter Rd.)	22.3	4.43
2352 (Newsome Rd.)	21.8	4.37
2487 (Frontier Rd.)	21.3	5.20
2529 (Surratt Rd.)	22.0	4.77
2572 (Lee Wilson Rd.)	22.1	4.80
2751 (Greentree Rd.)	21.4	4.83

No Data are Available For SR 2111

7.3 DCP Data

Figures A.1a through A.7c in Appendix A show plots of the DCP penetration in mm versus the number of blows. Three graphs present the data for each of the seven sites. The (a) graphs, in each of the three graph series, show plots of data for all seven tests from each site. The (b) graphs, in each series show plots of the data for the confined tests and the (c) graphs show plots of the data for the unconfined tests. The confined data were produced by running the penetration device through the asphalt, while the unconfined data were produced by removing a two by two foot square section of the asphalt and running the device within the asphalt-free area. The scale for all 21 graphs is the same so that comparisons among the graphs may be made. Table 7.4 summarizes the DCP results obtained from the profiles reported as average PR.

As the scale of all 21 graphs is the same, flatter slopes indicate lower PR values corresponding to a "stronger" soil. Conversely, the steeper slopes indicated a higher PR, or a "weaker soil." Measured DCP data in the field indicated that the confined PR data were consistently lower than the unconfined PR

Table 7.4 Summary of the DCP Findings as Synthesized from Figures A.1a through A.7c

Road	Figure Series (App A)	Confined		Unconfined	
		ABC PR (mm/blow)	Subgrade PR (mm/blow)	ABC PR (mm/blow)	SubgradePR (mm/blow)
2111 (Poole Rd)	1	3.1	18.2	3.9	24.0
2117 (Carter Rd)	2	2.2	7.9	3.4	7.4
2352(Newsome Rd)	3	2.4	32.0	5.0	25.4
2487 (Frontier Dr.)	4	2.6	30.0	3.1	39.4
2529 (Surratt Rd)	5	2.5	11.3	2.8	12.2
2572(Lee Wilson Rd)	6	2.1	5.7	2.8	6.3
2751(Greentree Rd)	7	5.5	33.7	3.9	37.4

In general, the unconfined PR values were higher than the confined values by approximately 20%. The exceptions to this trend were PR values for the ABC on SR 2751 (Greentree Rd.) and the subgrade on SR 2117 (Carter Rd.) and SR 2352 (Newsome Rd.) Because the differences are not large, these discrepancies are within expected variability of the test method.

7.4 FWD Data and Correlation

Although the FWD tests were included in this research program, they were conducted to provide complete database on the test sites for potential future use. The FWD data measured in the field at station 0 (location of weight drop) are shown in Figure 7.3. Each data point in Figure 7.3 is an average of three tests. Correlating the FWD deflection data with only the PR of the ABC layer proved fruitless as it was not possible to discern a consistent trend of correlation between PR-ABC and FWD data. This may be due to the fact that the FWD deflection data are a function of the multi-layered system encompassing the subgrade soil, the base layer, and the pavement overlay. It is reasonable to anticipate in this case that the measured deformation due to the impact weight will be a function of the module of the whole system which depends on the relative stiffness of each layer.

Accordingly the limited data shown in Figure 7.3 represent a correlation between

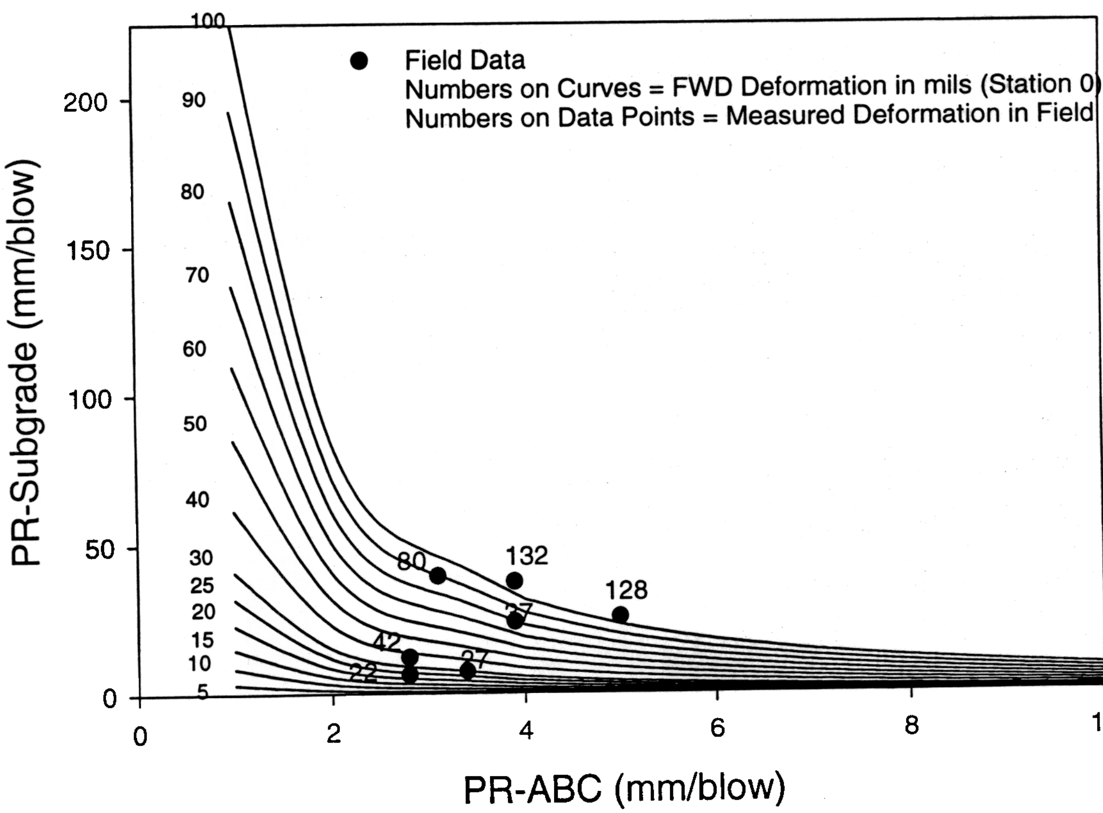

Figure 7.3 Variation of FWD Deflection Data with PR-ABC and PR-Subgrade Values

FWD data with the DCP data by focusing on predicting the FWD-generated moduli based on the DCP data and then using these moduli values to predict deformations based on elastic theory.

7.5 PR/CBR Field Results

Field PR-ABC and in-situ CBR field measurements are shown in Figure 7.4 along with predictions made using models developed in this research from the laboratory data and corrected for mold confinement. A reduction factor of 30% applied to the CBR values predicted from the laboratory-developed correlation was recommended by Harison (1987). Applying such a reduction factor to the CBR data evaluated from the laboratory-

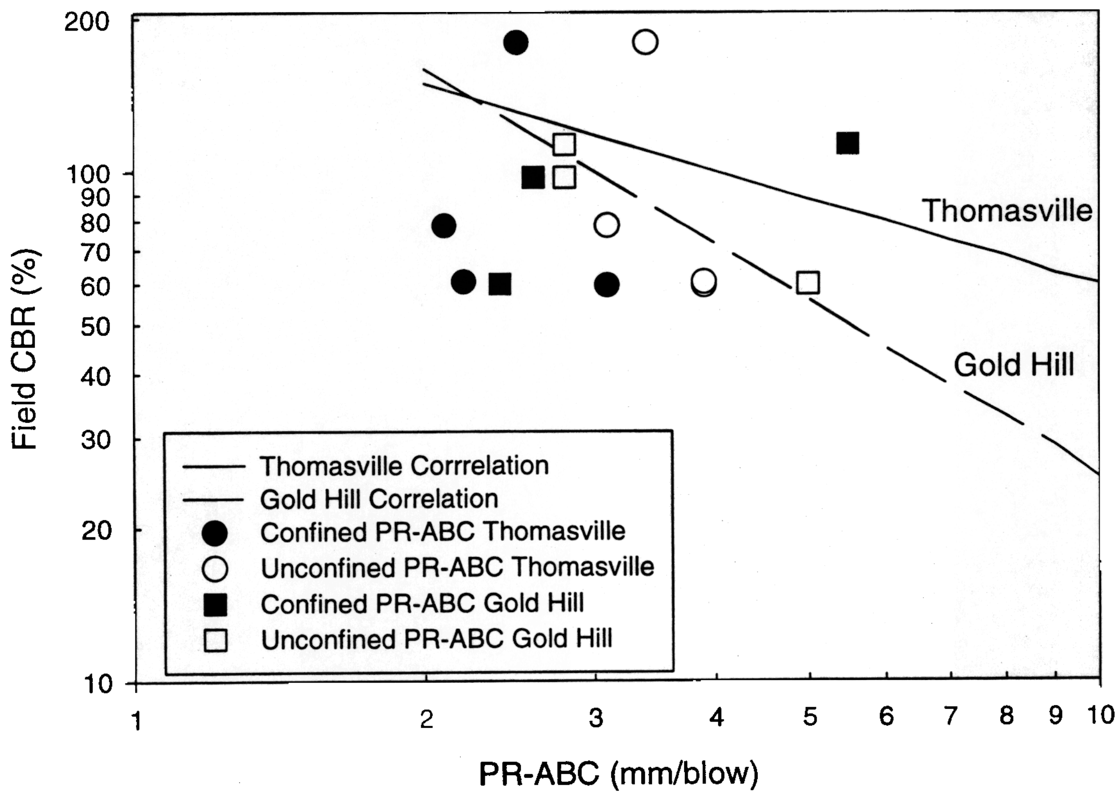

Figure 7.4 Field CBR as a Function of PR-ABC: Predicted Versus Measured

developed correlation, equations 9 and 10 are modified as follows:

<u>Thomasville</u>

Log (CBR) = 2.4 – 0.57 Log (PR, in mm/blow)

<u>Gold Hill</u>

Log (CBR) = 2.55 – 14 Log (PR, in mm/blow)

Comparing the laboratory and field data indicated that the laboratory-based model for Thomasville ABC overpredicts the field data and the Gold Hill ABC model seems to reasonably predict the field CBR values. However, and as shown in Figure 7.4, a discrepancy seems to appear in the field data and it is hypothesized that the measured field CBR values may not be a mere function of the PR of the ABC layer.

For example, the CBR corresponding to SR 2487 (Thomasville) was 78.2% at unconfined ABC-PR of 3.1 mm/blow while the CBR value for SR 2117 (Thomasville) was 179.3% at a higher unconfined ABC-PR value of 3.4 mm/blow. Further inspection of the test data reveals that the CBR data as measured in the field may not be only function of the PR (or the strength) measured for the ABC stone but also depends upon the thickness of the ABC stone specially when less than 152 mm (6 inches). In this case, the ABC thickness of SR 2487 was 89 mm (3.5 inches) compared to a thickness of 170 mm (6.7 inches) for SR 2117, which had higher field CBR value. Based on the stress distribution of a two-layer profile, as presented by Fox (1948), the stress bulb extends to a distance 2-3 times the diameter of the loaded area. In this case, the diameter of the CBR piston was 51 mm for a zone of influence of approximately 100-150 mm. Such a zone of influence will encompass a part of the subgrade in case of SR 2487. Accordingly, and even though the ABC-PR values for the two roads were comparable, the lower CBR value for SR 2487 can be explained by having PR-subgrade of 39.4 mm/blow for SR 2487 versus a value of 7.4 mm/blow for SR 2117.

8.0 PAVEMENT DISTRESS MODEL

A procedure is proposed for using the DCP PR data to evaluate the pavement distress state for prioritizing the need for remedial measures. Figure 8.1 shows a plot of the PR-subgrade versus the PR-ABC from data obtained in the field. Superimposed on Figure 8.1 are CBR data and the corresponding ABC thicknesses for the test sites (note that d=thickness of the ABC in the field) as well as the serviceability index. Also shown on Figure 8.1, is "pt=2.5" line representing the proportional requirement for PR-ABC and PR-subgrade values that, if satisfied, the pavement strength meets the criteria for terminal serviceability of 2.5. This line will be referred to as the "pt=2.5 criterion" and was constructed as follows:

i) Using the correlation developed in this report for residual soils, CBR values for the subgrade are predicted for assumed PR values,

ii) Using the CBR values of the subgrade, a structural number is determined and the required CBR value of a 202 mm (8 inch) layer of ABC stone is computed. These calculations are performed in accordance with the AASHO design method of pavement structures (1962),

iii) The estimated ABC CBR values are then used in equation (3) and the corresponding PR-ABC values are estimated, and,

iv) The predicted PR-subgrade and PR-ABC values are then used to construct the "pt=2.5" line shown in Figure 7.

These calculations were conducted assuming 18 kip equivalent axle load, regional factor of 1, ABC thickness of 203 mm (8 inches) and asphalt thickness of 51 mm (2 inches) with a layer coefficient of 0.44.

Inspecting Figure 8.1 reveals several important aspects of the potential use of the DCP data for pavement design. In general, the CBR values decreased with increasing PR values for the subgrade and the ABC layer. Data that plotted in the immediate vicinity of the "pt=2.5" line were for sites with serviceability values equal to 2 and 1, respectively (SR 2751 and SR 2487 were constructed with Thomasville ABC). Note that these two sites have PR-ABC values around 4 mm/blow which are approximately equal to the PR-ABC values for the two other sites constructed with Thomasville ABC (SR2111 and SR2117) and were rated with serviceability index of 3 or 4. However, the PR-subgrade values for SR 2751and SR 2487 exceeded 25 mm/blow. On the other hand, the "plotted to the left" two sites having serviceability equal to 4 and 3, respectively, yielded PR-subgrade values that were considerably less than 25 mm/blow, and ABC thicknesses that

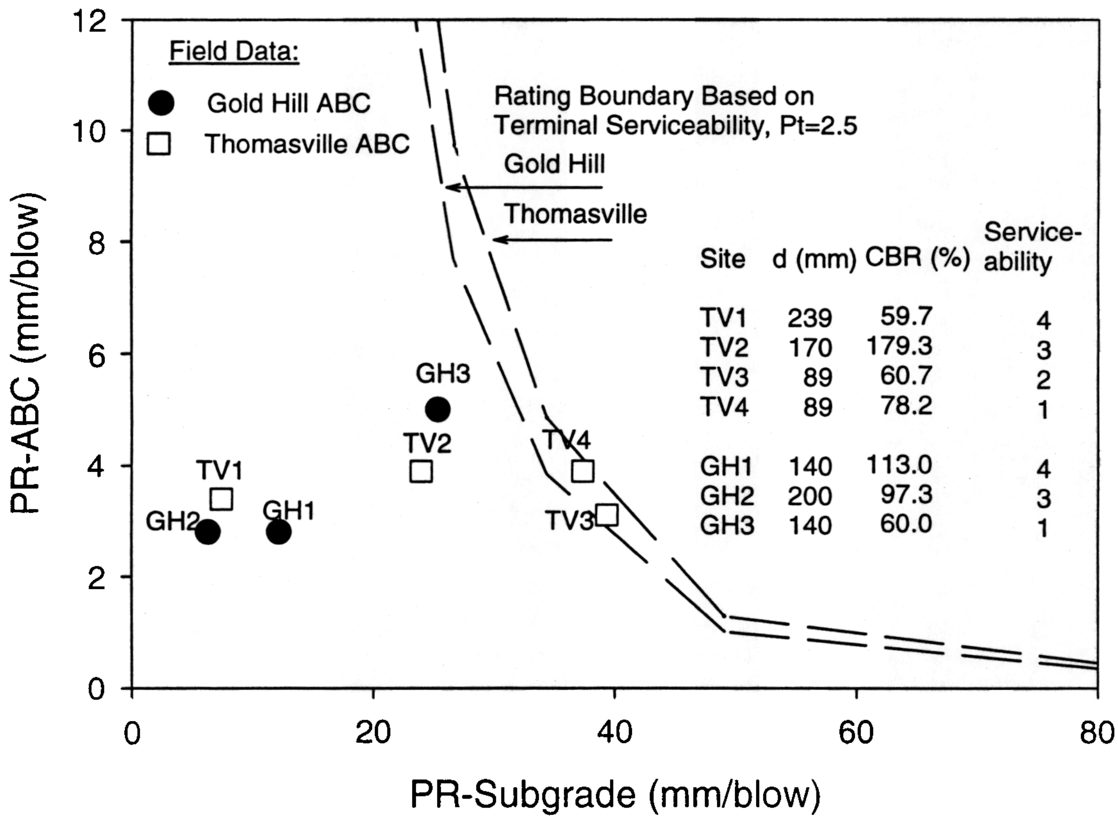

Figure 8.1 Pavement Distress Model: Performance Boundary and Field Comparisons

exceeded 152 mm (6 inches). One of these two sites was rated with high serviceability (4) even though the CBR of the ABC material was 60%. Nonetheless, it is hypotheised that the coupled contribution of the subgrade and the ABC material affects the serviceability level of the pavement. In additon, these results indicated that in the case of SR 2751 and SR 2487 that were rated low, permanent resurfacing will not be sufficient repair because low serviceability can be attributed to the low strength subgrade and the absence of a competent layer of ABC having sufficient thickness to dissipate wheel loads.

In the case of the three sites constructed using Gold Hill ABC, the two sites with serviceability of 3 and 4 were plotted well to the left of the "pt=2.5" line. The CBR values of the ABC layer for these two sites were 97% and 113%, respectively, the PR-ABC values were less than 4 mm/blow and the PR-subgrade values were less than 25 mm/blow. On the other hand, SR 2352 was rated with a serviceability value of 1. For this site, the CBR value was 60%, the stone thickness was 40 mm (5.5 inches), the PR-ABC was 4 mm/bow and the PR- subgrade was less than 25 mm/blow. This site provides an example where resurfaceing should increase the serviceability index because the PR data indicated competent subgrade and subbase layers and marginally accepteable ABC layer thickness.

Depending on the quality and type of the ABC and the subgrade soil, it is possible that material degradation takes place as the number of traffic cycles increases. Accordingly, and with time, sites with high serviceability plotted on Figure 8.1 can shift to the right and upward. If no degradation in strength properties is anticipated with time, then resurfacing will be sufficient to provide high servicability for these roads. In addition, it should be noted that the DCP only measures the in-situ strength of the material at the time at which the test is made. Changes in moisture content will change the strength of both the soil and pavement layers and this aspect needs to be considered when using the DCP to evaluate pavement condition.

8.1 Model Validation

Tests at three additional sites were conducted for the purpose of validating the developed procedure. Test conducted included FWD , DCP and CBR. Three 150 mm (6 in) diameter cores were cut into the BST pavement. The holes were spaced 1.2 m (4 feet) on center to repeat the distance between test locations during phase I of field testing. The asphalt was removed from the cored holes and the DCP was performed at the edge of each hole. Following the DCPT testing, an in-situ CBR test was performed on the ABC. The ABC layer was then removed to expose the subgrade and a CBR test was performed on the subgrade. Table 8.1 provides general description of the three test sites. Two of the test sites were constructed with Thomasville ABC and one site was constructed using Gold Hill ABC.

Table 8.1 – Summary of Test Sites Information, Phase II

Road	Asphalt Depth (inches)	ABC Depth (inches)	Average Daily Traffic[1]	Road Type	Other Information
2275 (John Lookabill Rd.)	7/8 TV	5.75	NA	Through Road	Paved June 1993, no resurfacing
1118 (Hugh Miller Rd.)	1.25 TV	7.5	NA	Connector Road	Paved May 1993, resurfaced 1998
2567 (Surratt Dr.)	1 GH	6	NA	Dead End	Paved June 1994, resurface October 1998

Unfortunately, problems were encountered with the in-situ CBR of the ABC and subgrade layers in this phase of testing. The in-situ CBR of the ABC ranged from 10% to 60 % and the three in-situ CBR subgrade tests yielded values that ranged from 1 to 3 %. These values were judged to be realistically low and therefore were not used in this report.

Figure 8.2 shows the PR data measured at the three test sites plotted in conjunction with the pavement distress model line "pt=2.5". At the time of this report, no serviceability rating had been provided by NCDOT for these three sites. One of the three sites (SR 2567) plot in the vicinity of the "pt=2.5" line which indicates a relatively low serviceability rating on the order of 1 or 2. However, since this road was resurfaced recently (October 98), such low serviceability may not be accurate. On the other hand, the points for SR 2275 and SR 1118 are placed well to the left of the "pt-2.5" which indicates a relatively high serviceability. In this case, the PR-ABC was less than 4 mm/blow and the PR-subgrade was less than 25 mm/blow.

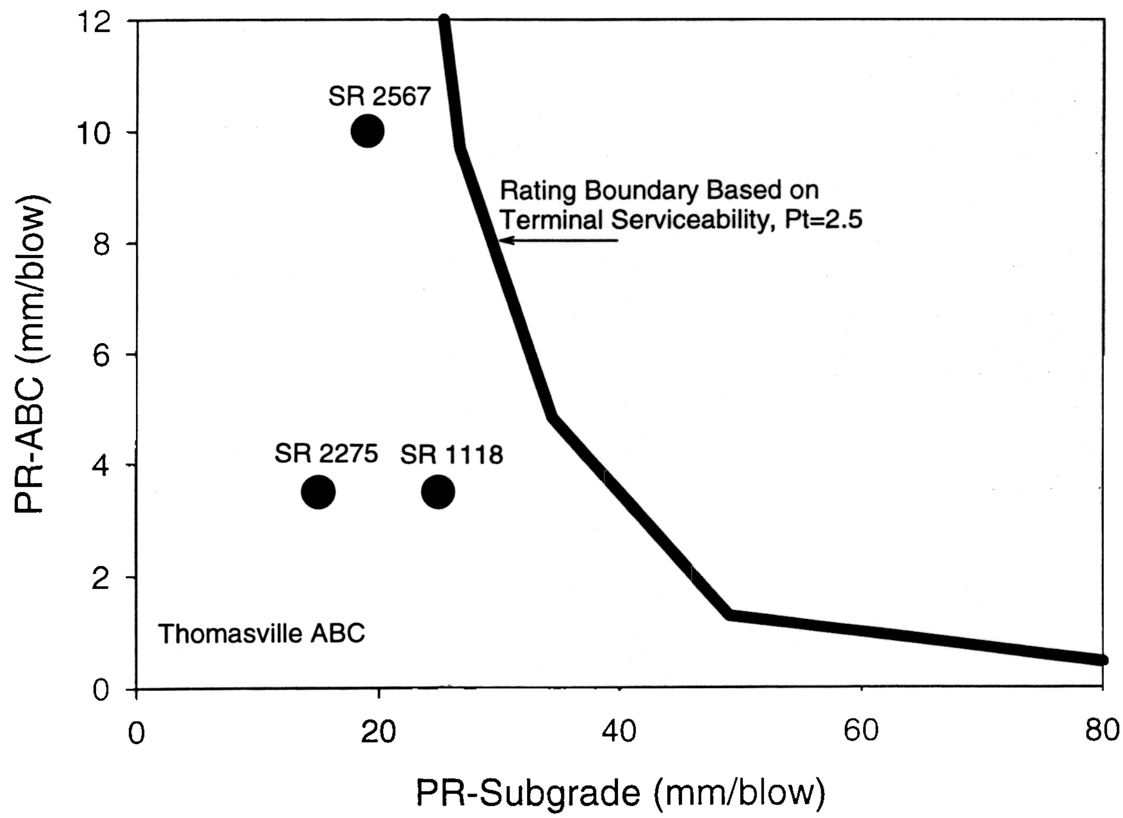

Figure 8.2 Pavement Distress Model Validation: Three Sites

9.0 SUMMARY AND CONCLUSIONS

This report summarizes the findings of a one-year research study sponsored by the North Carolina Department of Transportation on the use of the DCP to develop a pavement distress evaluation model. Work included laboratory and field testing programs as well as a modeling effort. In this report, a method was proposed by which the DCP PR data were utilized to evaluate the pavement condition. Such an evaluation is needed on a regular basis in order to prioritize pavement repairs. The principle idea of the research was to use the DCP data to determine the condition of the subase and ABC layers. Accordingly, if the structural integrity of the subgrade and ABC layers adequate, either resurfacing or treating the surface layer will be adequate. However, when structural integrity of either the ABC, or the subgrade is found inadequate, stabilization and soil improvement measures maybe needed and resurfacing alone will not be sufficient.

The laboratory work on the subgrade materials was performed on three residual soil types taken from test sites in Davidson County, North Carolina. Testing included compacting subgrade soil specimens in a 150 mm (6 in) mold, performing the CBR test on the prepared specimens, and then penetrating the specimens with the DCP probe. A similar program of laboratory testing was performed on ABC including the preparation of thirty-two CBR specimens using material from two different sources. The field testing included work at seven sites with three CBR tests, seven DCP penetrations, three nuclear gauge measurements, three FWD tests and one bulk sample extraction conducted at each site. A second phase of field testing was performed at three sites. Modeling work included development of correlations between the PR and CBR for subgrade soils, the PR and CBR for ABC, the PR and compaction unit weight, and the PR and moisture content for the subgrade soils. In addition, the PR-subgrade and PR- ABC data were combined to develop a pavement distress level to indicate the pavement's serviceability level if the test sites. Based on the results obtained in this study, the following conclusions are advanced:

1. The test data indicated that the CBR – DCP relationship was independent of moisture content and dry unit weight for the Piedmont residual soils utilized in this study. Kleyn (1975) and Harison (1989) also concluded that this relationship was independent of moisture content.

2. The test data showed that the CBR – DCP relationship was largely independent of soaking. Harison (1989) concluded that the CBR – DCP relationship was influenced by whether soaked or unsoaked specimens were used. Harison found the difference, however, was less than 10 %.

3. The relationship between the PR and CBR data for the Piedmont subgrade soils was best described with a model in the form of Log(CBR) = 2.53 – 1.14 Log(DCP).

4. The PR and the liquidity index (LI) are correlated as well as the PR and the degree of saturation (S). As the LI increased, the PR increased for LI values between –0.7 to 0.2. PR also increased with saturation for values between 30%-95%.

5. The PR-LI data were best correlated with an equation in the form of $LI = A \text{ Log } PR - B_m$. For the tested residual soils, the estimated parameters were "A" equal to 0.65 and $B_m = 1.2$. On the other hand, the PR-S data were best correlated with equation in the form of $S = 1 - e^{Cm*PR}$. Cm in this case was estimated equal to –0.065.

6. Using the compaction control model developed in this research, the average water content was underpredicted by 0.2% and the average dry unit weight was overpredicted by 0.3 kN/m^3.

7. A correlation between the Penetration Rate (PR) data from the DCP and the CBR was developed as Log (CBR) = A – B Log (PR, in mm/blow). The A and B coefficients in this case were equal to 2.4 and 0.55, respectively, and are specific to the types of ABC material used in this testing program.

8. A discrepancy in the field CBR data was explained by the possibility that some of the CBR values were affected by the strength of the underlying subgrade soil especially in cases where the thickness of the ABC layer was less than 100 mm (4 inches).

9. A simple model to predict the distress and serviceability levels of the pavement as "acceptable or unacceptable" was proposed following AASHO design guideline for flexible pavements. This model was developed using PR-subgrade and the PR-ABC values to construct a terminal serviceability (pt)=2.5 criterion representing the acceptable/unacceptable boundary.

10. The simple serviceability model for determining pavement condition was based on the coupled bearing contribution of both the subgrade and the ABC layers.

11. Out of seven test sites, the three test sites with serviceability equal to 4 and 3 had unconfined PR-ABC values less than 4mm/blow, PR-subgrade values less than 25 mm/blow, as well as ABC thichness on the order of 152 mm (6 inches).

It should be noted that the models developed in this research program need to be validated in the field. In addition, in the case of correlations to compaction parameters, a field calibration procedure is suggested in which moisture contents and dry densities are evaluated by alternative means, such as the sand cone device, and then compared to DCP-based values to determine whether adjustment is necessary. The developed pavement distress model is specific to the type of the ABC tested in this study. However, the framework for the procedure has been established and can be applied to other materials with the proper accounting for differences material characteristics and properties.

Future research is needed in order to more fully develop the pavement distress model presented in this study. Future research effort can include field testing encompassing CBR, DCP, and FWD in order to incorporate the deformation aspect of the design into the developed models. In addition, the model for compaction control should be further validated and established for different soil types. Other aspects of research should focus on incorporating a relationship between DCP and resilient modulus as well as the effect of the drainage conditions on all aspects.

10.0 REFERENCES

) AASHTO (1992) American Association of State Highway and Transportation Officials, T 255-92, Total Moisture Content of Aggregate by Drying, pp. 622-623.

2) AASHTO (1993) American Association of State Highway and Transportation Officials, T 27-93, Sieve Analysis of Fine and Coarse Aggregates, pp. 32-35

3) AASHTO (1993) American Association of State Highway and Transportation Officials, T 30-93, Mechanical Analysis of Extracted Aggregate, pp. 32-33

4) AASHTO (1993) American Association of State Highway and Transportation Officials, T 193-93, The California Bearing Ratio, pp.597-602.

5) AASHTO (1995) American Association of State Highway and Transportation Officials, T 99-95, The Moisture-Density Relations of Soils Using a 2.5-kg (5.5-lb) Rammer and a 305-mm (12-in.) Drop, pp. 300-306.

6) AASHTO (1995) American Association of State Highway and Transportation Officials, T 180-95, Moisture-Density Relations of Soils Using a 4.54-kg (10-lb) Rammer and a 457-mm (18-in.) Drop, pp. 560-566.

7) AASHTO (1996) American Association of State Highway and Transportation Officials, T 87-86, Dry Preparation of Disturbed Soil and Soil Aggregate Samples for Test, pp. 259-260.

8) AASHTO (1996) American Association of State Highway and Transportation Officials, T 88-93, Particle Size Analysis of Soils, pp. 262-272.

9) AASHTO (1997) American Association of State Highway and Transportation Officials, T2-91, Aggregate Sampling, pp.2-3.

10) AASHTO (1997) American Association of State Highway and Transportation Officials, T 238-97, Density Soil and Soil-Aggregate In-Place by Nuclear Methods (Shallow Depth), pp. 785-790.

11) AASHTO (1997) American Association of State Highway and Transportation Officials, T 239-97, Moisture Content of Soil and Soil-Aggregate In-Place by Nuclear Methods (Shallow Depth), pp. 791-794.

12) AASHTO (1997) American Association of State Highway and Transportation Officials, T 256-77, Pavement Deflection Measurements, pp. 624-627.

13) Black, W. P. M. (1961) "The Calculation of Laboratory and In-situ Values of California Bearing Ratio from Bearing Capacity Data," *Geotechnique, London,* 11.1:14-21.1961.

14) Ese, Dag., Myre, Jostein., Noss, Per Magne., and Vaernes, Einar (1994) "The use of Dynamic Cone Penetrometer (DCP) for road strengthening design in Norway," International Conference on Bearing Capacity of Roads and Airfield, Minneapolis, pp3-22. (also in the form of a report by Norwegian Road Research Laboratory, June 1995) .

15) Durnunoglu , H. T. and J. K. Mitchell. (1974) "Influence of Penetrometer Characteristics on Static Penetration Resistance," *Proc., European Symposium on Penetration Testing,* Stockholm, Sweden, 1974.

16) Harison, J. A. (1987) Correlation between California bearing ration and dynamic cone penetrometer strength measurement of soils. Proc Instn Civ. Engrs, Part2, Vol. 83, Technical Note No. 463.

7) Harison, J. A. 1987) "Correlation between California bearing ratio and dynamic cone penetrometer strength measurement of soils," Proc. Instn Civ. Engrs, Part 2, Vol 83, Dec, 833 – 844 Technical Note 463, Ground Engineering Group.

18) Harison, J. A. (1989) "In-situ CBR determination by DCP testing using a laboratory based correlation," Australian Road Research. v 19 n 4 Dec, p 313-317

19) Kleyn, E. G., " The Use of the Dynamic Cone Penetrometer (DCP)," Report 2/74 Transvaal Roads Department, July 1975

20) Livneh, M. (1991) "Verification of CBR and Elastic Modulus Values Derived From Local DCP Tests," *Proc. of the 9th Asian Regional Conf. on Soil Mechanics and Foundation Engrg.*, Vol , pp. 45-50, Bangkok.

21) Livneh, M. Ishai and Livneh, N.A 1992) "Automated DCP device versus manual DCP device," Road and Transport Research, Vol , No. 4, December 1992

22) Livneh, M., Ishai, and Livneh N. (1993) "Effect of Vertical Confinement on Dynamic Cone Penetrometer Strength Values in Pavement and Subgrade Evaluations," Transportation Research Record 1473, Highway Research Board, National Research Council, Washington D.C.

23) Marcu, A.; Popescu, M.; Abramescu, T.; Balacciu, C. (1982) "Comparison of the Results From Static and Dynamic Penetration Tests, In Situ Plate Tests and Laboratory Compressibility Tests," Penetration Testing, Proceedings of the European Symposium. Volume 1: Standard Penetration Test; Dynamic Probing /

Swedish Weight Sounding, National Society for Soil Mechanics and Foundation Engineering A. A. Balkema Rotterdam, pp 101-106.

24) North Carolina Department of Transportation. Pavement Condition Survey Manual. 1997/1998.

25) Notwatzki, E.A., and L.L. Karafiath (1972) "The Effect of Cone Angle on Penetration Resistance," Highway Research Record No. 405, Highway Research Board, National Research Council, Washington D.C.

26) Sowers, G. and Hedges, C., "Dynamic Cone for Shallow In-situ Penetration Testing," *Vane Shear and Cone Penetration Resistance Testing of In-situ Soils, ASTM STP 399,* Am. Soc. Testing Mats., 1966, p 29.

27) Tolia, D. S. (1977) "Interpretation of Dynamic Cone Penetration Tests," Ground Engineering vol 10, No. 7, p 37-41.

Appendix A

Figures A.1a through A.1c show plots of the data obtained from SR 2111 (Poole Rd.). From figure shown in A.1a, it was difficult to determine which data points were confined and which points were unconfined as no discernable differences in value or trend were observed between the unconfined and confined tests. Figure A.1b shows the data points for the confined tests and Figure A.1c shows the data points for the unconfined tests. Even with the data separated, it was difficult to distinguish any significant differences between the two data sets. Not until the PR of the ABC and of the subgrade were calculated were any differences detected.

Figures A.2a through A.2c show plots of the data obtained from SR 2117 (Carter Rd.). From plot A.2a, it was somewhat easier to determine the data points of the confined tests versus the unconfined tests. Figures A.2b and A.2c confirm the slight trend indicated in Figure A.2a. Figure A.2b shows a nice profile for determining the depth of asphalt. This depth was subtracted from the depth of transition from ABC to subgrade to obtain the ABC depth. The confined data was more consistent than the unconfined data. Note that both the confined data and the unconfined data indicated the same depth of transition from ABC to subgrade. Data of the three confined trials, however, provided more consistent results for the subgrade data. Reasons for the inconsistent data produced from the unconfined subgrade may include inconsistent stress release and disturbance of the ABC and subgrade with the removal of the asphalt. As previously stated, the PR for the unconfined subgrade is slightly lower than the PR for the confined subgrade.

Figures A.3a through A.3c plot the data obtained from SR 2352 (Newsome Rd.). From plot A.3a, it appeared that differences between the confined and unconfined data points were discernable. Figures A.3b and A.3c confirmed the visible difference suggested by Figure A.3a. The depth of transition from ABC to subgrade was indicated as the same depth by both the confined and unconfined plots. Both plots show consistent data for the ABC and subgrade. As depicted in the previous graph series, the unconfined PR data for the subgrade was less consistent than the confined, but to a much milder degree. A possible reason for the more consistent data obtained at this site is that the road featured in this series is about 15 years older than Carter Rd. and was subjected to commercial and residential traffic, while Carter Rd. was utilized by only residential vehicles. This difference in traffic conditions could easily explain the difference in subgrade profiles. Another possible reason for the differences is that both sections of road were fill. The fills were possibly different fill materials, but that information is not available. Another result contrary to what was expected is that the PR for the unconfined subgrade was lower than the PR for the confined subgrade. The PR indices were not much different, so the results are explainable by variability. The results may also be explained by incorrect DCP penetration angles.

Figures A.4a through A.4c plot the data obtained from SR 2487 (Frontier Rd.). Data in Figure A.4a suggested an obvious difference between the DCP confined and unconfined tests. Figures A.4b and A.4c confirmed this difference. Unlike the previous series, the depth of the transition from ABC to subgrade, differed between the confined and unconfined data points. Perhaps the ABC depth difference was due to variability in compaction thickness of the ABC at the different testing locations within the same site. Like other series, the unconfined data points were slightly less consistent than the confined series data points.

Figures A.5a through A.5c plot the data obtained form SR 2529 (Surratt Rd.). The plots of these seven tests were similar to series 1 in that it was difficult to distinguish between the confined and unconfined data points. To determine the PR of the ABC and subgrade, it was necessary to separate the confined and unconfined data points. Note the inconsistencies in both the confined and unconfined data. In both cases, there appeared to be a single outlier. For both sets of data, the single outlier may be attributed to a slight angle of penetration. This angle would result in the same indicated depth of transition from ABC to subgrade, but due to skin friction, the PR would be slightly lower, indicating a stronger soil or flatter slope. Note the outlier in both cases followed this trend.

Figures A.6a through A.6c show plots of the data obtained form SR 2572 (Lee Wilson Rd.). From Figure A.6a, confined and unconfined data points were not easily distinguished. The data from Figures A.6b and A.6c made it possible to determine the transition depth from ABC to subgrade. The transition depth determined from each graph corresponded with the design specification depth of approximately 200 mm. Contrary to the previous trends, the unconfined data points were more consistent than the confined data points. A plausible explanation for this effect could be the friction between the asphalt and the DCP while running the device at an angle. In other words if the DCP was penetrated at a slightly different angle for each trial, then the data would be rather inconsistent. Another explanation could be that roots or other debris were encountered during penetration. Finally, the most unsettling explanation is that the ABC and subgrade soil strength were variable.

Figures A.7a through A.7c show plots of the data obtained form SR 2751 (Greentree Rd.). From Figure A.7a it would appear that the difference between the confined and unconfined data were easily distinguished, however on closer inspection, it was evident that a confined outlier mimicked the behavior of the unconfined data points. The confined outlier data may be due to running a perfectly perpendicular test, while the others were systematically run at an angle, or more likely, the outlier test was run at a particularly weak point in the ABC which would increase the PR and generated data typical of subgrade strength. The unconfined data were rather consistent and indicated the same depth of transition from ABC to subgrade as the confined data.

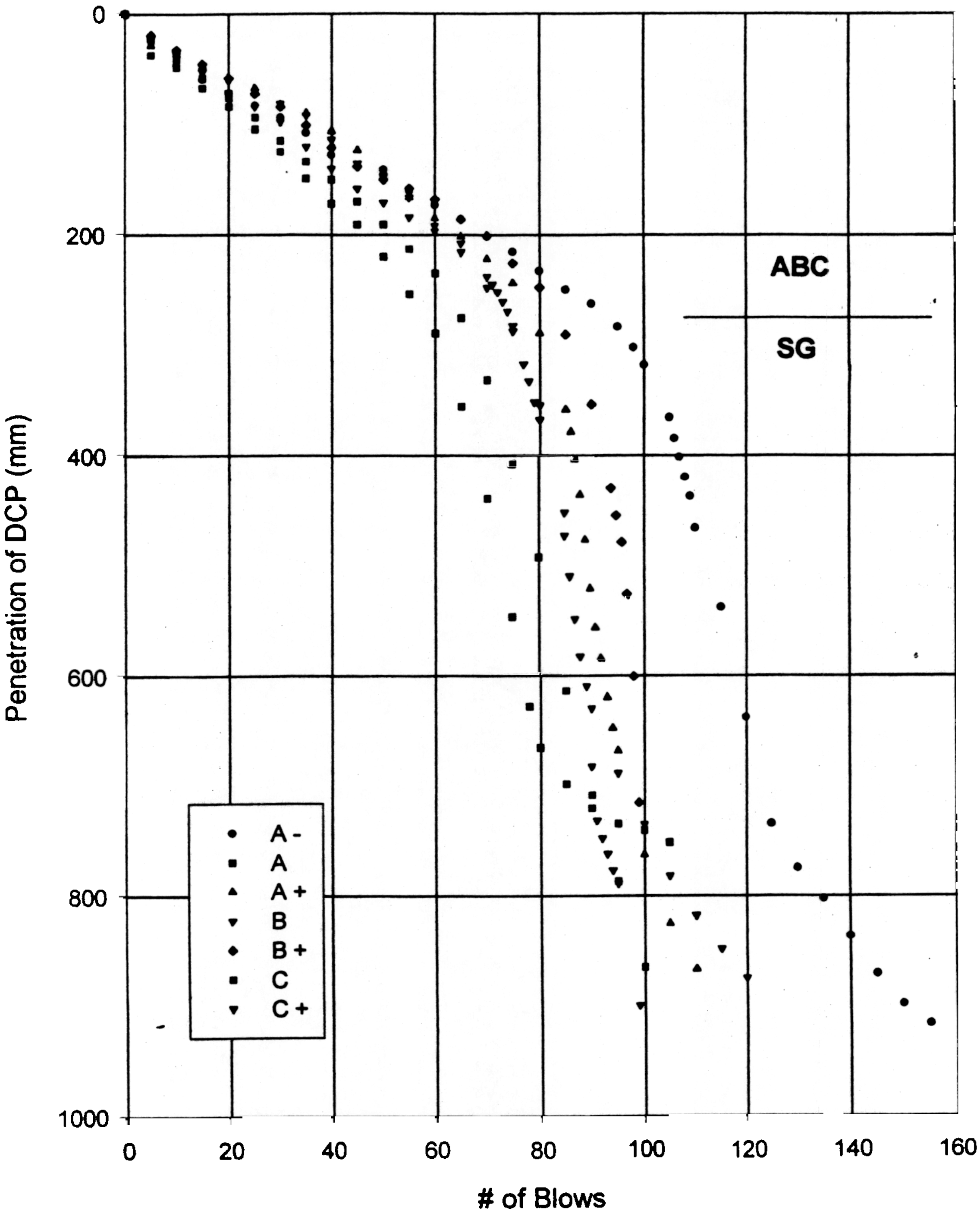

Figure A.1a SR 2111 (Poole Rd.) Penetration Depth Vs. # of Blows All Seven Tests

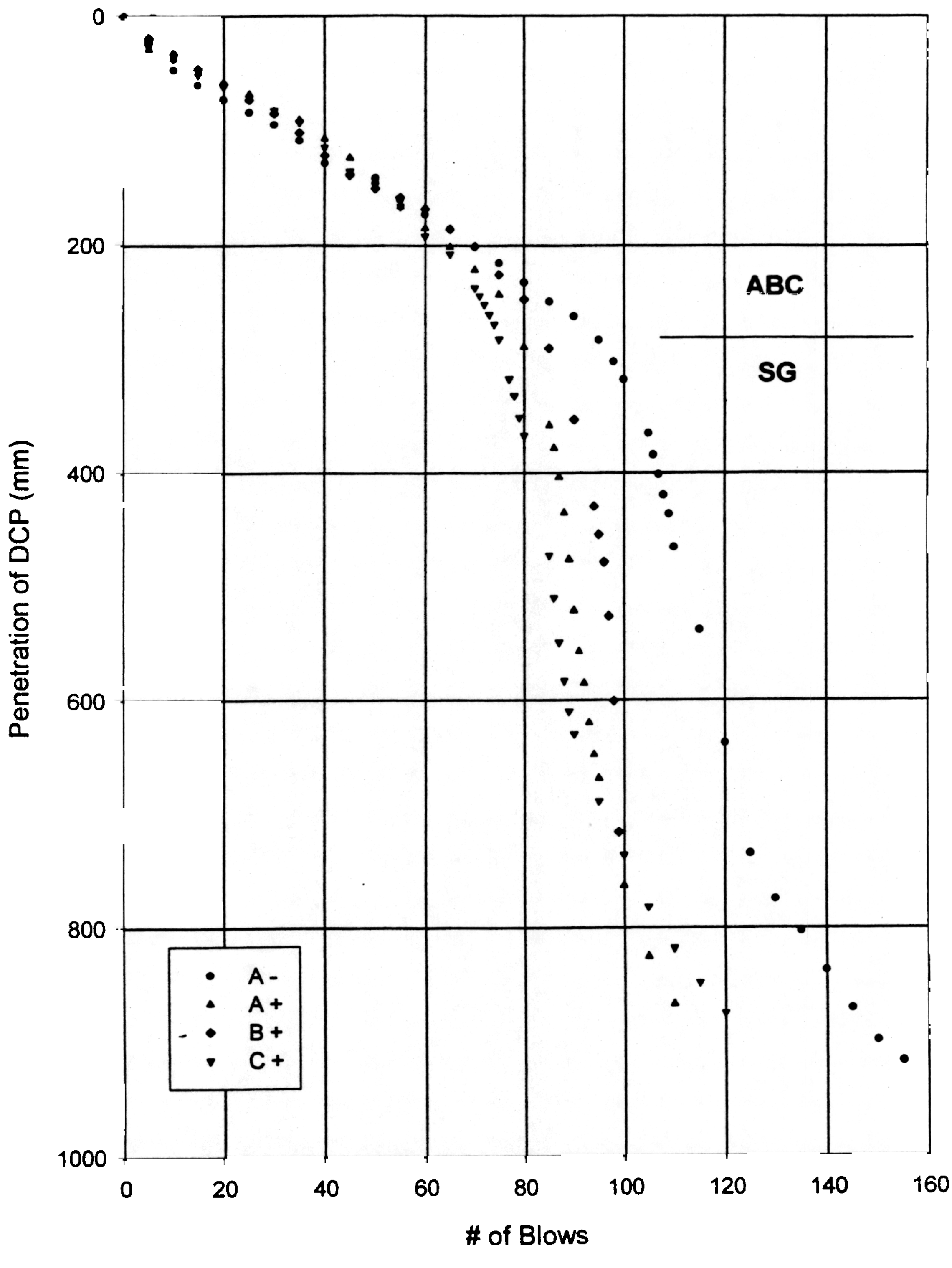

Figure A.1b SR 2111 (Poole Rd.) Penetration Depth Vs. # of Blows Confined

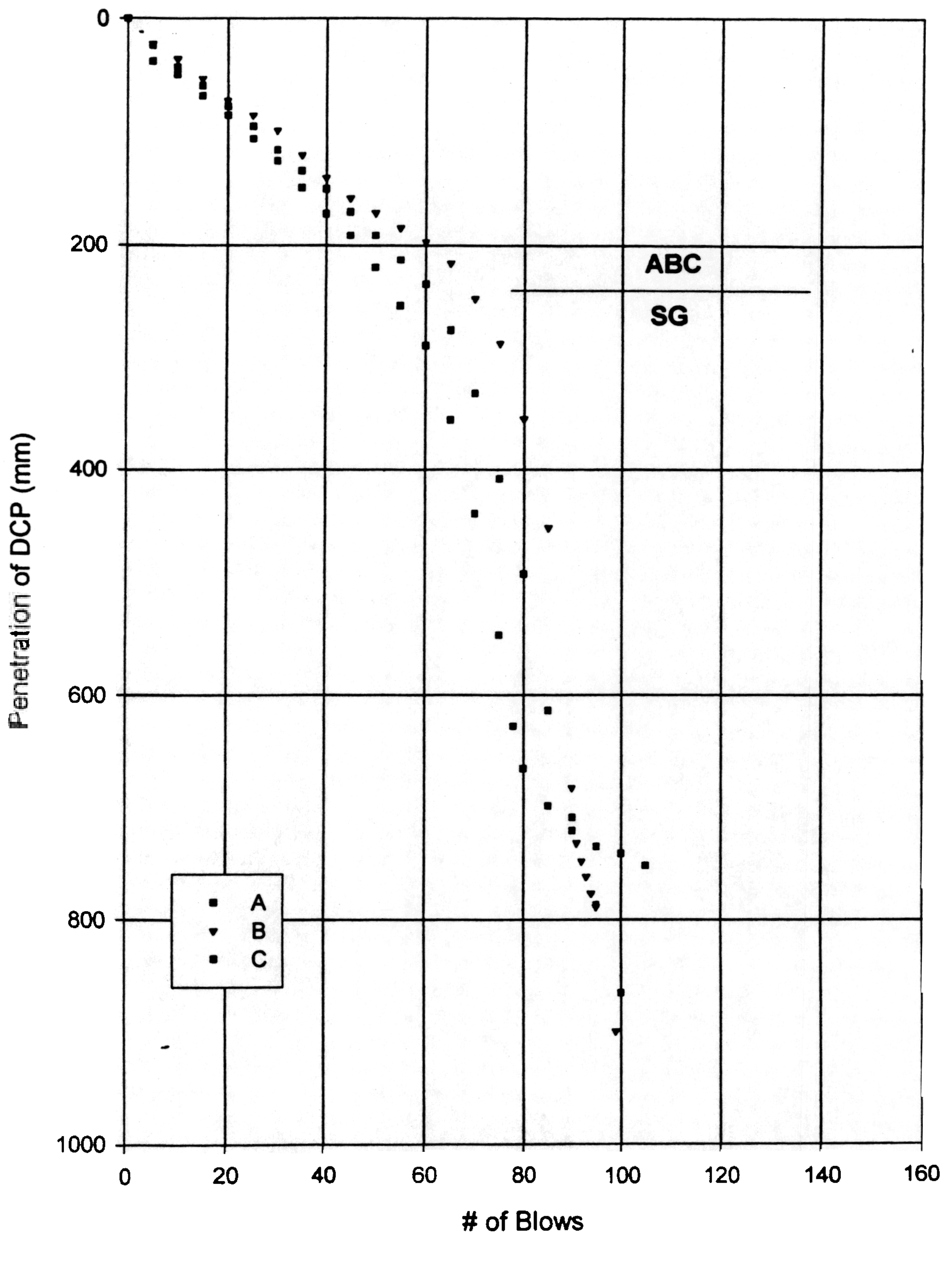

Figure A.1c SR 2111 (Poole Rd.) Penetration Depth Vs. # of Blows Unconfined

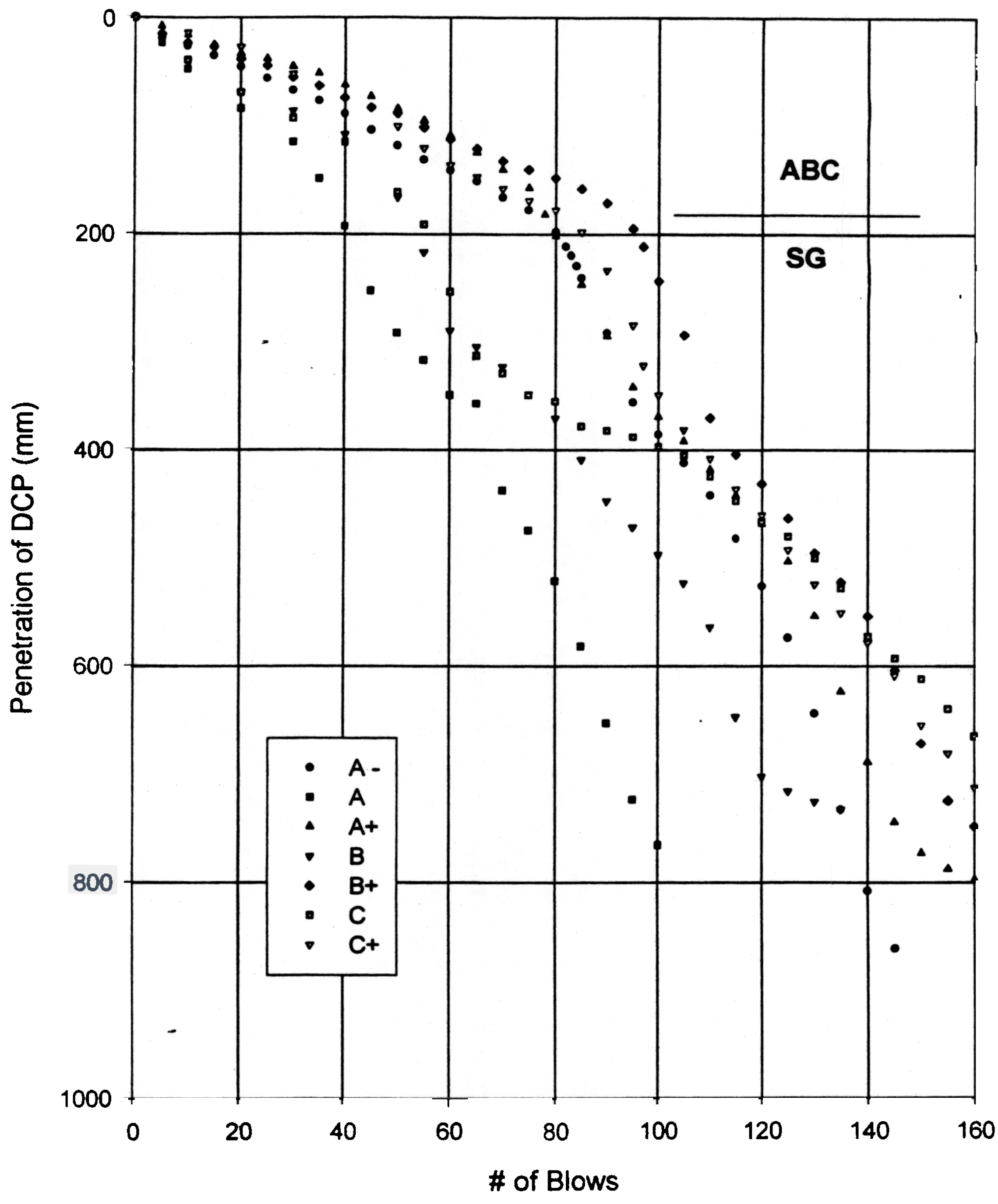

Figure A.2a SR 2117 (Carter Rd.) Penetration Depth Vs. # of Blows All Seven Tests

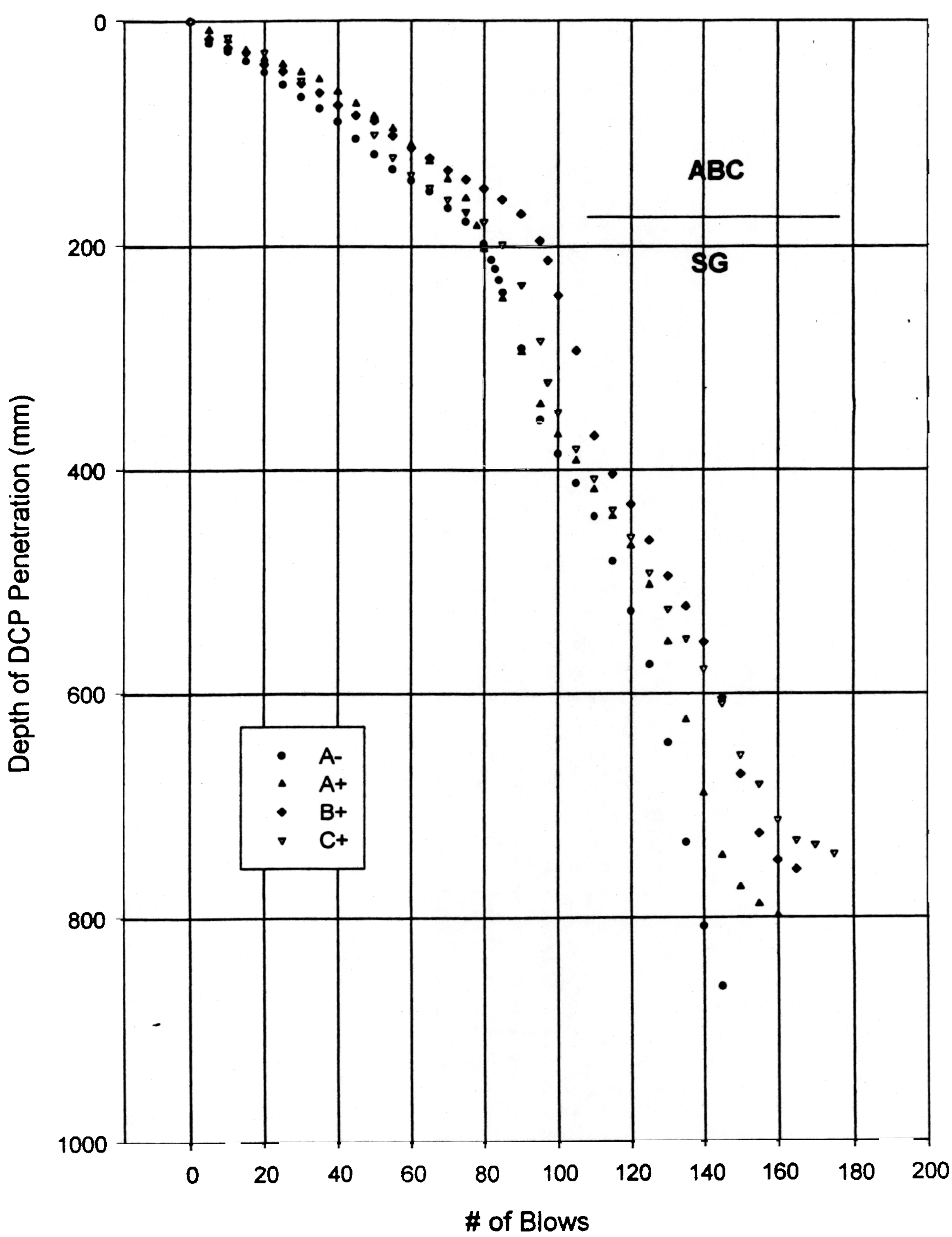

Figure A.2b SR 2117 Carter Rd Penetraion Depth Vs. # of Blows Confined

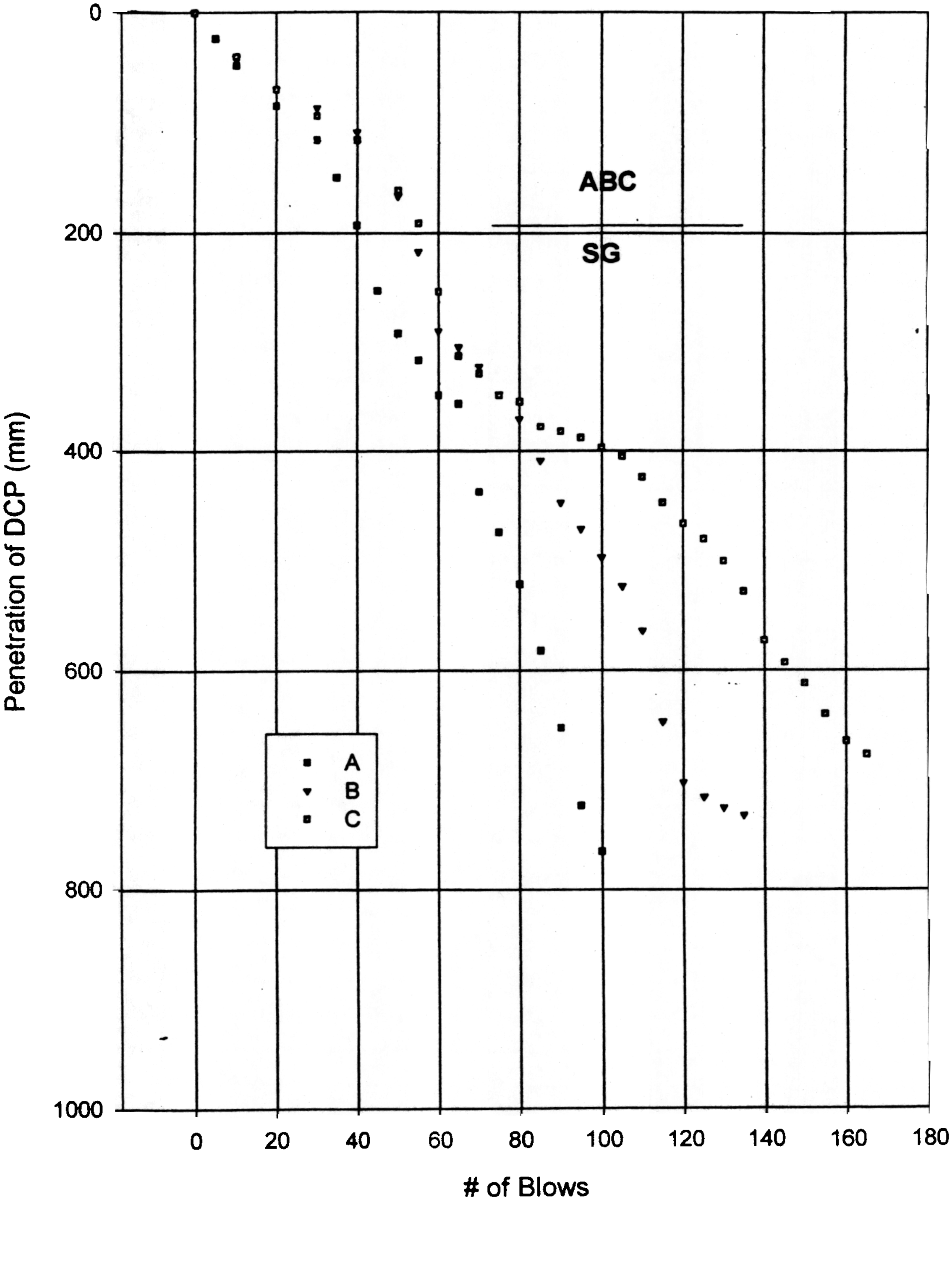

Figure A.2c SR 2117 Carter Rd Penetration Depth Vs. # of Blows Unconfined

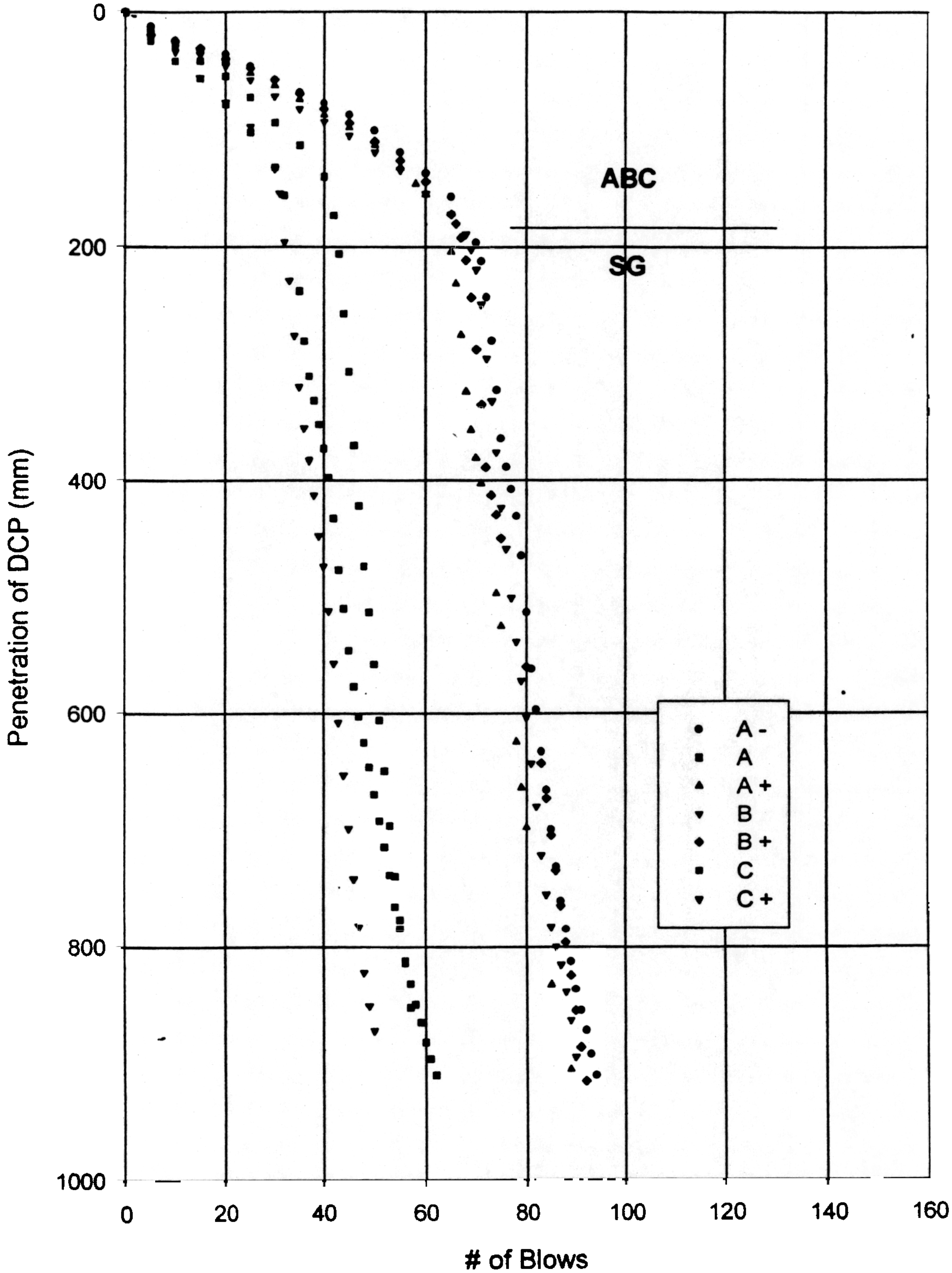

Figure A.3a SR 2352 (Newsome Rd.) Penetration Depth Vs. # Blows All Seven Tests

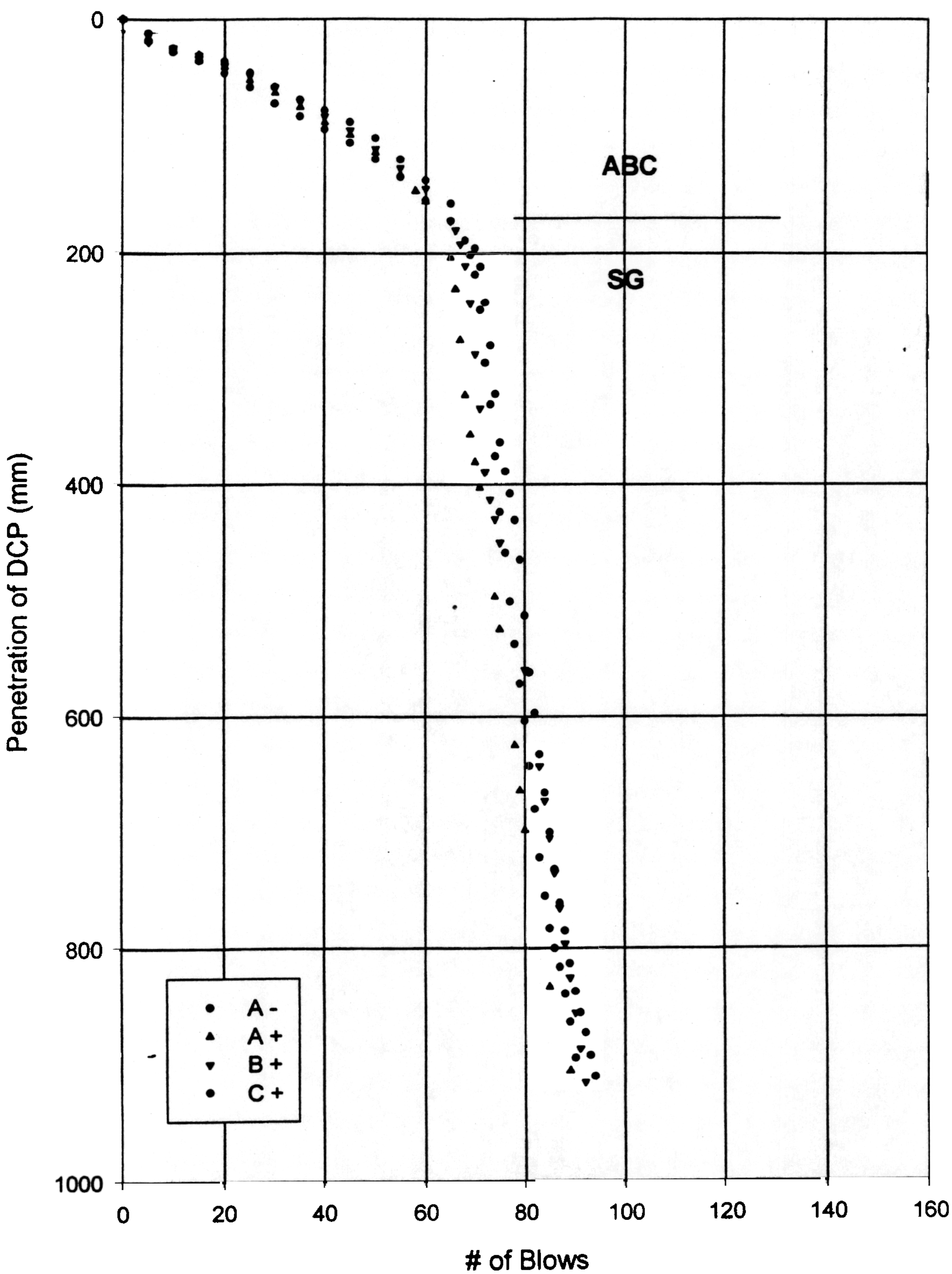

Figure A.3b SR 2352 (Newsome Rd.) Penetration Depth Vs. # of Blows Confined

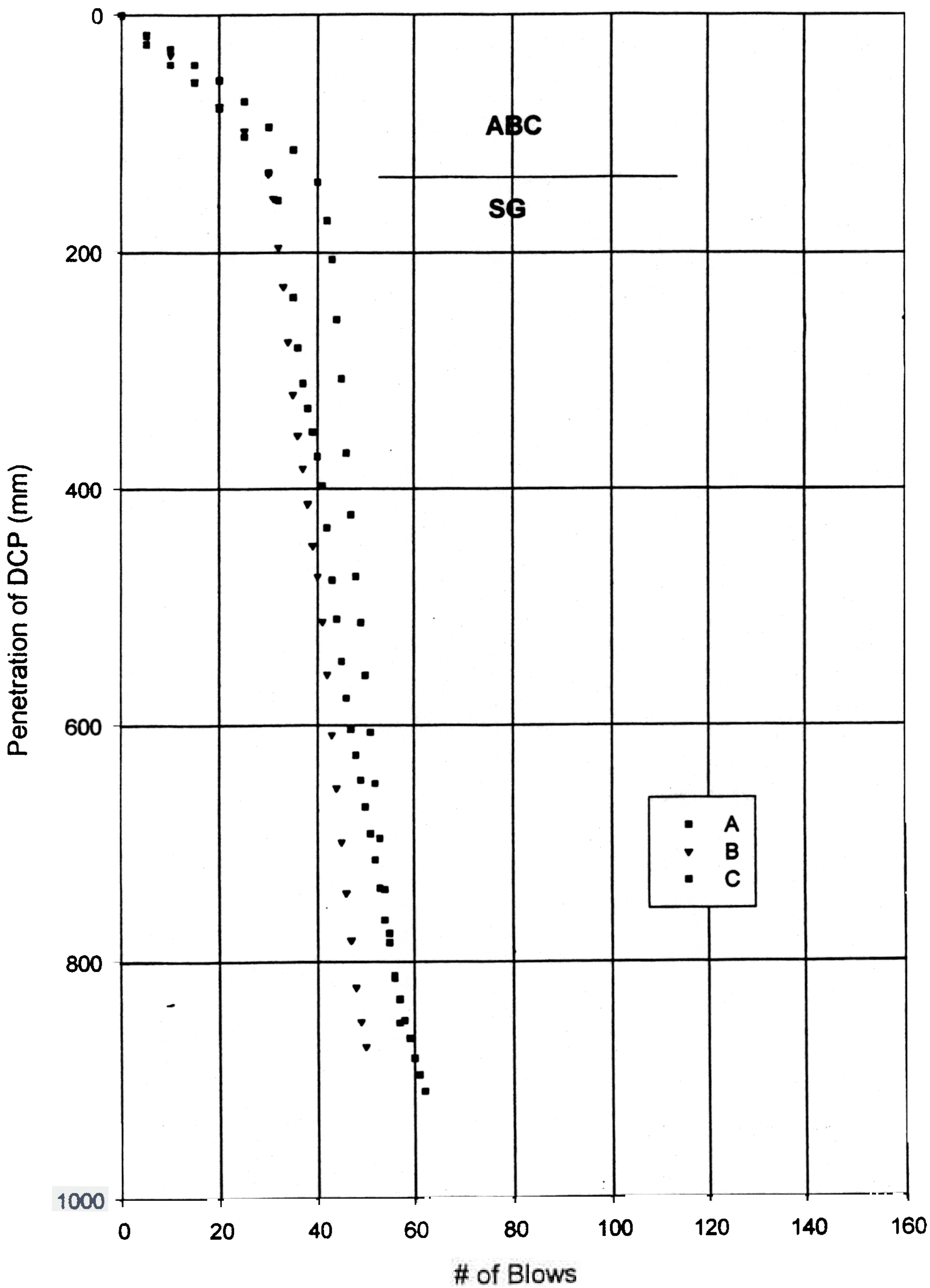

Figure A.3c SR 2352 (Newsome Rd.) Penetration Depth Vs.
# of Blows Unconfined

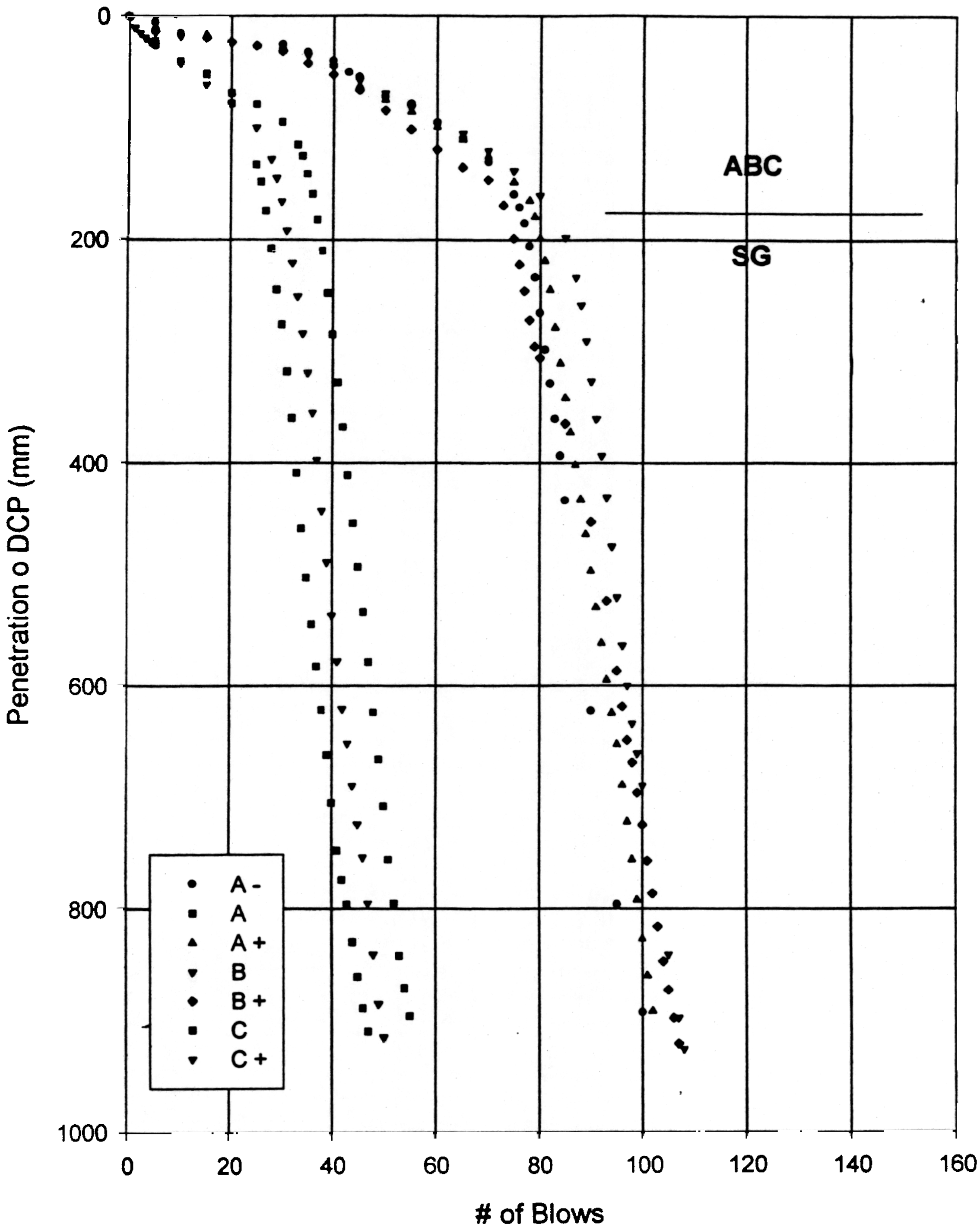

Figure A.4a SR 2487 (Frontier Dr.) Penetration Depth Vs. # of Blows All Seven Tests

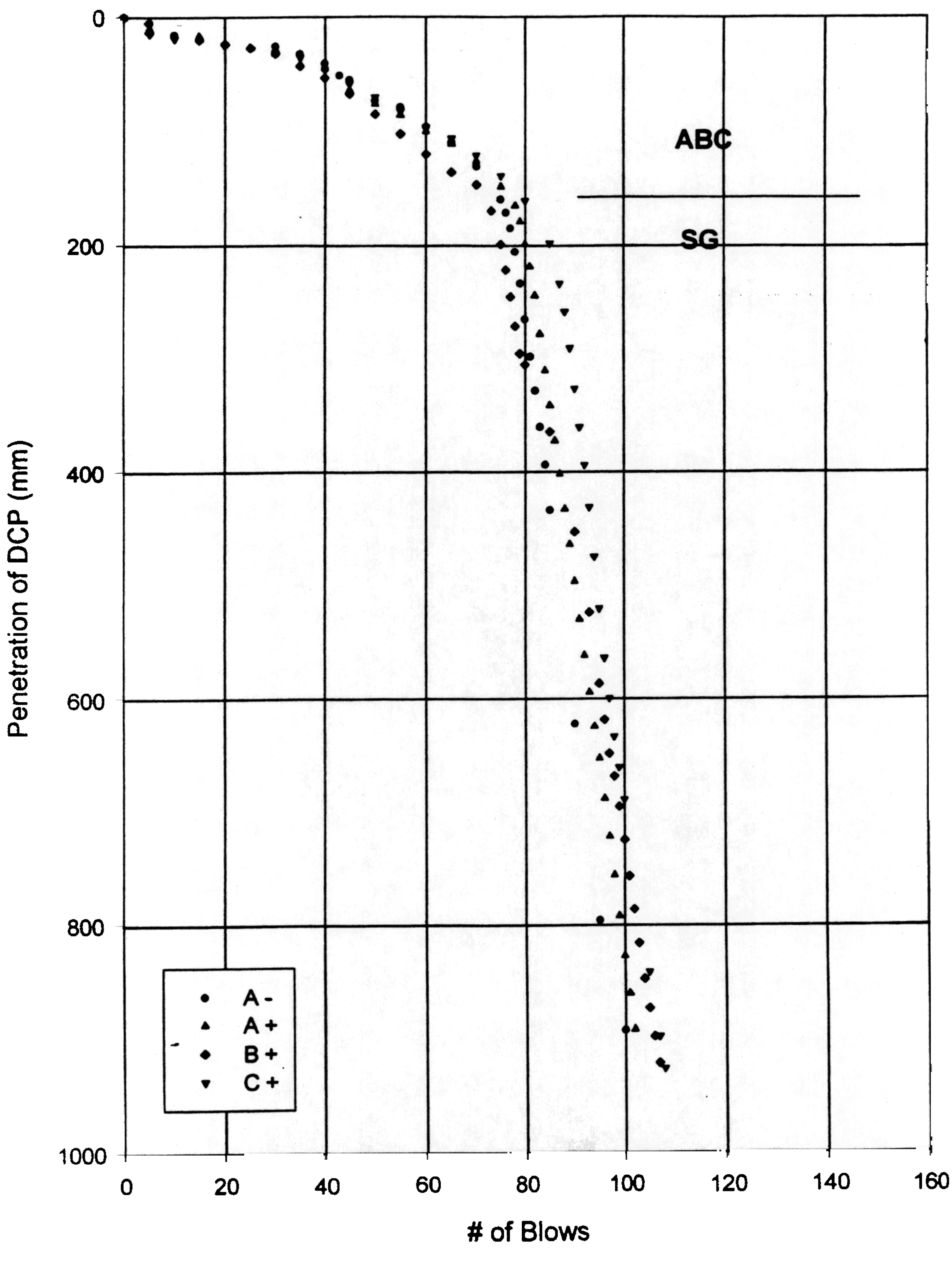

Figure A.4b SR 2487 (Frontier Rd.) Penetration Depth Vs. # of Blows Confined

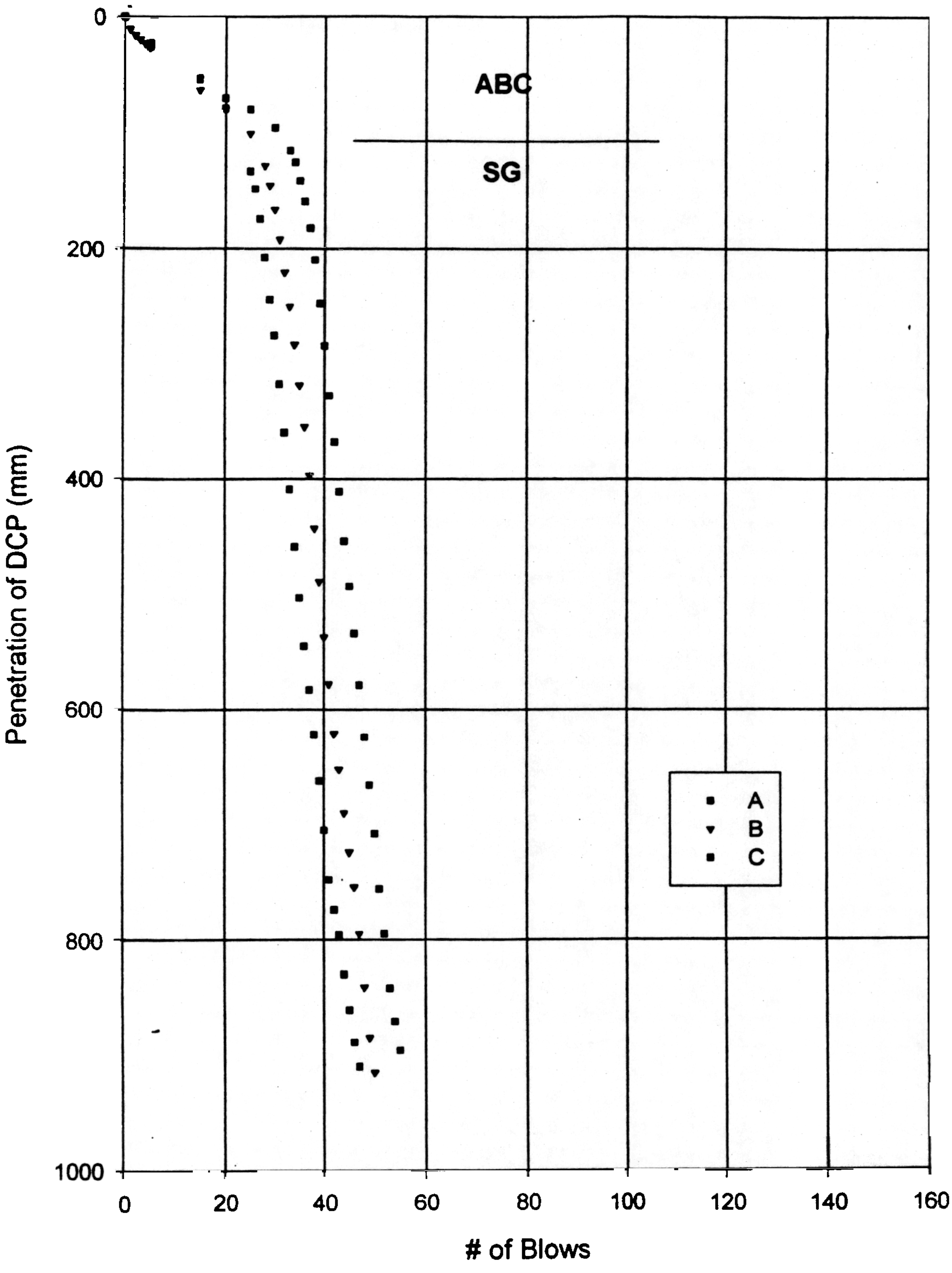

Figure A.4c SR 2487 (Frontier Rd.) Penetration Depth Vs. # of Blows Unconfined

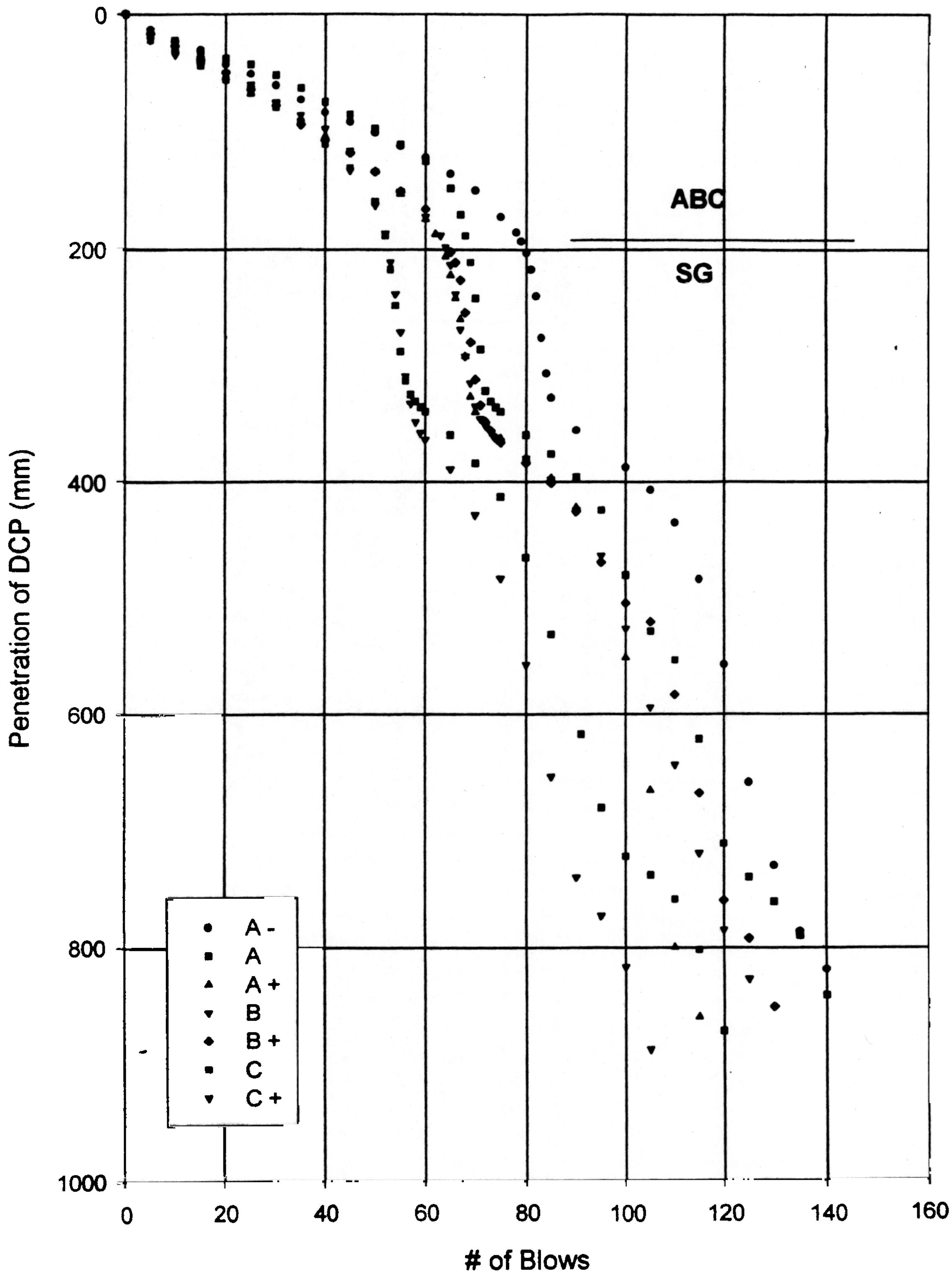

Figure A.5a SR 2529 (Surratt Rd.) Penetration Depth Vs. # of Blows All Seven Tests

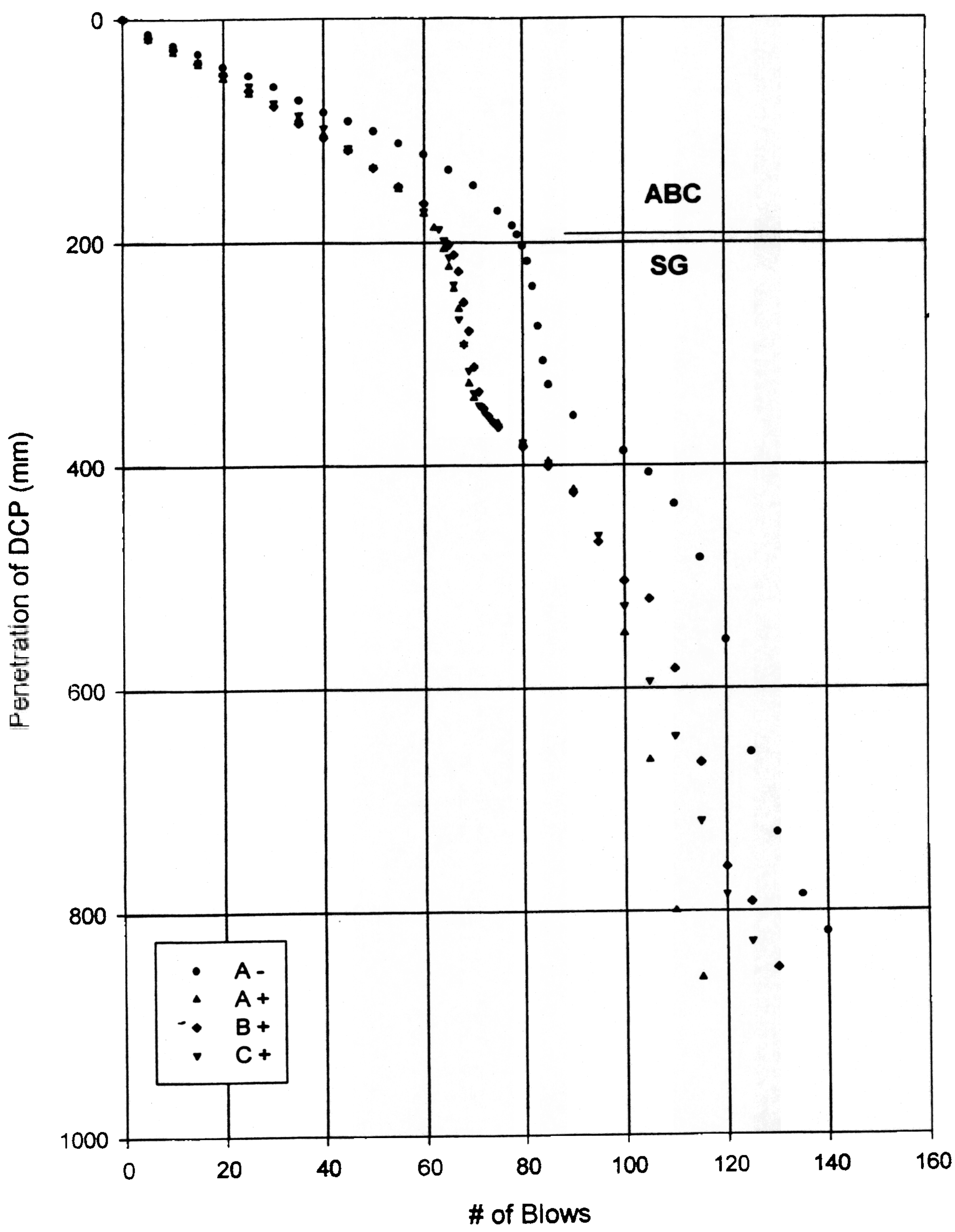

Figure A.5b SR 2529 (Surratt Rd.) Penetration Depth Vs. # of Blows Confined

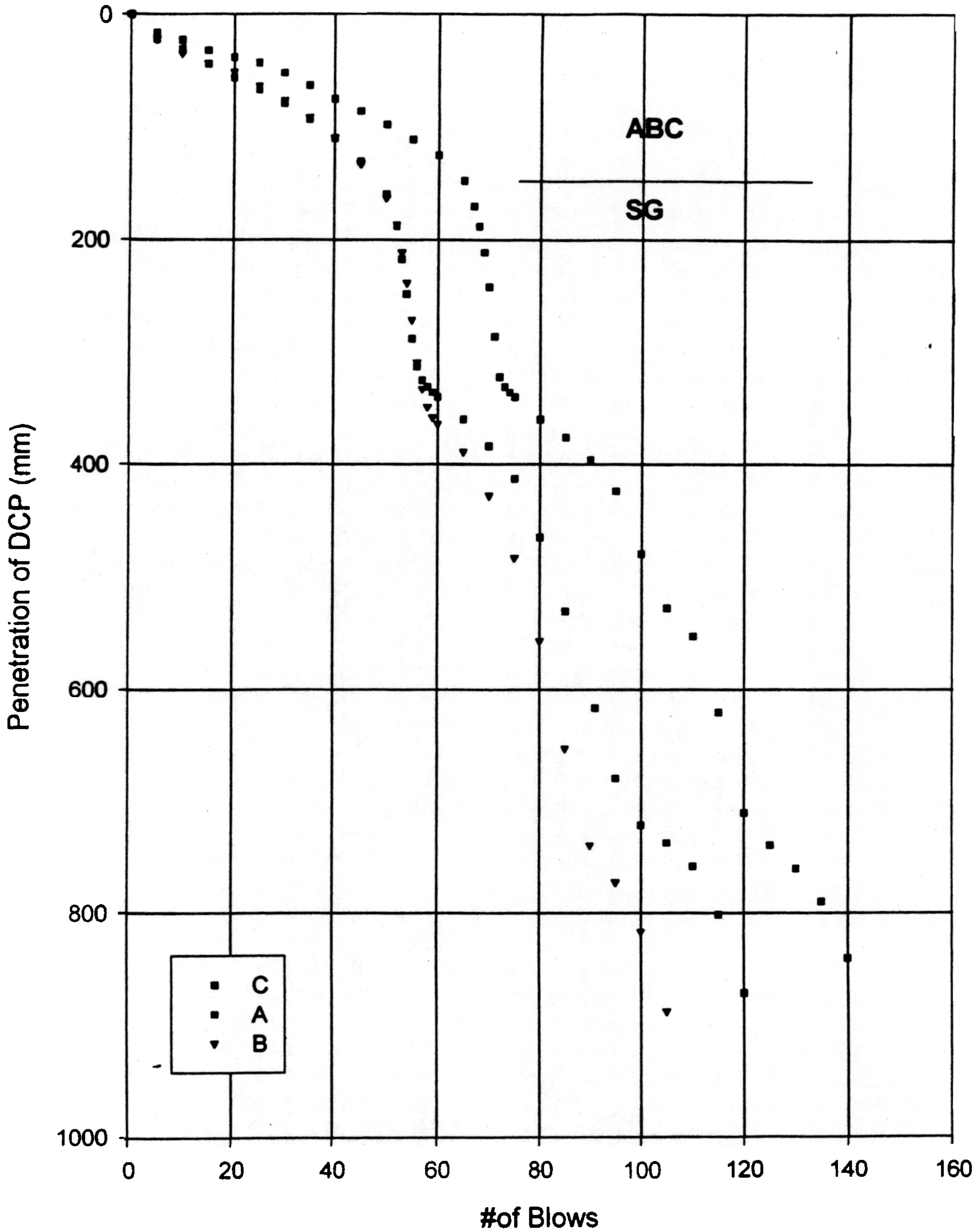

Figure A.5c SR 2529 (Surratt Rd.) Penetration Depth Vs. # of Blows Unconfined

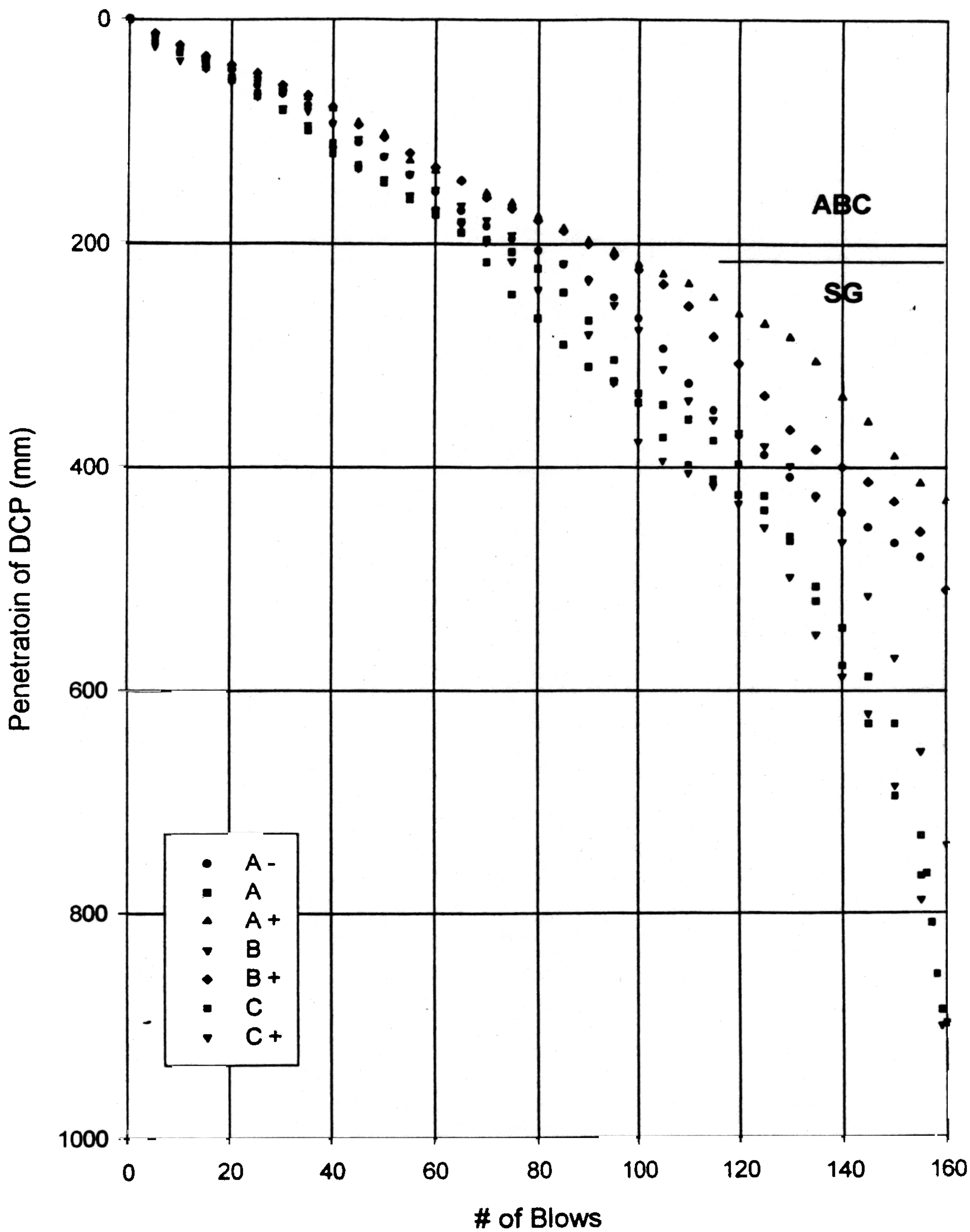

Figure A.6a SR 2572 (Lee Wilson Rd.) Penetration Depth Vs. # of Blows All Seven Tests

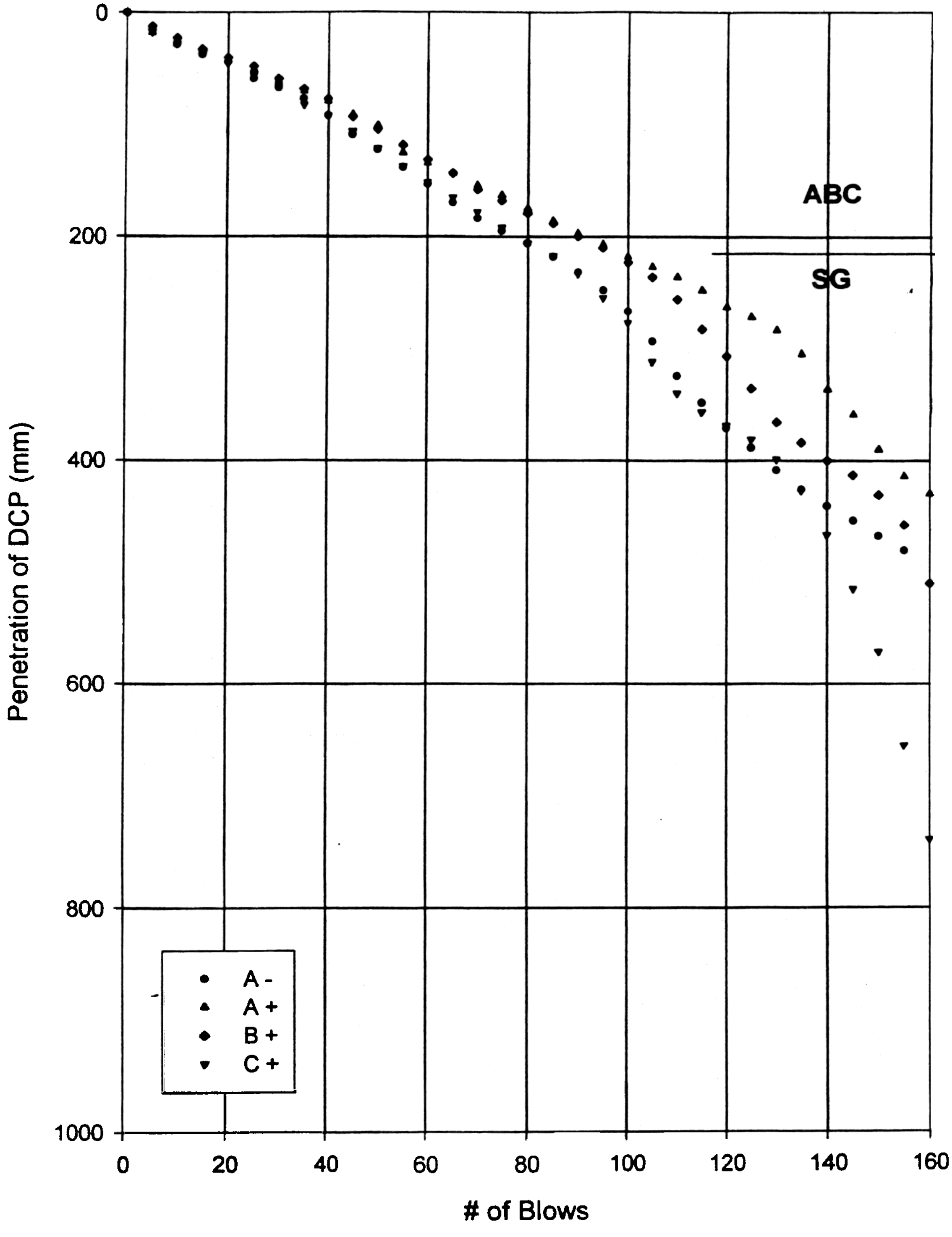

Figure A.6b SR 2572 (Lee Wilson Rd.) Penetration Depth Vs. # of Blows Confined

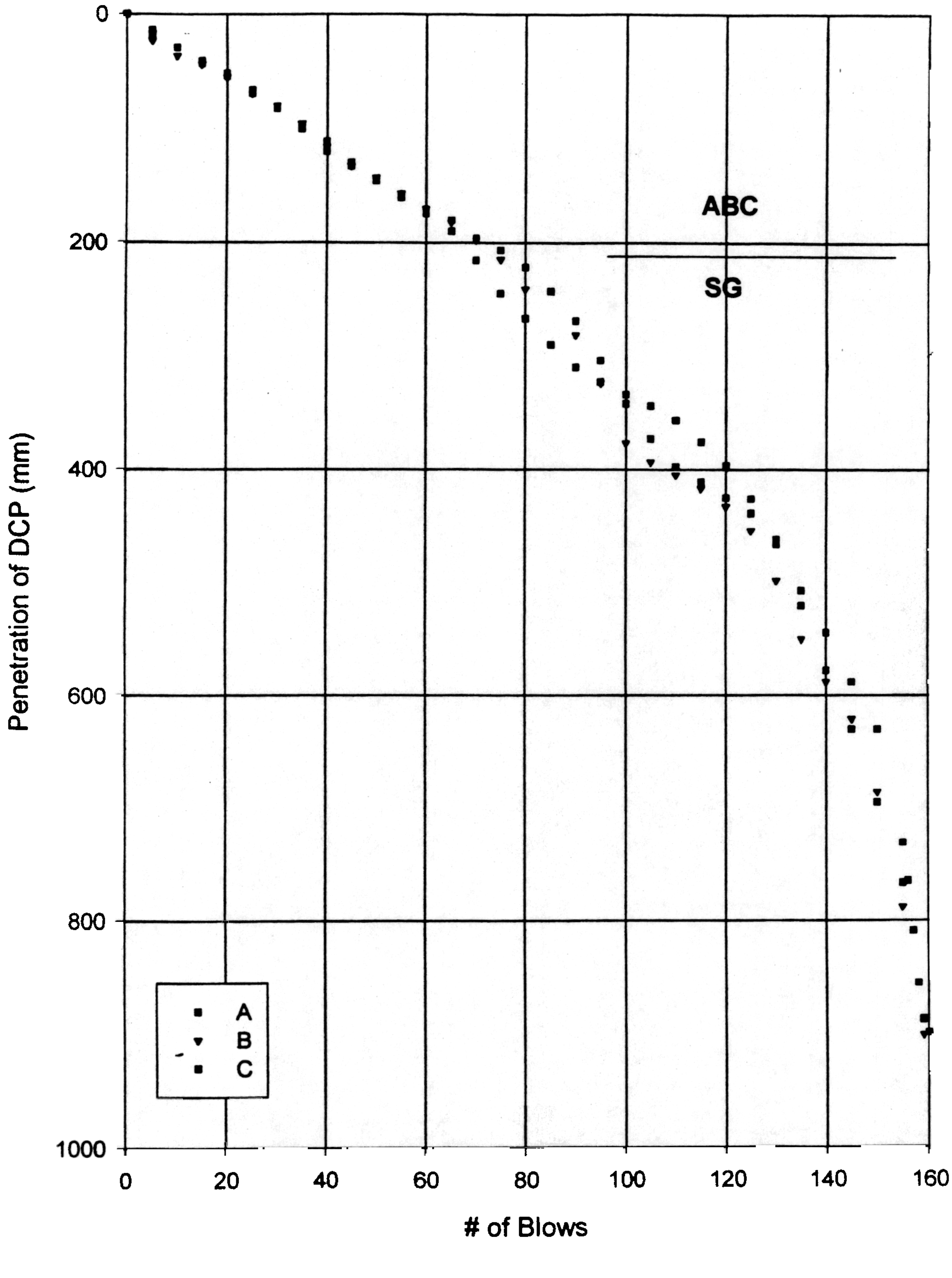

Figure A.6c SR 2572 (Lee Wilson Rd.) Penetration Depth Vs. # of Blows Unconfined

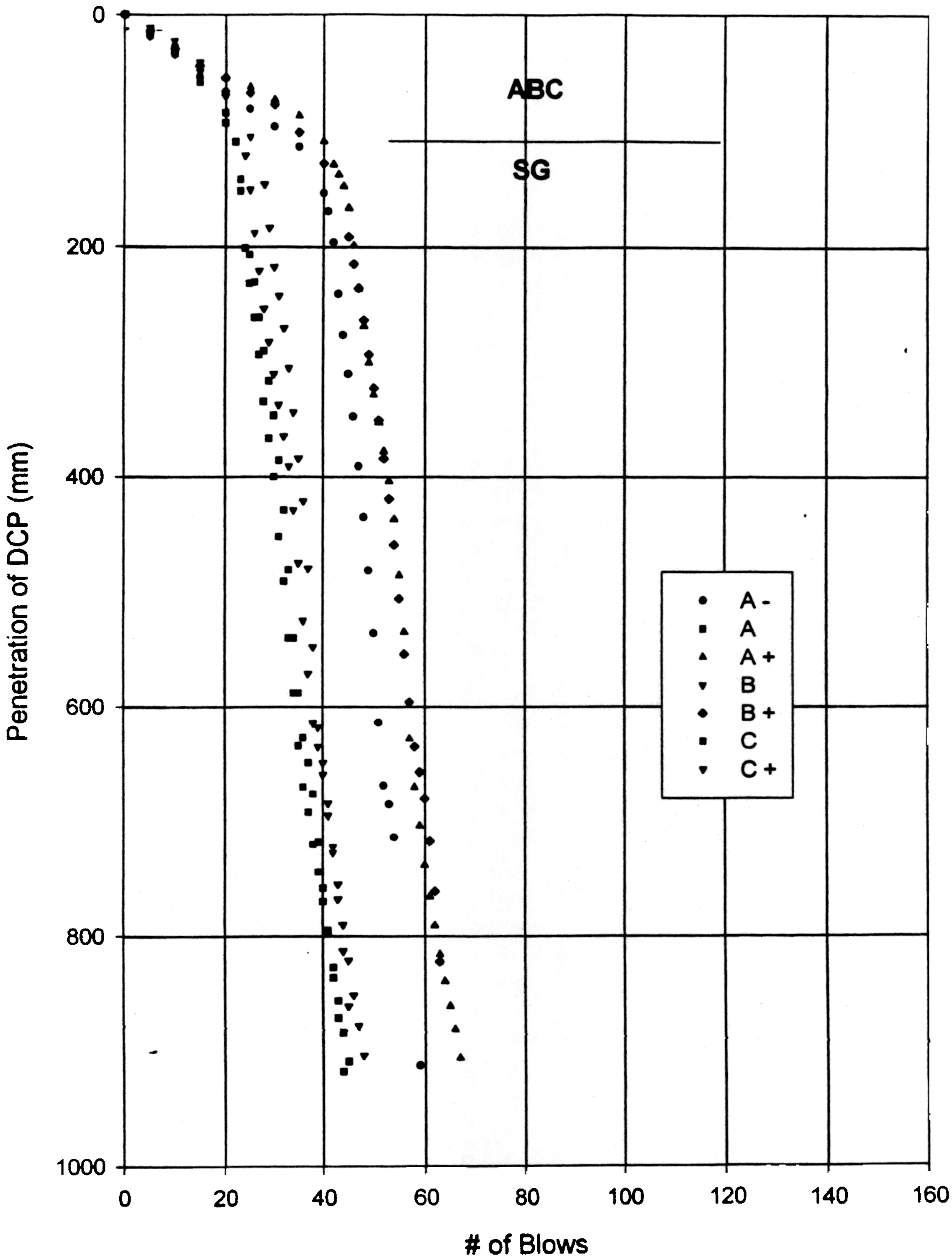

Figure A.7a SR 2751 (Greentree Rd.) Penetration Depth Vs. # of Blows All Seven Tests

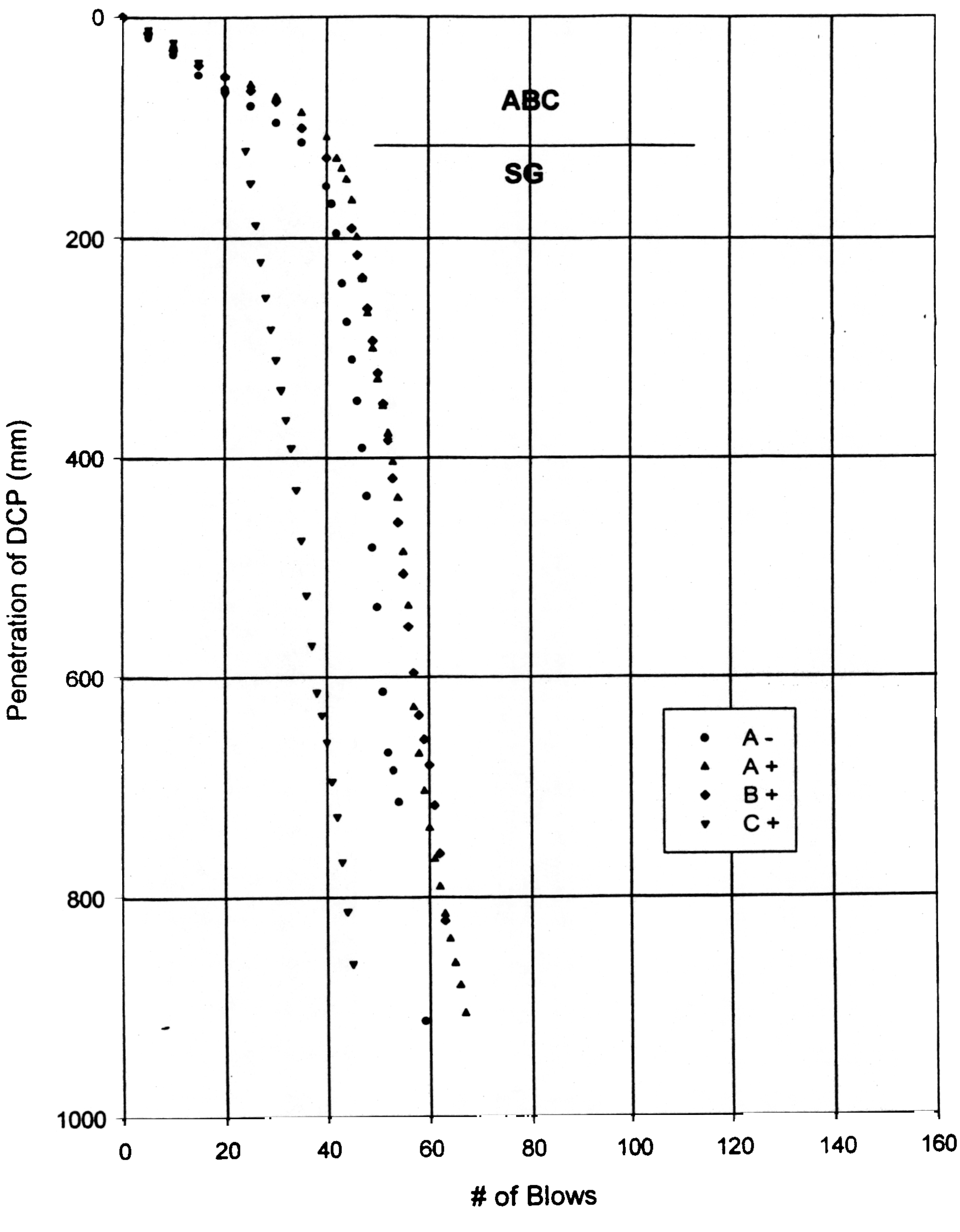

Figure A.7b SR 2751 (Greentree Rd.) Penetration Depth Vs. # of Blows Confined

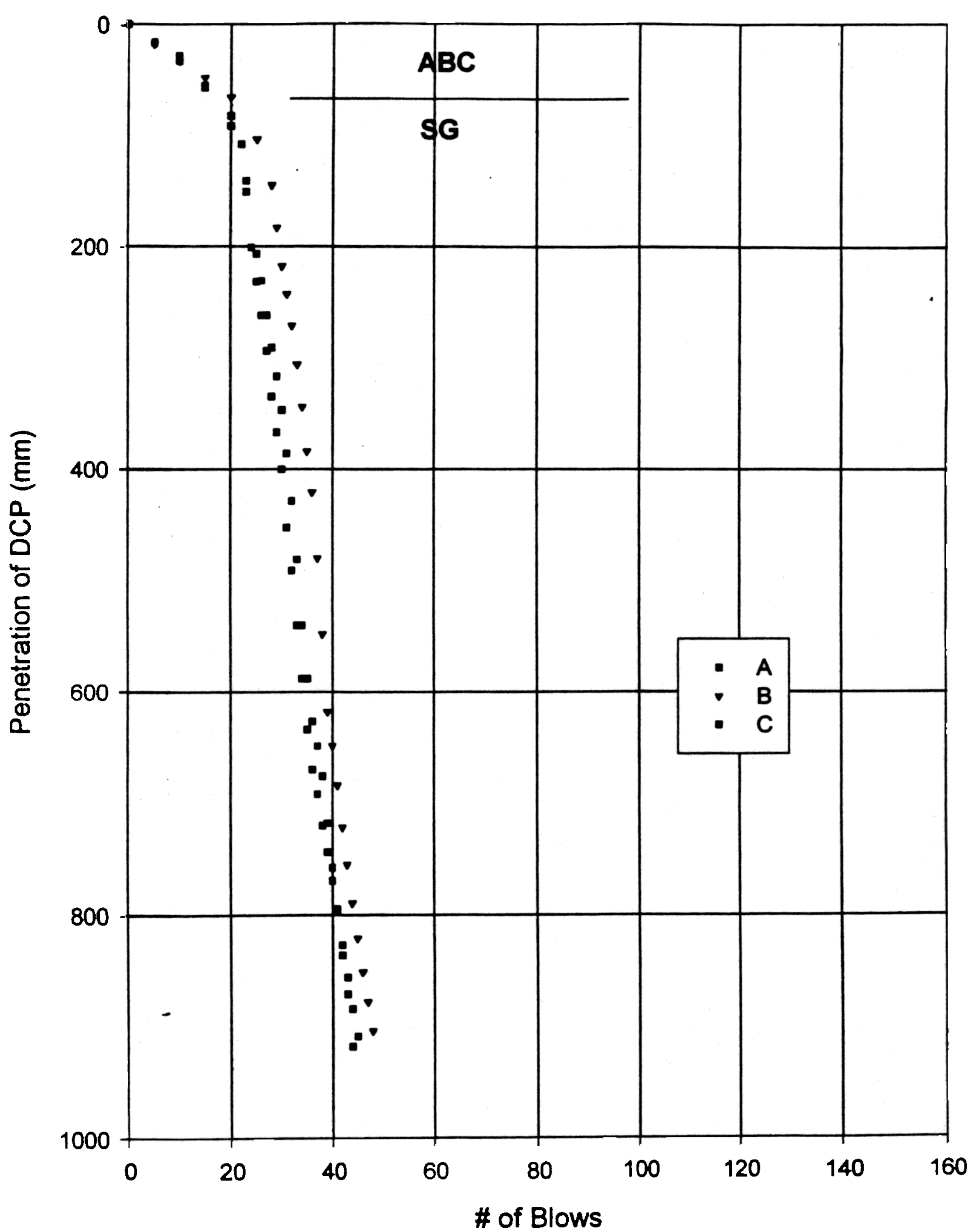

Figure A.7c SR 2751 (Greentree Rd.) Penetration Depth Vs. # of Blows Unconfined

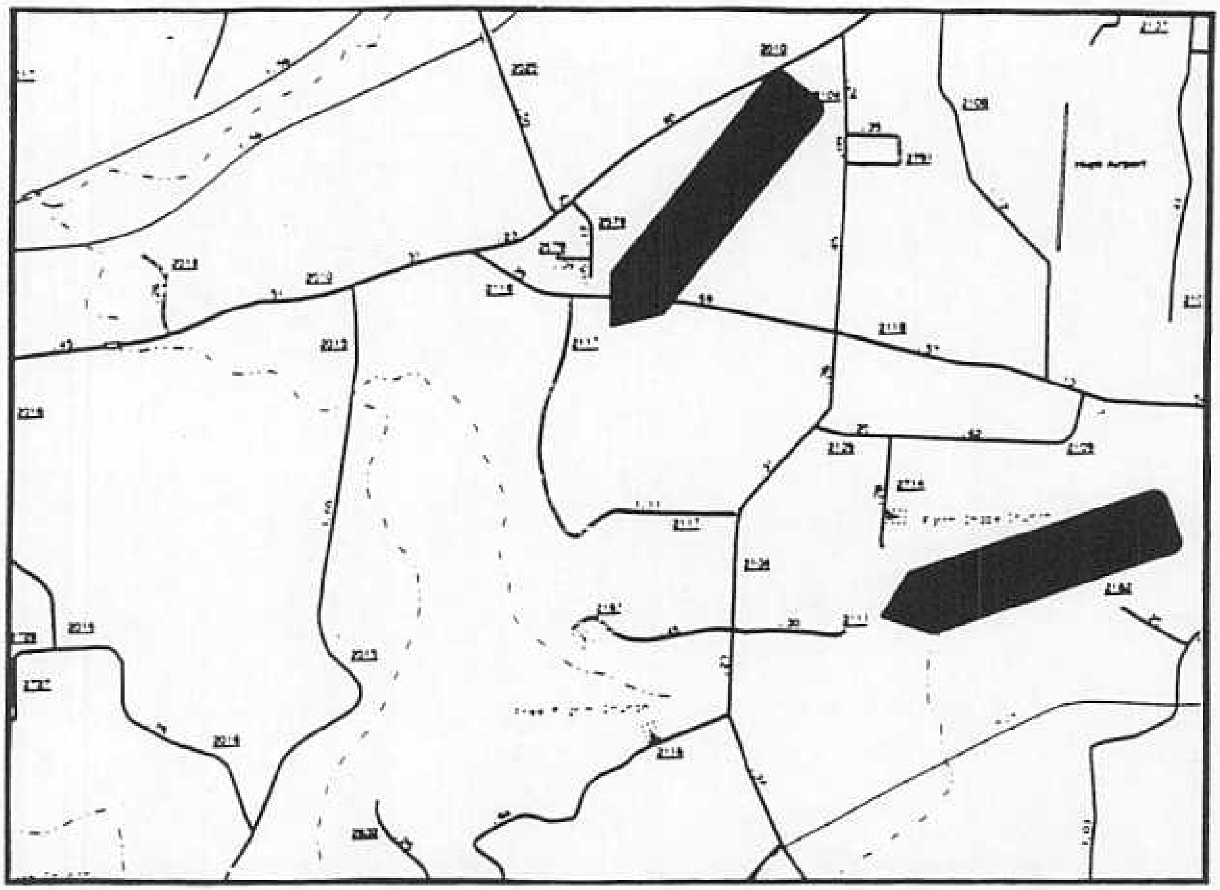

DAVIDSON COUNTY

NORTH CAROLINA

PREPARED BY THE

NORTH CAROLINA DEPARTMENT OF TRANSPORTATION
DIVISION OF HIGHWAYS - GIS UNIT

IN COOPERATION WITH THE

U.S.DEPARTMENT OF TRANSPORTATION
FEDERAL HIGHWAY ADMINISTRATION

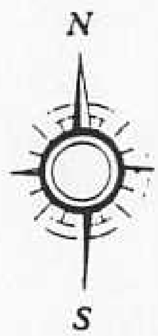

SCALE

1 0 1 MILES

Map A.8 Location of SR 2111 (Poole Rd.) and SR 2117 (Carter Rd.)

DAVIDSON COUNTY

NORTH CAROLINA

PREPARED BY THE

NORTH CAROLINA DEPARTMENT OF TRANSPORTATION
DIVISION OF HIGHWAYS - GIS UNIT

IN COOPERATION WITH THE

U.S.DEPARTMENT OF TRANSPORTATION
FEDERAL HIGHWAY ADMINISTRATION

SCALE

1 0 1 MILES

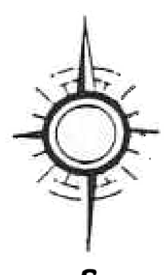

Map A.9 Location of SR 2352 (Newsome Rd.)

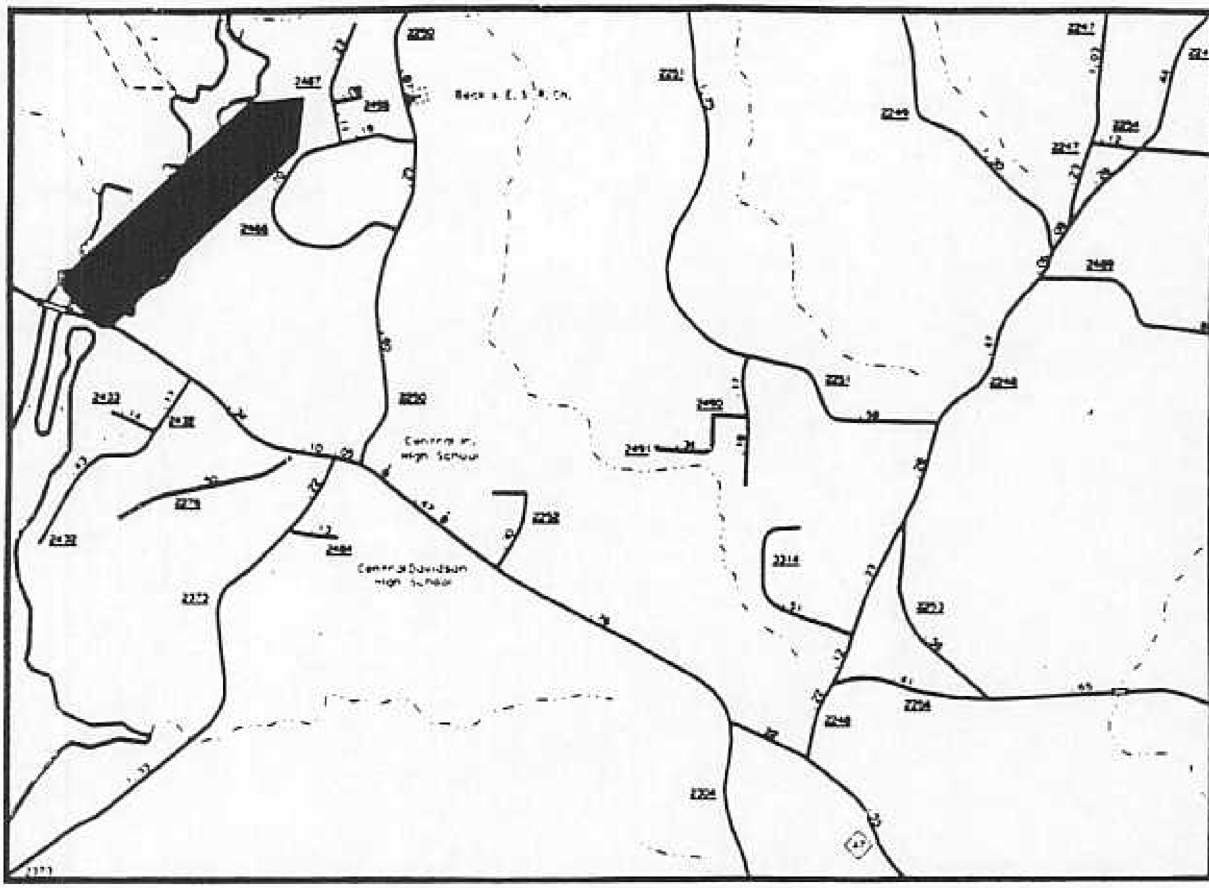

DAVIDSON COUNTY

NORTH CAROLINA

PREPARED BY THE

NORTH CAROLINA DEPARTMENT OF TRANSPORTATION
DIVISION OF HIGHWAYS – GIS UNIT

IN COOPERATION WITH THE

U.S.DEPARTMENT OF TRANSPORTATION
FEDERAL HIGHWAY ADMINISTRATION

SCALE

1 0 1 MILES

N

S

Map A.10 Location of SR 2487 (Frontier Dr.)

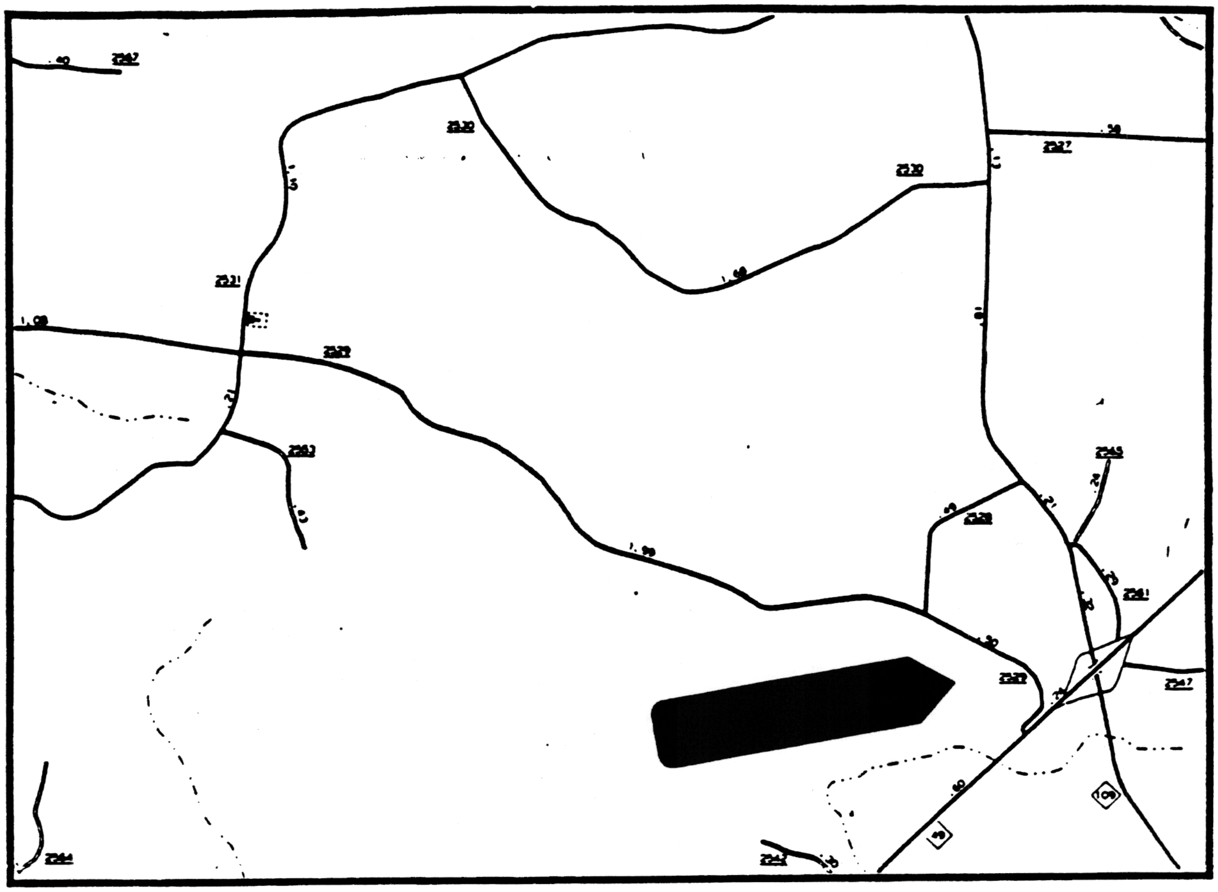

DAVIDSON COUNTY

NORTH CAROLINA

PREPARED BY THE

NORTH CAROLINA DEPARTMENT OF TRANSPORTATION
DIVISION OF HIGHWAYS - GIS UNIT

IN COOPERATION WITH THE

U.S.DEPARTMENT OF TRANSPORTATION
FEDERAL HIGHWAY ADMINISTRATION

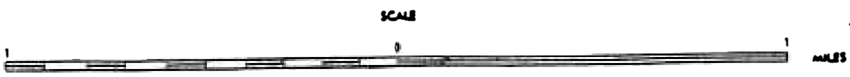

Map A.11 Location of SR 2529 (Surratt Rd.)

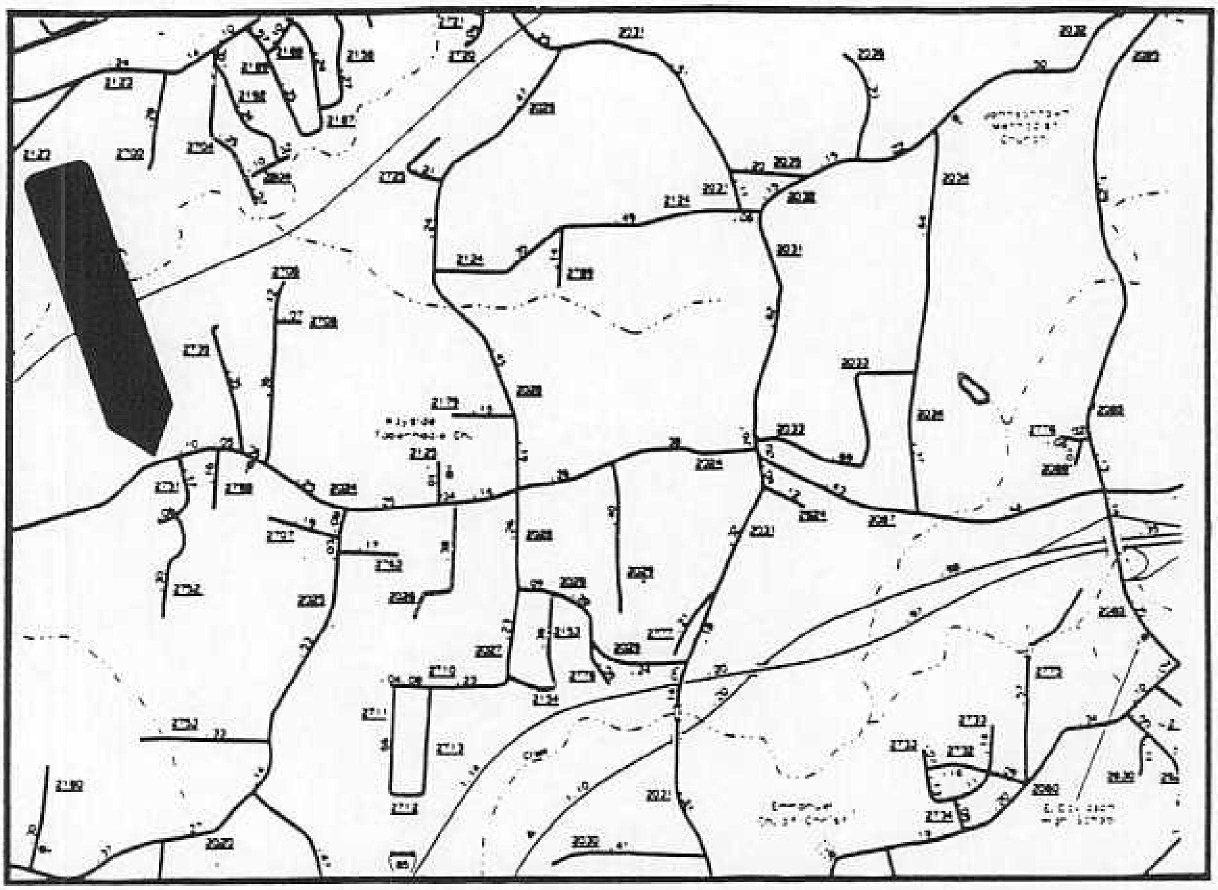

DAVIDSON COUNTY

NORTH CAROLINA

PREPARED BY THE

NORTH CAROLINA DEPARTMENT OF TRANSPORTATION
DIVISION OF HIGHWAYS - GIS UNIT

IN COOPERATION WITH THE

U.S.DEPARTMENT OF TRANSPORTATION
FEDERAL HIGHWAY ADMINISTRATION

SCALE

1 0 1 MILES

Map A.12 Location of SR 2751 (Greentree Rd.)

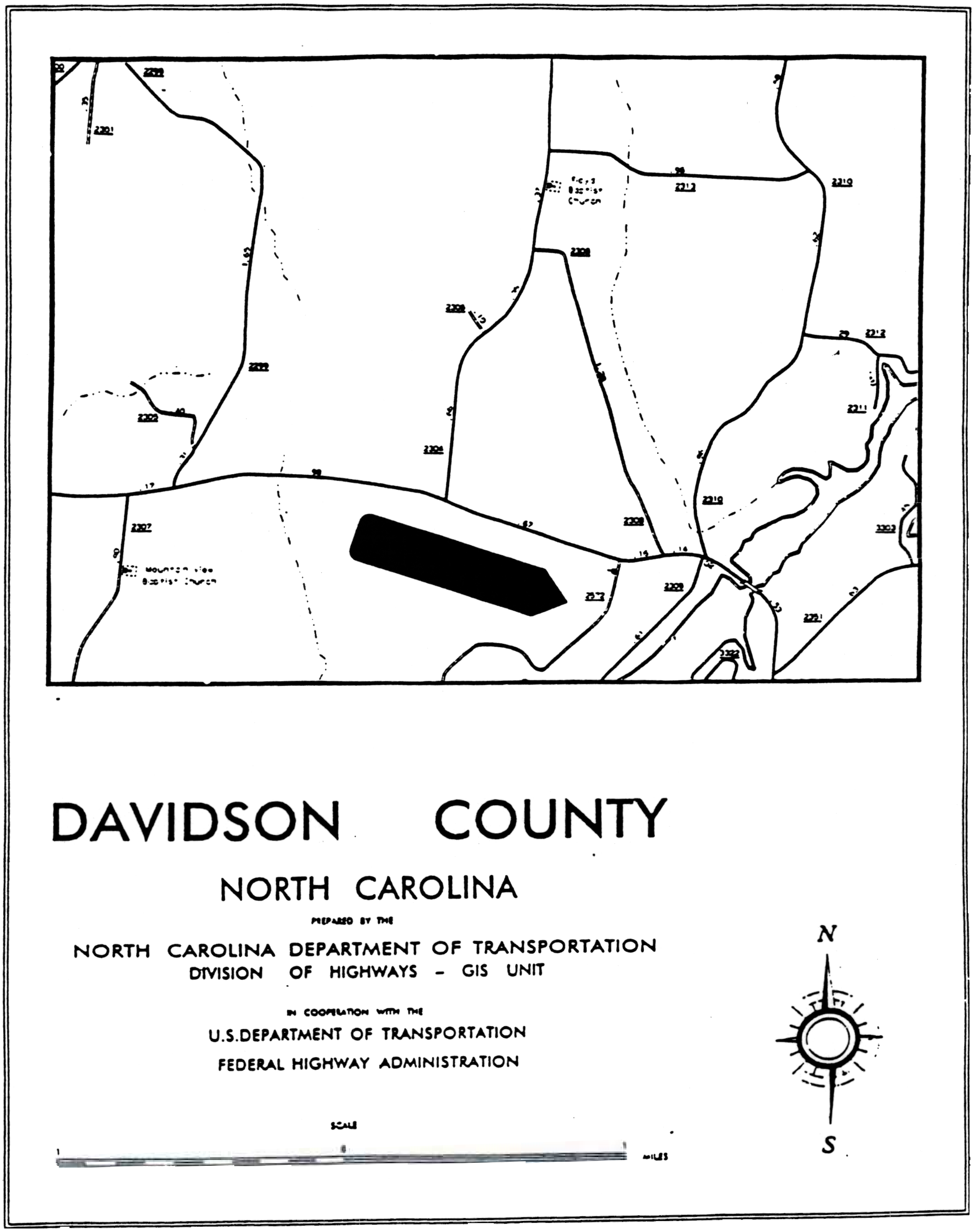

Map A.13 Location of SR 2572 (Lee Wilson Rd.)